



<https://theses.gla.ac.uk/>

Theses Digitisation:

<https://www.gla.ac.uk/myglasgow/research/enlighten/theses/digitisation/>

This is a digitised version of the original print thesis.

Copyright and moral rights for this work are retained by the author

A copy can be downloaded for personal non-commercial research or study,
without prior permission or charge

This work cannot be reproduced or quoted extensively from without first
obtaining permission in writing from the author

The content must not be changed in any way or sold commercially in any
format or medium without the formal permission of the author

When referring to this work, full bibliographic details including the author,
title, awarding institution and date of the thesis must be given

Enlighten: Theses

<https://theses.gla.ac.uk/>
research-enlighten@glasgow.ac.uk

PARALLEL-SURFACE THRUST BEARINGS

AT HIGH SPEEDS

A THESIS

presented to the University of Glasgow

for the degree of

Doctor of Philosophy

John Young, M.S., B.Sc., A.R.T.C., A.M.I.Mech.E

ProQuest Number: 10647547

All rights reserved

INFORMATION TO ALL USERS

The quality of this reproduction is dependent upon the quality of the copy submitted.

In the unlikely event that the author did not send a complete manuscript and there are missing pages, these will be noted. Also, if material had to be removed, a note will indicate the deletion.



ProQuest 10647547

Published by ProQuest LLC (2017). Copyright of the Dissertation is held by the Author.

All rights reserved.

This work is protected against unauthorized copying under Title 17, United States Code
Microform Edition © ProQuest LLC.

ProQuest LLC.
789 East Eisenhower Parkway
P.O. Box 1346
Ann Arbor, MI 48106 – 1346

GLASGOW
UNIVERSITY
LIBRARY

TABLE OF CONTENTS

	Page No.
Abstract	iv
Nomenclature	vi
Chapter I	
I.1 Introduction	1
Chapter II	
II.1 Critical Review of Published Theoretical Work	8
II.2 The Governing Equations of Lubrication between Parallel Surfaces	15
Chapter III	
III.1 Solution of Governing Equations for No Side Leakage	22
III.2 Solution by a Relaxation Method	27
III.3 General Solution taking account of Side Leakage	35
III.4 Numerical Comparisons of the Three Solutions	43
III.5 Friction in a Parallel Surface Bearing	71
III.6 Summary of Theoretical Work	74
Chapter IV	
IV.1 Description of Apparatus	80

	Page No.
Chapter V	
V.1 Experimental Procedure	101
V.2 Presentation of Experimental Results	106
V.3 Discussion of Results	127
Chapter VI	
VI.1 Conclusions	136
List of References	143
Acknowledgements	145
Appendix I - Tabulated Experimental Results	147
Appendix II -Calibration of Apparatus	158

ABSTRACT

On a few occasions thrust bearings composed of two opposing flat parallel surfaces, have shown some indications of fluid film lubrication. This behaviour is in contradiction to the classical lubrication theory, which requires some geometrical restriction or 'taper wedge' effect in the bearing clearance in order to produce a load-carrying oil film. A tentative explanation by Fogg suggested a 'thermal wedge' effect in which the restriction to oil flow in the bearing is caused by thermal expansion of the fluid as it passes through a space of constant area. Theoretical analyses of the problem have confirmed the thermal wedge as a possible contributing factor in developing a load-bearing fluid film, but no direct correlation of theory with practice has previously been made.

Towards this end, the theoretical analysis of the thermal wedge effect in a parallel surface bearing has been extended in this thesis to include the important effect of side leakage. General equations for temperature distribution, and for bearing pressure and load-carrying capacity for a sector pad have been developed, and from these were obtained characteristic equations which can be applied directly to an actual bearing, and which can be used to produce theoretical performance curves.

A high-speed experimental apparatus was designed and built and tests were conducted on a parallel-surface thrust bearing, over a wide range of operating conditions. Readings of bearing friction, load, film thickness, oil flow and temperatures around the bearing were taken for a large number of tests. The maximum bearing pressure which could be carried without excessive friction and temperature rise was about 60 to 70 psi, which is in accordance with values for the old-fashioned horseshoe marine bearings. The experimental results were plotted and compared with the theoretical performance curves. Although a certain amount of scatter is evident in the experimental points, sufficient correlation is shown to confirm the thermal wedge behaviour, within the range of test conditions.

It is concluded that the thermal wedge effect does exist and is of importance in a parallel surface bearing at high speeds and low loads. However, in order to produce a high load-carrying capacity, a parallel surface bearing of a type similar to the test bearing would be required to operate with a film thickness of about 0.0002 inches and a temperature rise around the bearing pad of some 300°F. These values are outside the limits of normal lubrication practice, and thus it would seem that, while the thermal wedge effect may be of interest in certain high-speed low-load applications, it is not important in normal thrust bearing practice.

NOMENCLATURE

The following symbols are used throughout the text. As far as possible, standard symbols are used. Any symbol not listed is defined where it first appears.

x, y, z	Cartesian coordinates
u, v, w	Velocities in the x, y and z directions
U	Velocity of the moving surface
p	Pressure
ρ	Density
μ	Viscosity
t	Temperature rise above inlet
T	Temperature or Torque
h	Film thickness
q	Rate of Flow
E	Internal Energy
σ	Specific Heat
J	Mechanical Equivalent of Heat
λ	Coefficient of Thermal Expansion
β	Coefficient of Viscosity Variation
r, θ	Polar Coordinates
τ	Shear Stress
ω	Angular Velocity
α	Included Angle of Sector Pad
b	Expansion Coefficient related to bearing angle.

A, B, C	Constants of Integration
Q, K, G, \bar{g}_n , \bar{p}_n	Functions defined in text
L	Length of Bearing Pad
P	Non-dimensional Pressure
D	Non-dimensional Density
M	Non-dimensional Viscosity
R, \odot	Non-dimensional Variables
a	Grid size in relaxation process, or Influence Coefficient.
F	Residual Coefficient or Force
W	Load on Bearing

CHAPTER I.

I. 1. Introduction.

Note: The experimental work for this thesis was done during the period, January 1954 to August 1956, and the thesis was compiled before March 1959.

CHAPTER II. 1. Introduction

Since the problem of hydrodynamic lubrication was first analysed by Osborne Reynolds in 1886, perhaps the most important point to emerge from the development of his work is the principle of the "taper wedge." This postulates that fluid film lubrication is not possible unless there is a geometrical restriction of the clearance space between the bearing surfaces in the direction of relative motion. The restriction may be arranged, by using tilting pads or fixed taper lands as in thrust bearings, or may happen fortuitously as in the case of a journal bearing where the restriction occurs when an applied load causes the journal to run eccentrically in the bearing. Or indeed, strictly speaking, the restriction may not be tapered, as bearings with various non-linear functions of film thickness variation, including a stepped surface bearing, have been operated quite successfully. Specifically the geometrical "taper wedge" requirement precludes the possibility of film lubrication existing between two parallel surfaces in relative motion.

Experimental data and practical experience of parallel-surface thrust bearings, which were in general use before the introduction of the Michell and Kingsbury tilting pad bearings, generally agreed with this conclusion. Any thrust load which these parallel bearings did carry was at low speeds with high friction coefficients, and could be attributed to boundary lubrication and the oiliness of the lubricant. Although some discrepancy was noted (Newbiggin (1) and Lasche (2)) in that parallel surface bearings sometimes performed better than expected,

the phenomenon had no definite characteristics and was not examined in detail.

It was not until 1946 that a positive contribution was made by Fogg (3) who reported high load carrying capacity and low friction in parallel thrust bearings operating at high rotational speeds. Because the work was done under conditions of war-time security, many details of the running conditions, dimensions of the bearings and results obtained were not reported in full. However, from the magnitude of the loads carried, the low coefficients of friction, the absence of metallic contact and a general relationship between friction and the viscosity-speed-load parameter, enough evidence was produced to suggest that film lubrication did occur (Fig.1). It was stressed that the bearings were plain annular rings with white-metalled faces, in which a number of sharp-edged grooves were cut radially across the surface. Every effort was made to ensure that there was no geometric taper present. The only apparent difference between the test bearing and the old-fashioned parallel surface bearing was that very high rotational speeds were used. (The actual speeds were not reported, but it has since been learned that the test speeds were about 14,000 and 19,000 rpm). A tentative explanation of the results was given, which suggested that a pressure was developed because of the differential expansion of the lubricant as it passed through the bearing. In effect, a restriction was caused, not by passing a constant volume of oil through a converging passage, but by passing an expanding volume through a parallel passage - the so-called 'thermal wedge' effect.

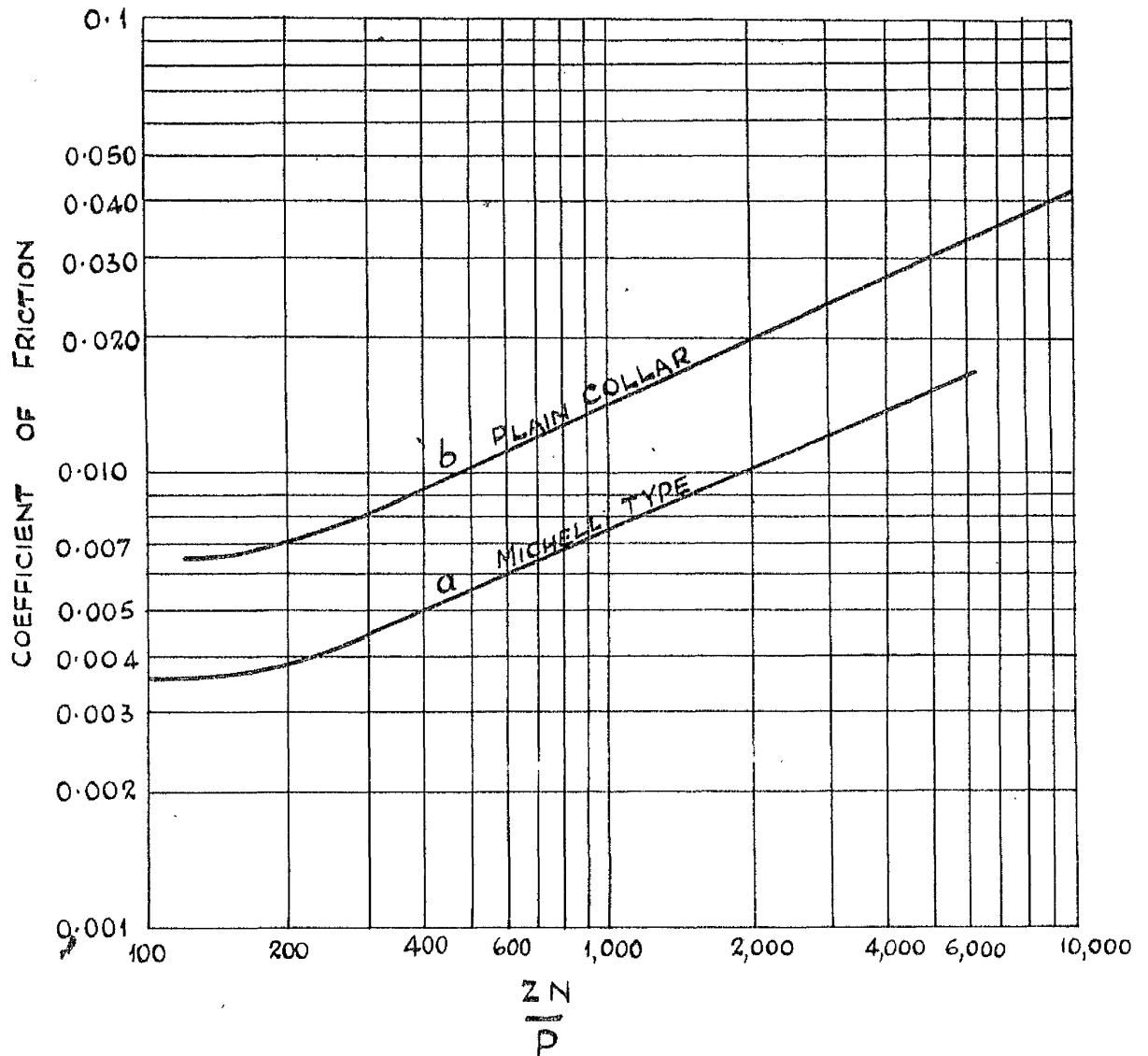


FIG. 1. CHARACTERISTICS OF BEHAVIOUR OF MICHELL
TYPE AND PLAIN COLLAR BEARINGS (FOGG)

This novel suggestion caused an immediate re-examination of Reynolds equation, and several solutions were produced in which the assumption of mass continuity through the bearing replaced the former assumption of volume continuity, thus taking account of the expansion of the lubricant. Some of these solutions are discussed in detail later, and according to them, it seems possible to produce a load-carrying lubricating film between parallel plates, dependent on the 'thermal wedge' effect.

In spite of a convincing amount of theoretical work, there still remains some dubiety about the existence and effect of a 'thermal wedge' film in an actual bearing, because so far as is known, no positive correlation between theory and experiment has been made. The new solutions to Reynolds equation which followed Fogg's work could not be checked against his experiments because not enough detail was given; and generally the solutions themselves were obtained by making simplifications - in particular the fairly common assumption of no side leakage, which implies an infinitely wide bearing - which had but little physical justification, and which made comparisons difficult.

One further experimental paper by Kettleborough (4), did little to clarify the situation. This author recorded a pressure distribution for a parallel surface bearing (with some difficulty and showing obvious discrepancies because of the very small film thicknesses involved), but was unable to record any temperature gradient around the film in the circumferential direction. The friction coefficients were much greater than comparable values from

Fogg's paper, but the difference in running speeds prevented a direct comparison (Fig. 2). It is stated that hydrodynamic lubrication did exist in this bearing, although again, no correlation with theory was attempted.

It would appear, therefore, that the 'thermal wedge' can only operate under certain conditions, which have not yet been clearly defined, although the effect seems to be more evident at high speeds.

It was considered that a useful contribution could be made by recording the operating characteristics - the friction, film thickness, temperature around the bearing, and so on - of a parallel surface bearing over a wide range of speeds and loads and analysing the results; by showing whether or not the temperature gradient exists and is sufficient to produce the necessary expansion to provide a pressure film; and finally, by expanding the existing theoretical work to include the effect of side leakage, in order to demonstrate whether the results obtained are in agreement with theory.

It was with these objectives in view that this research was undertaken.

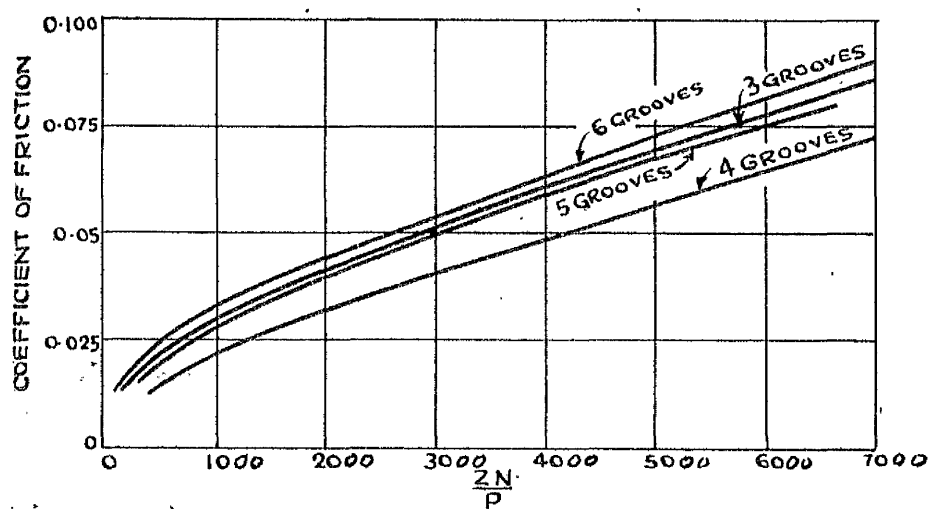
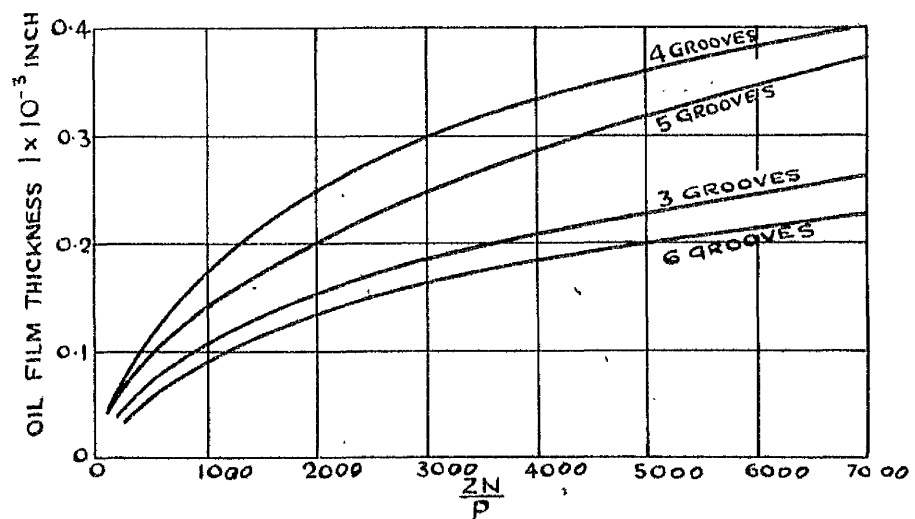


FIG. 2. VARIATION OF FILM THICKNESS
AND COEFFICIENT OF FRICTION.
(KETTLEBOROUGH)

CHAPTER II

- II. 1. Critical Review of Published Theoretical Work.

- II. 2. The Governing Equations of Lubrication between Parallel Surfaces.

CHAPTER II

II. 1. Critical Review of Published Theory

The publication of Fogg's paper provoked a comprehensive discussion in which opinions were divided. Several contributors expressed beliefs that side leakage from a bearing would more than counter any expansion effect of the oil, and that thermal distortion might cause a geometric taper, which would be of more consequence in producing a pressure film than would be a thermal wedge.

No theoretical or experimental evidence was produced to substantiate this side of the argument at that time.

Supporting the thermal wedge idea, Bower (5) produced an analysis of the problem in a simplified form, in which he assumed no side leakage, and ab initio linear variations of density, viscosity, and film thickness along the bearing, viz:-

$$\rho = \rho_0 (1 + a x_1)$$

$$h = h_0 (1 + b x_1)$$

$$\nu = \nu_0 (1 + c x_1)$$

where ' x_1 ' defines the distance of a point along the bearing as a fraction of the total length L . He then tabulated the load capacity of the bearing for various values of 'a', 'b', and 'c', and concluded that a bearing could carry a load by an expansion effect only, i.e. for ' $a > 0$ ' and ' $b = 0$ ', but that for similar conditions the effect of varying 'b' was much greater than varying 'a'. This latter conclusion, of course, assumes the same minimum film thickness for a parallel and

taper bearing, carrying the same load at the same conditions, an assumption which need not be true. Since the load carrying capacity varies as $1/h_0^2$, if conditions are favourable for maintaining a very thin film, a parallel surface bearing should be able to carry a useful load. While these arbitrary variations give a reasonable approximation to the conditions met with in a bearing, nevertheless they tend to mask the true state of affairs, and the derived equations have little physical significance.

Similarly, Shaw (6) gave a solution, in which he allowed a linear variation of density but kept the viscosity constant. Again, a comparison of the load-carrying capacities of tilting-pad and parallel surface types of bearing was made on the basis of equal film thickness, which led to the conclusion that a parallel surface bearing has a load capacity of about 1/10 that of a similar tilting-pad bearing (Fig. 3). Shaw also states that while the variable density theory explains the operation of a parallel surface bearing at low speeds and moderate loads, it does not explain satisfactorily the high load carrying capacity at high speeds, claimed by Fogg. In the discussion of this paper, Professor Shaw was criticised for the assumption of a lubricant which maintains a constant viscosity, but has a density varying with temperature. Besides being physically untenable, this assumption leads to an erroneous pressure distribution, when used to derive the pressure equation. Blok (7) states that the density and viscosity cannot be chosen arbitrarily but that the problem should be specified by four basic equations:-

- (a) a pressure equation
- (b) an energy or heat balance equation.

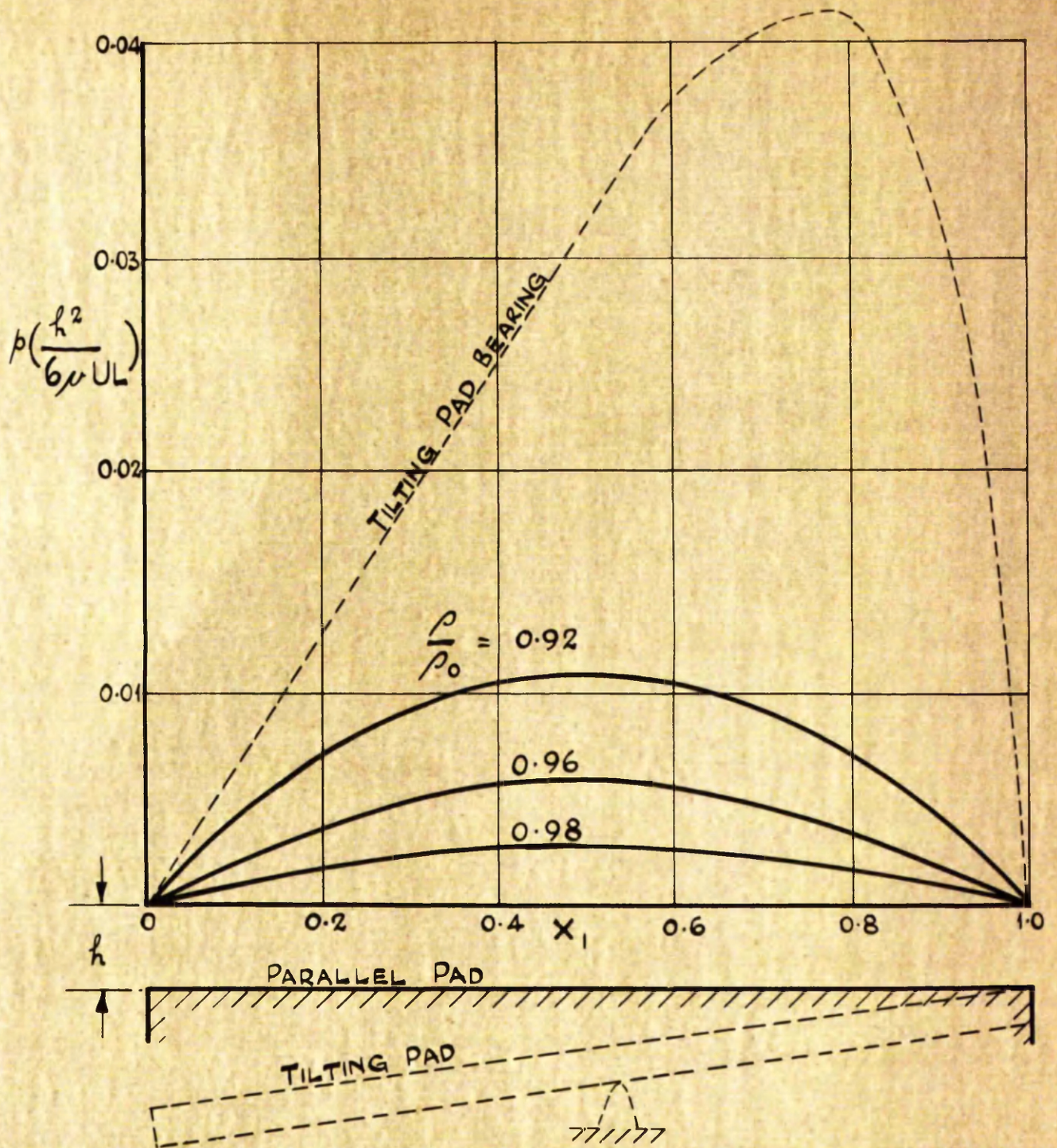


FIG. 3. VARIATION OF PRESSURE ALONG PARALLEL SURFACE THRUST BEARING (SHAW).

- (c) a temperature-viscosity relationship and
- (d) a temperature-density relationship for the lubricant.

Cameron and Wood (8) had earlier used such a procedure, but their work was not published until recently (8a), and in consequence was little known. Corresponding to the four basic equations above, these authors used

- (a) the general Reynolds equation with density as a variable

$$\frac{\partial}{\partial x} (\rho q_x) + \frac{\partial}{\partial y} (\rho q_y) = 0$$

- (b) an energy equation (derived by assuming adiabatic flow, similar to that of Christopherson (9))

$$\frac{\partial}{\partial x} (t \rho q_x) + \frac{\partial}{\partial y} (t \rho q_y) = \frac{U}{\sigma J} \left[\frac{h}{2} \frac{\partial p}{\partial x} + \frac{U \rho}{h} \right]$$

- (c) an exponential variation of absolute viscosity with temperature

$$\nu = k e^{\left[\frac{b}{t+95} \right]}$$

where 'k' and 'b' are constant for a particular oil and $t_1 = \text{deg. Centigrade}$, and

- (d) a linear variation of density with temperature.

$$\rho = \rho_0 (1 - \lambda t)$$

Hence two simultaneous partial differential equations in pressure and temperature were developed, which being rather complicated, were integrated for the simplified case of negligible side leakage only. Numerical values were obtained for a variety of conditions, and it was observed that the introduction of an appropriate constant value of viscosity did not seriously affect the results obtained.

It is to be noted, however, that this use of a constant viscosity value is at the calculation stage, and not in the derivation of the pressure distribution equation, as in Shaw's paper.

An error of omission in the energy equation above was noted by Cope (10) who presented a complete mathematical analysis of the hydrodynamic bearing. Starting with the fundamental equations of flow, - a mass-continuity equation; a momentum or Navier-Stokes equation; and a very complete energy equation - Cope developed his thesis carefully, any simplifying assumptions being made only after consideration of the orders of magnitude of the terms involved. This author also arrived at two equations in pressure and temperature, the pressure equation being similar to that of Cameron and Wood, but the temperature equation differing by an amount dependent on the work done on an element of the lubricant by the pressure forces exerted by the surrounding fluid - omitted by Cameron and Wood. The difference is only important at higher values of pressure gradient.

In the present notation, Cope's equations are

$$\frac{\partial}{\partial x} \left\{ \rho h \left(1 - \frac{h^2}{6\nu u} \frac{\partial p}{\partial x} \right) \right\} - \frac{\partial}{\partial y} \left\{ \frac{\rho h^3}{6\nu u} \cdot \frac{\partial p}{\partial y} \right\} = 0$$

$$\left(1 - \frac{h^2}{6\nu u} \frac{\partial p}{\partial x} \right) \frac{\partial t}{\partial x} - \left(\frac{h^2}{6\nu u} \frac{\partial p}{\partial y} \right) \frac{\partial t}{\partial y} = \frac{2\nu u}{\rho \alpha h^2} \left\{ 1 + \frac{h^4}{12\nu^2 u^2} \left[\left(\frac{\partial p}{\partial x} \right)^2 + \left(\frac{\partial p}{\partial y} \right)^2 \right] \right\}$$

A simplified derivation of these equations follows in Section 2 of this Chapter. These equations are again too complicated for direct integration, and are solved by Cope for the case of a rectangular pad with no side leakage, with a simplified equation of state and law of viscosity

variation. Cope concludes that for successful lubrication, a wedging action is necessary and this may be achieved (1) geometrically, by decreasing the film thickness, or (2) thermally, by decreasing the oil density, in the direction of motion. The relative importance of these two "wedges" would depend on the particular application, the thermal wedge assuming importance under conditions of small film thickness, and when the lubricant had a small viscosity-temperature variation and a large coefficient of thermal expansion.

A similar solution, but one derived in a practical rather than purely mathematical manner is that of Osterle, Charnes and Saibel (11). The energy equation used by these authors was developed in a separate paper (12), and is identical to that of Cope. Again, the equations are evaluated for an infinite bearing only, and although some numerical values are given, correlation with experimental results would be difficult because of the "no side leakage" assumption.

From the foregoing analyses, it can be seen that while the "thermal wedge" effect is theoretically valid, it still remains to be demonstrated that theory and experiment can be correlated. In order to do this, the effect of side leakage, previously neglected for convenience in integration, must be taken into account. Only by so doing can the load-carrying capacity, coefficient of friction, film thickness and other operating characteristics of a sector pad bearing - the usual practical type - be calculated.

It should perhaps be noted at this point that while this thesis is concerned essentially with the phenomenon of the thermal wedge and

its analysis, the author is not proposing that a parallel surface bearing operating on a thermal wedge principle is a practical proposition - at least not in the normal operating range of plain thrust bearings. In addition, the effect of viscosity-temperature variation has been minimized, not because of lack of importance, but in order to clarify the density-temperature relationship. Recent analyses by Zienkiewicz (13) and Cameron (14) indicate that the variation of viscosity in a high speed bearing is possibly more important than the density variation.

II. 2. Governing Equations of Lubrication between Parallel Surfaces

The following analysis concerns the steady flow of an incompressible viscous fluid between parallel plates, which are moving relative to one another at a speed high enough that density variations become important. Under these conditions, there are two equations governing the flow; the first is a general expression of the well-known Reynolds equation, in which the variation of density is included; and the second is an energy equation, expressing the constancy of energy in the fluid. The equations are briefly re-developed below for the sake of continuity, in a rather less formal manner than is mathematically proper.

Referring to Fig. 4a, since 'h' is small, it is reasonable to assume:-

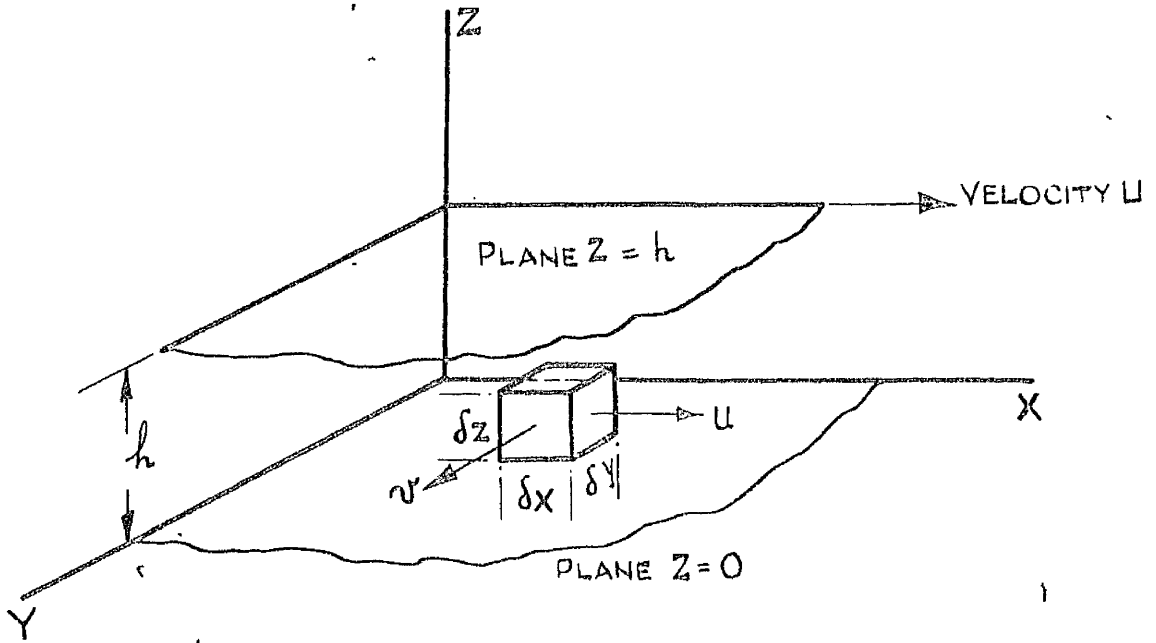
1. That variations of the variables, except velocity are not important in the Z direction.
i.e. $p, \rho, t, \nu,$ are functions of x and y only.
2. That velocity gradients are important only in the Z direction.

$$\frac{\partial u}{\partial z} \gg \frac{\partial u}{\partial x} \quad \text{and} \quad \frac{\partial v}{\partial z} \gg \frac{\partial v}{\partial y}$$

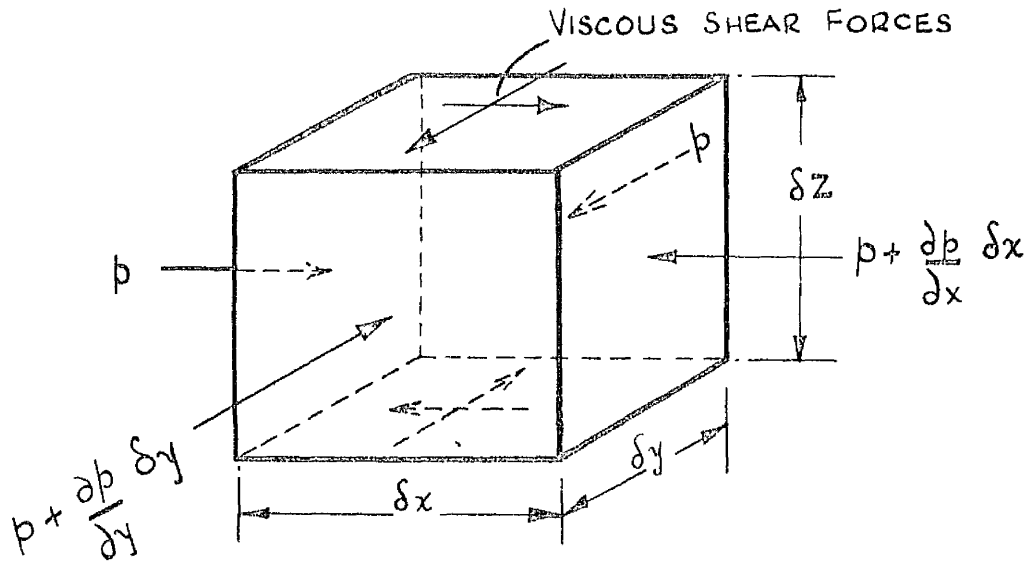
3. That the fluid velocity in the Z direction is negligible.

$$w = 0$$

Consider a small rectangular element of fluid $\delta x, \delta y, \delta z$ as in Fig. 4b.



4a. PARALLEL PLATES IN RELATIVE MOTION



4b. RECTANGULAR ELEMENT OF FLUID

The viscous shear forces on the lower face are

$$-\mu \frac{\partial u}{\partial z} \delta x \cdot \delta y \quad \text{and} \quad -\mu \frac{\partial v}{\partial z} \delta x \cdot \delta y$$

The corresponding forces on the upper face are

$$\mu \left(\frac{\partial u}{\partial z} + \frac{\partial^2 u}{\partial z^2} \delta z \right) \delta x \cdot \delta y \quad \text{and} \quad \mu \left(\frac{\partial v}{\partial z} + \frac{\partial^2 v}{\partial z^2} \delta z \right) \delta x \cdot \delta y$$

The algebraic sum of these forces plus a difference of fluid pressure forces = change in momentum of the element.

$$\left(\mu \frac{\partial^2 u}{\partial z^2} - \frac{\partial p}{\partial x} \right) \delta x \delta y \delta z = m \delta x \delta y \delta z \frac{du}{dt} \quad \dots (1)$$

and similar equations for the 'y' direction.

The momentum terms $m \frac{du}{dt}$ and $m \frac{dv}{dt}$ are small and can be neglected. (Cope, 10)

$$\left. \begin{aligned} \mu \frac{\partial^2 u}{\partial z^2} - \frac{\partial p}{\partial x} &= 0 \\ \mu \frac{\partial^2 v}{\partial z^2} - \frac{\partial p}{\partial y} &= 0 \end{aligned} \right\} \quad \dots (2)$$

Integrating

$$\left. \begin{aligned} u &= \frac{1}{\mu} \frac{\partial p}{\partial x} \left(\frac{1}{2} z^2 + A_1 z + A_2 \right) \\ v &= \frac{1}{\mu} \frac{\partial p}{\partial y} \left(\frac{1}{2} z^2 + B_1 z + B_2 \right) \end{aligned} \right\} \quad \dots (3)$$

since 'p' and ' μ ' are independent of 'z'.

Boundary conditions are

$$\left. \begin{array}{l} u = 0 \\ v = 0 \end{array} \right\} \text{ at } z = 0$$

∴ A_2 and B_2 are zero.

$$\text{and } \left. \begin{array}{l} u = U \\ v = 0 \end{array} \right\} \text{ at } z = h$$

$$\text{Thus } \left. \begin{array}{l} u = \frac{1}{\mu} \frac{\partial p}{\partial x} \left\{ \frac{1}{2} z^2 + z \left(\frac{\nu U}{h} \frac{\partial p}{\partial x} - \frac{h}{2} \right) \right\} \\ v = \frac{1}{\mu} \frac{\partial p}{\partial y} \left\{ \frac{1}{2} z^2 - \frac{1}{2} z h \right\} \end{array} \right\} \dots (4)$$

The volume of flow per unit width from $z = 0$ to $z = h$ will be

$$q_x = \int_0^h u \, dz \quad \text{and} \quad q_y = \int_0^h v \, dz$$

$$\text{Thus } \left. \begin{array}{l} q_x = -\frac{h^3}{12\mu} \frac{\partial p}{\partial x} + \frac{U h}{2} \\ q_y = -\frac{h^3}{12\mu} \frac{\partial p}{\partial y} \end{array} \right\} \dots (5)$$

Since the density variation is to be considered, the equation of mass continuity is used instead of the usual volume continuity.

$$\frac{\partial}{\partial x} (\rho \cdot q_x) + \frac{\partial}{\partial y} (\rho \cdot q_y) = 0 \quad \dots (6)$$

there being no flow in the Z direction.

Substituting for 'q' in equation (6) gives a general Reynolds equation

$$\frac{\partial}{\partial x} \left(\frac{\rho h^3}{12\mu} \frac{\partial p}{\partial x} \right) + \frac{\partial}{\partial y} \left(\frac{\rho h^3}{12\mu} \frac{\partial p}{\partial y} \right) = \frac{\partial}{\partial x} \left(\frac{\rho U h}{2} \right) \quad \dots (7)$$

which gives the pressure distribution through the bearing, provided that the variations of viscosity and density are known.

In order to obtain the correct temperature variation through the bearing, it is necessary to consider the exchange of energy in the fluid.

Cope (10) gives a complete energy equation whereby for a fluid element, the rate of decrease of internal energy and the work done by pressure in compressing the fluid is equated to the sum of the heat energy conducted away and the rate at which work is done against viscosity. It may be considered as implicit in assumption (1) above that the heat transfer from fluid to bearing surface is negligible. That is, the process is adiabatic and the heat developed by friction goes only to raise the temperature of the fluid. By comparing the relative magnitudes of the various terms in the energy equation for typical physical conditions, Cope shows that this adiabatic assumption is justifiable and reduces the equation to

$$J \rho \left(u \frac{\partial E}{\partial x} + v \frac{\partial E}{\partial y} \right) = \nu \left\{ \left(\frac{\partial u}{\partial z} \right)^2 + \left(\frac{\partial v}{\partial z} \right)^2 \right\} \dots (8)$$

where the internal energy above inlet conditions is $E = \sigma t$

Substituting values of velocities and velocity gradients from equation (4) and integrating across the film, the energy equation becomes

$$\begin{aligned} \sigma \rho J \left[\left(\frac{U h}{2} - \frac{1}{\nu} \frac{\partial p}{\partial x} \frac{h^3}{12} \right) \frac{\partial t}{\partial x} - \left(\frac{h^3}{12 \nu} \frac{\partial p}{\partial y} \right) \frac{\partial t}{\partial y} \right] \\ = \frac{h^3}{12 \nu} \left[\left(\frac{\partial p}{\partial x} \right)^2 + \left(\frac{\partial p}{\partial y} \right)^2 \right] + \frac{U^2 \nu}{h} \dots (9) \end{aligned}$$

The two equations obtained, equation (7) for pressure and equation (9) for temperature cannot be solved independently, since viscosity and density appearing in (7) are functions of temperature

mainly, and pressure terms appear in equation (9). For a complete solution these two equations must be solved simultaneously for p and t . This process would certainly prove laborious and it is doubtful if a solution of any practical value would be obtained by rigorous means.

However, an understanding of the behaviour of the thermal wedge can be obtained by making certain simplifying assumptions in the original equations; or by solving by means of a numerical method. Solutions thus obtained are presented in the following chapter.

CHAPTER III

- III. 1. Solution of Governing Equations for No Side Leakage.
- III. 2. Solution by a Relaxation Method.
- III. 3. General Solution taking account of Side Leakage.
- III. 4. Numerical Comparisons of the Three Solutions.
- III. 5. Friction in a Parallel Surface Bearing.
- III. 6. Summary of Theoretical Work.

CHAPTER III

Three solutions of the governing equations (7) and (9) are given here. Of these, solutions III. 1 and III. 2, while original in their application to this problem, owe a certain debt to the work of Osterle, Charnes and Saibel (11) and Christopherson (9) respectively. Solution III. 3 is quite new and so far as is known, is the first general solution of these equations to include the effect of side leakage.

III. 1. Solutions of Governing Equations for No Side Leakage.

The simplest solution is obtained by assuming an infinitely wide bearing, in which there is no side leakage, i.e. all variations with respect to 'y' can be neglected. The equations then become

$$\frac{d}{dx} \left[\rho \left(\frac{Uh}{2} - \frac{h^3}{12\nu} \frac{dp}{dx} \right) \right] = 0 \quad \dots (10)$$

and

$$\rho \propto \int \left[\frac{Uh}{2} - \frac{h^3}{12\nu} \frac{dp}{dx} \right] \frac{dt}{dx} = \frac{h^3}{12\nu} \left[\frac{dp}{dx} \right]^2 + \frac{U^2 \mu}{h} \quad \dots (11)$$

Integrating equation (10)

$$\rho \frac{Uh}{2} - \frac{\rho h^3}{12\nu} \frac{dp}{dx} = A_3 \quad \dots (12)$$

At the point of maximum pressure $\frac{dp}{dx} = 0$ and $\rho = \rho_m$

Hence
$$A_3 = \rho_m \frac{Uh}{2}$$

and
$$\frac{1}{\nu} \frac{dp}{dx} = \frac{6U}{h^2} \left(1 - \frac{\rho_m}{\rho} \right) \quad \dots (13)$$

Substituting this value of $\frac{dp}{dx}$ in equation (11) gives

$$\rho \sigma \int \left\{ \frac{uh}{2} - \frac{h^3}{12\nu} \left[\frac{6U\nu}{h^2} \left(1 - \frac{\rho_m}{\rho} \right) \right] \right\} \frac{dt}{dx}$$

$$= \frac{h^3}{12\nu} \left\{ \frac{36U^2\nu^2}{h^4} \left(1 - \frac{\rho_m}{\rho} \right)^2 \right\} + \frac{U^2\nu}{h}$$

which becomes after simplification

$$\frac{1}{\nu} \frac{dt}{dx} = \frac{2U}{h^2 \sigma \rho_m} \left[1 + 3 \left(1 - \frac{\rho_m}{\rho} \right)^2 \right] \quad \dots (14)$$

Now consider the variations of viscosity and density with pressure and temperature. The pressures encountered in a bearing of this type are comparatively low, and so it is permissible to take μ and ρ as functions of t only. The laws of variation are derived from standard tables of properties (15) for the oils used. Curves of viscosity/temperature and density/temperature are plotted (Fig. 5) and it is seen that to a good approximation, the viscosity variation is exponential and the density variation is linear over the range of temperature encountered in the experimental bearing. Thus the viscosity variation is taken as

$$\mu = \mu_0 e^{-\beta t} \quad \dots (15)$$

and the density variation

$$\rho = \rho_0 (1 - \lambda t) \quad \dots (16)$$

where β and λ are established for each oil used. Introducing these relationships into equations (13) and (14) and expanding according to the binomial theorem they become

$$\frac{dp}{dx} = -\mu_0 e^{-\beta t} \frac{6U}{h^2} \lambda (t - t_m) \quad \dots (17)$$

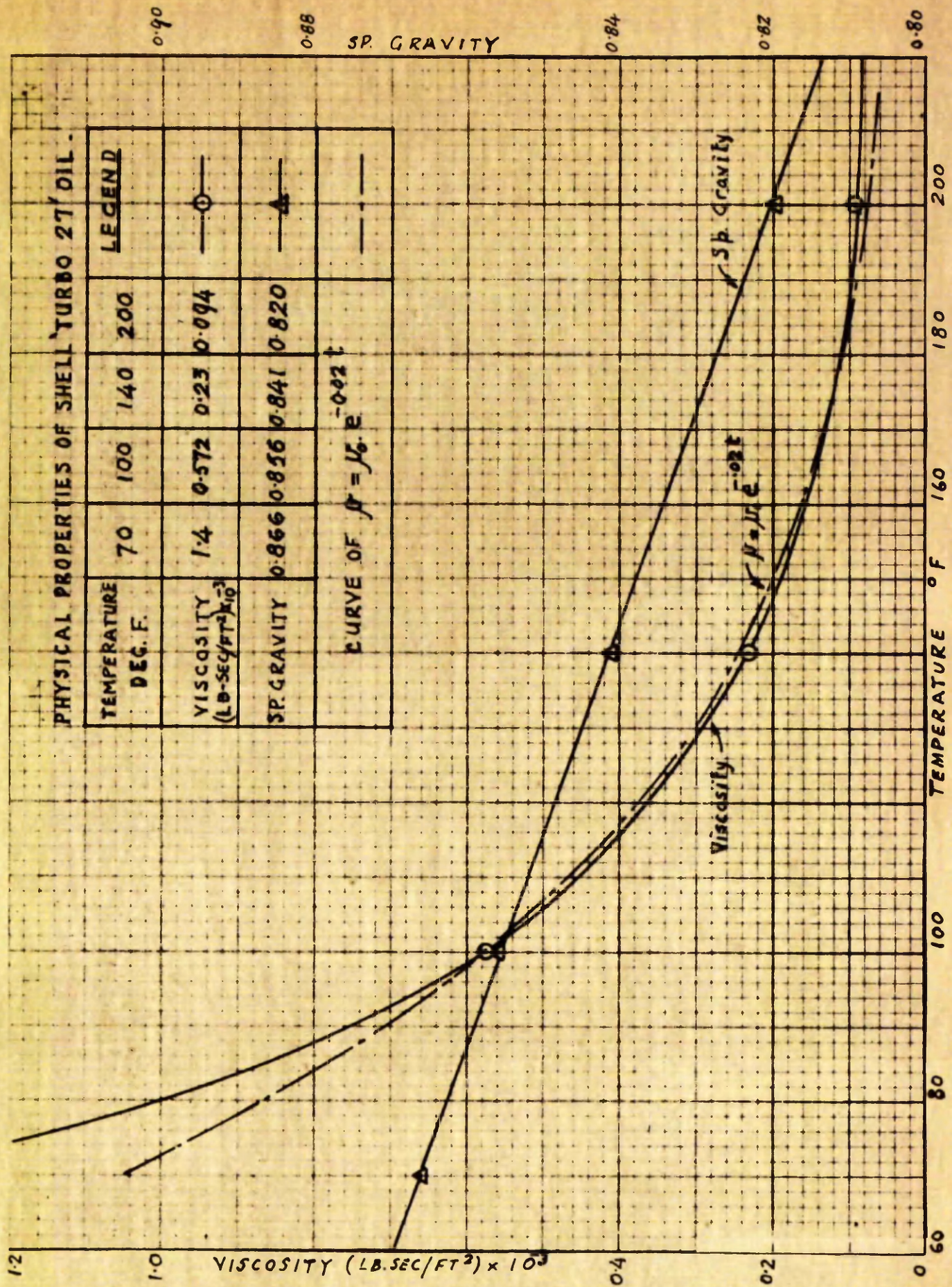


FIG. 5 VARIATION OF VISCOSITY AND SPECIFIC GRAVITY OF SHELL 'TURBO 27'.

and

$$e^{\beta t} \frac{dt}{dx} = \frac{2 U \nu_0}{h^2 \sigma J \rho_m} \quad \dots (18)$$

having neglected terms containing λ^2 and higher powers, since λ is small

Equation (18) can be integrated thus :

$$\frac{1}{\beta} \frac{d}{dx} (e^{\beta t}) = \frac{2 U \nu_0}{h^2 \sigma J \rho_m} \quad \dots (19)$$

Hence

$$e^{\beta t} = G_1 x + A_4 \quad \dots (20)$$

where

$$G_1 = \frac{2 U \nu_0 \beta}{h^2 \sigma J \rho_m}$$

and $t = 0$ at $x = 0$

$$\therefore A_4 = 1$$

$$t = \frac{1}{\beta} \ln (G_1 x + 1) \quad \dots (21)$$

Substituting this value of t in the pressure equation (17)

$$\frac{dp}{dx} = \frac{-\nu_0}{G_1 x + 1} \frac{6 U \lambda}{h^2 \beta} \ln \left(\frac{G_1 x + 1}{G_1 x_m + 1} \right) \quad \dots (22)$$

Integrate by substituting $y = G_1 x + 1$, $\frac{dy}{dx} = G_1$

$$\text{let } G_2 = \frac{6 \nu_0 U \lambda}{h^2 \beta}$$

$$p = -G_2 \int \frac{\ln y}{y} \frac{1}{G_1} dy + G_2 \int \frac{\ln(G_1 x_m + 1)}{y} \frac{1}{G_1} dy$$

$$p = -\frac{G_2}{G_1} \left\{ \frac{[\ln(G_1 x + 1)]^2}{2} - \ln(G_1 x_m + 1) \ln(G_1 x + 1) \right\} + A_5 \quad \dots (23)$$

At $x = x_m$, $p = p_m$

$$\therefore A_5 = p_m - \frac{3 U \nu_0 \lambda}{h^2 \beta G_1} [\ln(G_1 x_m + 1)]^2$$

$$p = p_m - \frac{3 U \nu_0 \lambda}{h^2 \beta G_1} \left[\ln \left(\frac{G_1 x + 1}{G_1 x_m + 1} \right) \right]^2 \quad \dots (24)$$

$$p = p_m - \frac{3}{2} \lambda \sigma J \rho_m (t - t_m)^2$$

... (25)

End conditions are $p = 0$ at $x = 0, L$
i.e. $t = 0, t_L$

$$0 = p_m - \frac{3}{2} \lambda \sigma J \rho_m (t_m)^2$$

and $0 = p_m - \frac{3}{2} \lambda \sigma J \rho_m (t_L - t_m)^2$

$$\therefore t_L = 2 t_m$$

... (26)

$$t_L = \frac{1}{\beta} \ln(G_1 L + 1)$$

... (27)

$$t_m = \frac{1}{2\beta} \ln(G_1 L + 1)$$

... (28)

and $p_m = \frac{3}{2} \lambda \sigma J \rho_m (t_m)^2$

... (29)

where $\rho_m = \rho_0 (1 - \lambda t_m)$

Substituting these values for t_m and p_m in equations (21) and (25) gives the evaluation of t and p . These equations are evaluated for a particular set of conditions in Section 4 of this chapter.

III. 2. Solution by a Relaxation Method

A rigorous solution of the two simultaneous equations in pressure and temperature being impracticable, the most accurate results are obtained by a numerical method. One such method is a relaxation process first applied to lubrication by Christopherson (9).

Consider the equations (7) and (9) in polar coordinates which refer to a sector pad, Fig. 6, with boundaries $\theta = 0$ and α , $r = r_0$ and r_1 .

The Reynolds equation becomes

$$\frac{\partial}{\partial \theta} \left(\frac{h^3 \rho}{\nu} \frac{\partial p}{\partial \theta} \right) + r \frac{\partial}{\partial r} \left(\frac{h^3 \rho}{\nu} r \frac{\partial p}{\partial r} \right) = 6 \omega^2 r^2 \frac{\partial}{\partial \theta} (\rho h) \quad \dots (30)$$

and the energy equation

$$\begin{aligned} J \rho \sigma \left\{ \left(\frac{\omega h}{2} - \frac{1}{r^2} \frac{h^3}{12\nu} \frac{\partial p}{\partial \theta} \right) \frac{\partial t}{\partial \theta} - \frac{h^3}{12\nu} \frac{\partial p}{\partial r} \frac{\partial t}{\partial r} \right\} \\ = \frac{h^3}{12\nu} \left\{ \left(\frac{\partial p}{\partial r} \right)^2 + \frac{1}{r^2} \left(\frac{\partial p}{\partial \theta} \right)^2 \right\} + \frac{\omega^2 r^2 \nu}{h} \quad \dots (31) \end{aligned}$$

These two equations are rendered suitable for computation by writing them in a non-dimensional form and transforming conformally the sector pad to a rectangle.

$$\text{Let } p = P \frac{6\nu_0 \omega \alpha r_0^2}{h^2} ; \quad \rho = D \rho_0 ; \quad \nu = M \nu_0$$

$$\text{Change the variables by putting } \theta = \Theta \alpha ; \quad r = r_0 e^{\alpha R} \quad \dots (32)$$

The equations then become

$$\frac{\partial}{\partial \Theta} \left(\frac{D}{M} \frac{\partial P}{\partial \Theta} \right) + \frac{\partial}{\partial R} \left(\frac{D}{M} \frac{\partial P}{\partial R} \right) = e^{2\alpha R} \frac{\partial D}{\partial \Theta} \quad \dots (33)$$

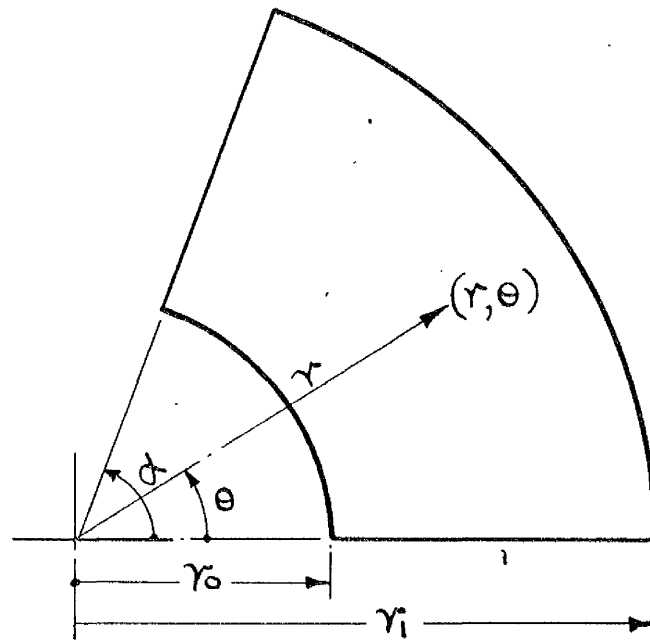


FIG. 6. SECTOR PAD OF CIRCULAR BEARING.

and

$$\left(1 - \frac{1}{M} e^{-2\alpha R} \frac{\partial P}{\partial \Theta}\right) \frac{\partial t}{\partial \Theta} - \left(\frac{1}{M} e^{-2\alpha R} \frac{\partial P}{\partial R}\right) \frac{\partial t}{\partial R} =$$

$$\left(\frac{6\nu_0 \omega \alpha r_0^2}{J \rho_0 \sigma h^2}\right) \frac{1}{D} \left\{ \frac{1}{M} \left[\left(\frac{\partial P}{\partial R}\right)^2 + \left(\frac{\partial P}{\partial \Theta}\right)^2 \right] e^{-2\alpha R} + \frac{M}{3} e^{2\alpha R} \right\} \quad \dots (34)$$

Equations (33) and (34) now refer to a rectangular pad with boundaries $\Theta = 0$ and 1 ,

$$R = 0 \text{ and } \frac{1}{\alpha} \ln \frac{r_1}{r_0}$$

Pressure Equation

Consider now the identity used by Christopherson (9) adapted to the present problem

$$\nabla^2 \left(\frac{D}{M} P \right) = P \nabla^2 \left(\frac{D}{M} \right) + \frac{D}{M} \nabla^2 P + 2 \frac{\partial}{\partial \Theta} \left(\frac{D}{M} \right) \frac{\partial P}{\partial \Theta} + 2 \frac{\partial}{\partial R} \left(\frac{D}{M} \right) \frac{\partial P}{\partial R} \quad \dots (35)$$

where the operator $\nabla^2 = \frac{\partial^2}{\partial \Theta^2} + \frac{\partial^2}{\partial R^2}$

Equation (35) can be written

$$\frac{\partial}{\partial \Theta} \left(\frac{D}{M} \right) \frac{\partial P}{\partial \Theta} + \frac{D}{M} \frac{\partial^2 P}{\partial \Theta^2} + \frac{\partial}{\partial R} \left(\frac{D}{M} \right) \frac{\partial P}{\partial R} + \frac{D}{M} \frac{\partial^2 P}{\partial R^2} = \frac{\partial D}{\partial \Theta} e^{2\alpha R} \quad \dots (36)$$

From (35) and (36) is obtained

$$\nabla^2 \left(\frac{D}{M} P \right) - 2 \frac{\partial D}{\partial \Theta} e^{2\alpha R} = P \nabla^2 \left(\frac{D}{M} \right) - \frac{D}{M} \nabla^2 P \quad \dots (37)$$

If w is any polynomial function, then the operator ∇^2 can be

expressed in a finite difference form by the equation

$$a^2 \nabla^2 w = \sum_n w - 4 w_c + \text{terms in } a^4 + \text{etc} \dots \dots \dots (38)$$

where the summation sign refers to four points equally spaced on a circle, radius 'a' with centre at point 'C', or to a grid covering the bearing thus:-

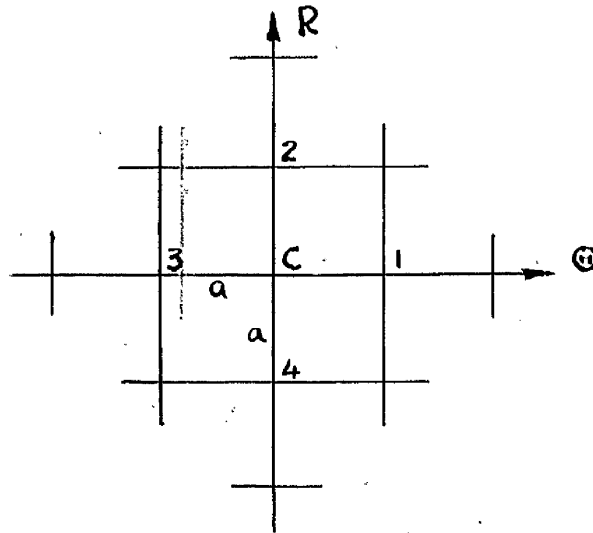


Fig. 7.

Substituting this expression in equation (37) gives

$$\sum_{n=1}^4 \left[\left(\frac{D}{M} \right)_n + \left(\frac{D}{M} \right)_c \right] P_n - P_c \sum_{n=1}^4 \left[\left(\frac{D}{M} \right)_n + \left(\frac{D}{M} \right)_c \right] = 2 a^2 \frac{\partial D}{\partial \Theta} e^{2\alpha R} \dots (39)$$

Equation (39) gives the pressure P_c at any points 'C' on the grid in terms of the four surrounding points 1, 2, 3, and 4. One equation of this type is obtained for each intersection of the grid, except at the boundaries where the pressure is specified as being zero, so that by solving this set of simultaneous equations, the complete pressure distribution is found. The relaxation method is suitable for this type of problem and has been fully described elsewhere (9, 19).

Briefly, any values are assumed initially for P at the various intersections and the 'residuals' F are computed.

$$F = \sum_1^4 \left[\left(\frac{D}{M} \right)_n + \left(\frac{D}{M} \right)_c \right] P_n - P_c \sum_1^4 \left[\left(\frac{D}{M} \right)_n + \left(\frac{D}{M} \right)_c \right] - 2a^2 \frac{\partial D}{\partial \alpha} e^{2\alpha R} \dots (40)$$

Next a diagram of the influence coefficients, defined by

$$\left. \begin{aligned} a_{cn} &= \left(\frac{D}{M} \right)_c + \left(\frac{D}{M} \right)_n \\ a_{cc} &= \sum_1^4 \left[\left(\frac{D}{M} \right)_n + \left(\frac{D}{M} \right)_c \right] \end{aligned} \right\} \dots (41)$$

is constructed (Fig. 8). The effect of any change ΔP on the residuals is then

$$\begin{aligned} - a_{cc} \Delta P & \text{ at each point which is altered} \\ + a_{cn} \Delta P & \text{ at each of the surrounding four points 'n' } \end{aligned}$$

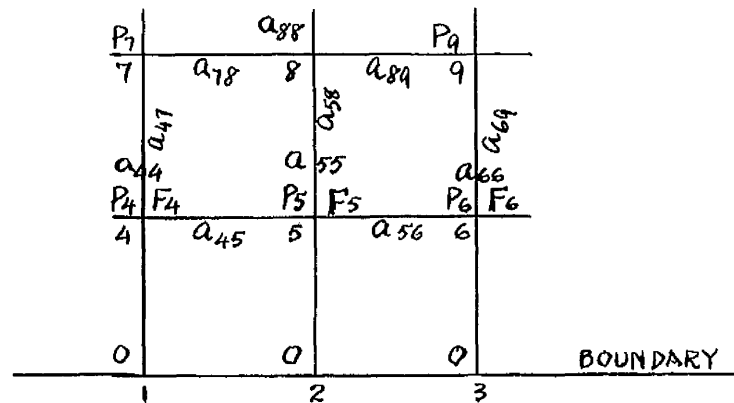


FIG. 8.

The assumed values of P are now 'relaxed,' i.e. the values are altered in such a way that the residuals are reduced to zero, or to a value which is considered negligible.

Energy Equation:

The energy equation (34) can be rewritten in a finite-difference form thus

$$\left(1 - \frac{e^{-2\alpha R}}{M_c} \frac{P_1 - P_3}{2a} \right) \frac{t_1 - t_3}{2a} - \left(\frac{e^{-2\alpha R}}{M_c} \frac{P_2 - P_4}{2a} \right) \frac{t_2 - t_4}{2a} = \frac{1}{D_c} \left\{ \frac{e^{-2\alpha R}}{M_c} \left[\left(\frac{P_1 - P_3}{2a} \right)^2 + \left(\frac{P_2 - P_4}{2a} \right)^2 \right] + \frac{M_c}{3} e^{2\alpha R} \right\} \frac{6\nu_0 \omega d r_0^2}{J \rho_0 \sigma h^2} \dots (42)$$

If the pressure distribution is known, the above equation is first applied to the inlet edge of the bearing, where M is unity. On this boundary, the approximation can be used that

$$\frac{t_1 - t_c}{a} = \left(\frac{\partial t}{\partial \theta} \right)_c$$

Using this approximation in equation (42) the temperatures at the first row of points are obtained. Thereafter equation (42) can be applied and temperatures on succeeding rows are found, working along the length of the bearing. According to Christopherson, no serious cumulative errors occur at the downstream end because any slight error in temperature, say on the high side, results in a decrease in viscosity, and a decrease in friction work, giving a consequent smaller temperature increment. The process seems to be inherently stable.

Equations Solved Simultaneously.

These finite difference equations (30) and (42) can be used individually to find one variable provided the other is known, i.e. if the temperature distribution is known, equation (39) gives the pressure, and if the pressure is known equation (42) gives the temperature. In order to solve the problem completely, the two systems must be compatible.

As a first approximation, the pressure distribution is taken as zero all over the bearing and the resulting temperature distribution is calculated, say t_1 . Corresponding to a temperature distribution t_1 , a pressure distribution P_1 is obtained by applying equation (39).

Using the new pressure P_1 a new temperature t_2 is evolved and from it, a pressure distribution P_2 . This process could be repeated indefinitely, but generally it is found that t_2 and P_2 are very close to the required solutions.

Load-Carrying Capacity.

The load carried by the sector pad is obtained by integrating the pressure over the area of the pad.

$$\begin{aligned} \text{Load } W \text{ per pad} &= \int_{r=r_0}^{r_1} \int_{\theta=0}^{\alpha} p \, dA \\ &= \int_{r_0}^{r_1} \int_0^{\alpha} p r \, d\theta \, dr \end{aligned} \quad \dots (43)$$

Changing the variables and limits of integration, using the transforms at the beginning of the section, the equation becomes

$$W = \frac{6\nu_0 \omega \alpha^3 r_0^4}{h^2} \int_{R=0}^{R_1} \int_{\theta=0}^{\theta_1} P e^{2\alpha R} \, d\theta \, dR. \quad \dots (44)$$

This may be integrated numerically over the equivalent rectangular pad by an application of Simpson's $\frac{1}{3}$ Rule, first in one direction and then the other.

For a uniform spacing 'a' in a square network, the load W' for the area is

$$W' = \frac{a^2}{9} \sum (k_n P_n e^{2\alpha R}) \quad \dots (45)$$

where ' k_n ' is a multiplying factor given in the following diagram:

	1	4	2	4	1
4		16	8	16	4
2		8	4	8	2
4		16	8	16	4
1		4	2	4	1

FIG. 9. Multiplying Factor for Numerical Integration

The value of W' may be found by dividing the equivalent rectangular bearing into suitable square areas, constructing for each area a table of values of $P_n e^{2\alpha R}$ for the grid intersections, multiplying by the appropriate k factor and making the summations.

III. 3. General Solution taking account of Side Leakage.

The effect of the side leakage in a parallel surface thrust bearing in which the film thickness is normally very small, may be quite considerable (Swift, 16). Although the relaxation solution (III.2) takes account of side leakage, a separate full calculation is required for every change in running conditions of each bearing, so that a great amount of computation would be required to obtain the overall pattern of behaviour for a bearing operating under thermal wedge conditions. It is desirable, therefore, to derive a general solution which takes account of flow in two directions even at the expense of making certain simplifications in other terms of the equations.

Consider then a sector pad of a circular bearing (Fig. 6) for which the governing equations in pressure and temperature are rewritten in polar co-ordination, as in Section III. 2.

$$\frac{\partial}{\partial \theta} \left(\frac{h^3 \rho}{\nu} \frac{\partial p}{\partial \theta} \right) + r \frac{\partial}{\partial r} \left(\frac{h^3 \rho}{\nu} r \frac{\partial p}{\partial r} \right) = 6 \omega r^2 h \frac{d\rho}{d\theta} \quad \dots (30)$$

$$\int \rho \sigma \left\{ \frac{\omega h}{2} \frac{dt}{d\theta} - \frac{h^3}{12\nu} \left(\frac{\partial p}{\partial r} \frac{dt}{dr} + \frac{1}{r^2} \frac{\partial p}{\partial \theta} \frac{dt}{d\theta} \right) \right\} \\ = \frac{h^3}{12\nu} \left[\left(\frac{\partial p}{\partial r} \right)^2 + \frac{1}{r^2} \left(\frac{\partial p}{\partial \theta} \right)^2 \right] + \frac{\omega^2 r^2 \nu}{h} \quad \dots (31)$$

It is necessary to make two simplifications:

1. Assume constant kinematic viscosity, $\frac{\nu}{\rho}$. This assumption cannot be justified physically as the variation of viscosity with temperature is an important factor in the performance of a thermal wedge bearing, but it is slightly more correct than the assumption of constant absolute viscosity, a common simplification made in numerous analyses (6; 17; etc.), since both ν and ρ vary with temperature in the same direction.

If the value of viscosity used is chosen correctly at some average figure for the bearing, the errors in pressure and load values predicted may be small, although the distribution patterns will be incorrect.

2. Assume no variation of density in the radial direction. This is fairly reasonable, since the temperature variation across the bearing is smaller than the variation around the bearing, as may be observed from the experimental results in Chapter V, and in Appendix I.

Pressure Distribution

The pressure equation (30) can now be written

$$\frac{h^3}{r^2} \frac{\partial^2 p}{\partial \theta^2} + r \frac{h^3}{r^2} \frac{\partial}{\partial r} \left(r \frac{\partial p}{\partial r} \right) = 6 \omega r^2 h \frac{\partial \rho}{\partial \theta} \quad \dots (46)$$

Then

$$\frac{\partial^2 p}{\partial \theta^2} + r \frac{\partial}{\partial r} \left(r \frac{\partial p}{\partial r} \right) = K r^2 g(\theta) \quad \dots (47)$$

where $K = \frac{6 \omega r}{h^2 \rho}$ and $g(\theta)$ is a function of

' θ ' only, since ρ is independent of r .

The boundary conditions are

$$p = 0 \text{ at } r = r_0 \text{ and } r_1$$

and $p = 0$ at $\theta = 0$ and α

This equation may be solved by use of a finite Fourier sine transform (Sneddon, 18)

By definition, let $\bar{p}_n = \int_0^\alpha p \sin\left(\frac{\pi n \theta}{\alpha}\right) d\theta$... (48)

Then $p = \frac{2}{\alpha} \sum_{n=1}^{\infty} \bar{p}_n \sin\left(\frac{\pi n \theta}{\alpha}\right)$... (49)

Multiply equation (47) by $\sin\left(\frac{\pi n \theta}{\alpha}\right)$ and integrate between the limits $\theta = 0$ and α .

$$\int_0^\alpha \frac{\partial^2 p}{\partial \theta^2} \sin\left(\frac{\pi n \theta}{\alpha}\right) d\theta + \int_0^\alpha r \frac{d}{dr} \left(r \frac{dp}{dr} \right) \sin\left(\frac{\pi n \theta}{\alpha}\right) d\theta = \int_0^\alpha K r^2 g(\theta) \sin\left(\frac{\pi n \theta}{\alpha}\right) d\theta$$

Consider the first term of the equation and integrate by parts.

$$\int_0^\alpha \frac{\partial^2 p}{\partial \theta^2} \sin\left(\frac{\pi n \theta}{\alpha}\right) d\theta = \left[\frac{\partial p}{\partial \theta} \sin\left(\frac{\pi n \theta}{\alpha}\right) \right]_0^\alpha - \frac{\pi n}{\alpha} \int_0^\alpha \frac{\partial p}{\partial \theta} \cos\left(\frac{\pi n \theta}{\alpha}\right) d\theta \quad \dots (50)$$

and $\sin\left(\frac{\pi n \theta}{\alpha}\right)$ and p are both zero at $\theta = 0$ and α

Therefore 1st Term = $-\frac{\pi n}{\alpha} \int_0^\alpha \frac{\partial p}{\partial \theta} \cos\left(\frac{\pi n \theta}{\alpha}\right) d\theta$

Integrate by parts again:- $-\left[\frac{\pi n}{\alpha} p \cos\left(\frac{\pi n \theta}{\alpha}\right) \right]_0^\alpha - \left(\frac{\pi n}{\alpha}\right)^2 \int_0^\alpha p \sin\left(\frac{\pi n \theta}{\alpha}\right) d\theta$

1st Term = $-\left(\frac{\pi n}{\alpha}\right)^2 \bar{p}_n$

Therefore Equation becomes

$$-\left(\frac{\pi n}{\alpha}\right)^2 \bar{p}_n + r \frac{d}{dr} \left(r \frac{d}{dr} \bar{p}_n \right) = K r^2 \bar{g}_n \quad \dots (51)$$

where

$$\bar{g}_n = \int_0^\alpha g(\theta) \sin\left(\frac{\pi n \theta}{\alpha}\right) d\theta \quad \dots (52)$$

Solving for \bar{p}_n the complementary function is

$$\bar{p}_n = r^k \quad \text{where } k = \pm \left(\frac{\pi n}{\alpha}\right)$$

and the particular integral is $\bar{p}_n = C_n \cdot r^2$

where C_n is found to be

$$\frac{K \bar{g}_n}{4 - (\frac{\pi n}{\alpha})^2}$$

Hence the solution is

$$\bar{p}_n = A_n r^{\frac{\pi n}{\alpha}} + B_n r^{-\frac{\pi n}{\alpha}} + \frac{K \bar{g}_n}{4 - (\frac{\pi n}{\alpha})^2} r^2 \quad \dots (53)$$

provided that $(\frac{\pi n}{\alpha})^2 \neq 4$.

$\bar{p}_n = 0$ when $p = 0$, i.e. at $r = r_0$ and r_1

hence A_n and B_n can be evaluated.

Thus

$$\bar{p}_n = \frac{K \bar{g}_n}{4 - (\frac{\pi n}{\alpha})^2} \left[\left(\frac{r_0^{\frac{2+\frac{\pi n}{\alpha}}{\alpha}} - r_1^{\frac{2+\frac{\pi n}{\alpha}}{\alpha}}}{r_1^{\frac{2\pi n}{\alpha}} - r_0^{\frac{2\pi n}{\alpha}}} \right) r^{\frac{\pi n}{\alpha}} + \left(\frac{r_0^{\frac{2-\frac{\pi n}{\alpha}}{\alpha}} - r_1^{\frac{2-\frac{\pi n}{\alpha}}{\alpha}}}{r_1^{\frac{-2\pi n}{\alpha}} - r_0^{\frac{-2\pi n}{\alpha}}} \right) r^{-\frac{\pi n}{\alpha}} + r^2 \right] \quad \dots (54)$$

This expression can be evaluated for any point on the bearing summing from $n = 1$ to $n = \infty$ provided \bar{g}_n is known,

$$\bar{g}_n = \int_0^\alpha g(\theta) \sin\left(\frac{n\pi\theta}{\alpha}\right) d\theta$$

and

$$g(\theta) = \frac{\partial \rho}{\partial \theta}$$

The density ρ is in reality a function of temperature mainly; but the temperature increase through the bearing is almost linear, (Cameron and Wood, 8) so a reasonable approximation is:

$$\rho = \rho_0 (1 + b\theta) \quad \dots (55)$$

Therefore $g(\theta) = \rho_0 b = \text{constant.}$

Then

$$\begin{aligned} \bar{g}_n &= \int_0^\alpha \rho_0 b \sin\left(\frac{n\pi\theta}{\alpha}\right) d\theta \\ &= \rho_0 b \left[\frac{-\cos n\pi + 1}{\frac{n\pi}{\alpha}} \right] \end{aligned} \quad \dots (56)$$

$$\bar{g}_n = 0 \quad \text{if } n \text{ is even}$$

$$\bar{g}_n = \frac{2\rho_0 b \alpha}{\pi n} \quad \text{if } n \text{ is odd.}$$

Hence for any point on the bearing, the pressure 'p' can be found

by Eq. (46).
$$p = \frac{2}{\alpha} \sum_1^\infty \bar{p}_n \sin\left(\frac{n\pi\theta}{\alpha}\right)$$

In practice the series is rapidly convergent, and 'p' may be evaluated by summing the first four or five terms only.

Load-Carrying Capacity.

Equation (46) establishes the value of the pressure at any point on a sector pad of a plane-surface bearing. The load carried by the pad is obtained by integrating this expression over the sector area.

$$\begin{aligned} \text{Load } W \text{ per pad} &= \int_{r_0}^{r_1} \int_0^\alpha p r \, d\theta \, dr \\ &= \int_{r_0}^{r_1} \int_0^\alpha r \frac{2}{\alpha} \sum_1^\infty \bar{P}_n \sin\left(\frac{n\pi\theta}{\alpha}\right) d\theta \, dr \end{aligned} \quad \dots (57)$$

and \bar{P}_n is independent of θ

$$\begin{aligned} \text{load } W \text{ per pad} &= \int_{r_0}^{r_1} r \frac{2}{\alpha} \sum_1^\infty \bar{P}_n \frac{-\alpha}{n\pi} \left[\cos \frac{n\pi\theta}{\alpha} \right]_0^\alpha dr \end{aligned} \quad \dots (58)$$

$$\begin{aligned} &= -\frac{2}{n\pi} \int_{r_0}^{r_1} r \sum_1^\infty \bar{P}_n (\cos n\pi - 1) dr \\ &= \left. \begin{aligned} &= 0 && \text{for 'n' even} \\ &= \int_{r_0}^{r_1} \frac{4}{n\pi} r \sum_1^\infty \bar{P}_n dr && \text{for 'n' odd.} \end{aligned} \right\} \quad \dots (59) \end{aligned}$$

Substituting for \bar{P}_n from equation (54), and integrating

$$\begin{aligned} W \text{ per pad} &= \frac{4}{n\pi} \frac{K \bar{q}_n}{4 - \left(\frac{n\pi}{\alpha}\right)^2} \left\{ \frac{1}{\frac{n\pi}{\alpha} + 2} \left(\frac{r_0^{2 + \frac{n\pi}{\alpha}} - r_1^{2 + \frac{n\pi}{\alpha}}}{r_1^{\frac{2n\pi}{\alpha}} - r_0^{\frac{2n\pi}{\alpha}}} \right) \left(r_1^{\frac{n\pi}{\alpha} + 2} - r_0^{\frac{n\pi}{\alpha} + 2} \right) + \right. \\ &\quad \left. + \frac{1}{-\frac{n\pi}{\alpha} + 2} \left(\frac{r_0^{2 - \frac{n\pi}{\alpha}} - r_1^{2 - \frac{n\pi}{\alpha}}}{r_1^{-\frac{2n\pi}{\alpha}} - r_0^{-\frac{2n\pi}{\alpha}}} \right) \left(r_1^{2 - \frac{n\pi}{\alpha}} - r_0^{2 - \frac{n\pi}{\alpha}} \right) + \frac{r_1^4 - r_0^4}{4} \right\} \end{aligned}$$

$$\text{Let } \frac{r_1}{r_0} = R_1$$

$$W \text{ per pad} = \frac{48 \omega \mu_0 b \alpha r_0^4}{\pi^2 h^2} \sum_1^\infty \frac{1}{n^2 [4 - \left(\frac{n\pi}{\alpha}\right)^2]} \left[\frac{R_1^4 - 1}{4} - \frac{(R_1^2 - R_1^{-\frac{n\pi}{\alpha}})^2}{\left(\frac{n\pi}{\alpha} + 2\right)(1 - R_1^{\frac{2n\pi}{\alpha}})} - \frac{(R_1^{\frac{n\pi}{\alpha}} - R_1^{-\frac{n\pi}{\alpha}})^2}{\left(\frac{n\pi}{\alpha} - 2\right)(R_1^{\frac{2n\pi}{\alpha}} - 1)} \right] \quad (60)$$

This summation also converges rapidly and can easily be evaluated by taking the first four or five values of 'n'.

Temperature Distribution

Simplifications may be made in the energy equation (31), using the method of Cope (10), by assuming a representative set of conditions for a high speed bearing and examining the orders of magnitude of the individual terms. The values employed are taken from the experimental work of this thesis, and from Kettleborough (4). For a light lubricating oil the density is about 50 lb/ft³, specific heat 0.5 and viscosity 0.0005 lb.sec/ft² at 100°F. A bearing of mean radius 1 in. with 1 in. breadth of pad, angular velocity 1000 rad/sec and film thickness 0.0005 is reasonable. For such a bearing, the pressure will be in the order of 100 lb/in² (Kettleborough, 4) and the pressure gradients $\frac{\partial p}{\partial r}$ and $\frac{\partial p}{\partial \theta}$ will not exceed 10⁶ and 10⁵ respectively in ft. lb. units. Thus, evaluating approximately equation (31) to obtain an order of magnitude equation

$$\rho \alpha \left\{ \left[\frac{\omega h}{2} - \frac{h^3}{12\nu r^2} \frac{\partial p}{\partial \theta} \right] \frac{\partial t}{\partial \theta} - \left[\frac{h^3}{12\nu} \frac{\partial p}{\partial r} \right] \frac{\partial t}{\partial r} \right\} = \frac{h^3}{12\nu} \left[\left(\frac{\partial p}{\partial r} \right)^2 + \frac{1}{r^2} \left(\frac{\partial p}{\partial \theta} \right)^2 \right] + \frac{\omega^2 r^3 \nu}{h}$$

$$2 \times 10^4 \left\{ \left[10^{-2} - 2 \times 10^4 \right] \frac{\partial t}{\partial \theta} - 10^{-5} \frac{\partial t}{\partial r} \right\} \approx 10^{-11} \left[10^{12} + 10^{12} \right] + 10^5 \dots (61)$$

It can be seen that the terms containing $\left(\frac{\partial p}{\partial r} \right)^2$ and $\left(\frac{\partial p}{\partial \theta} \right)^2$ are of the same order, 10¹, compared with 10⁵ for the other term on the right hand side of the equation, and thus they may be neglected with little loss of accuracy. Likewise, on the left hand side of the equation, the $\frac{\partial t}{\partial r}$ term, itself smaller than $\frac{\partial t}{\partial \theta}$, has a coefficient of 10⁻⁵ compared to a coefficient of order 10⁻² for $\frac{\partial t}{\partial \theta}$ and it too can be neglected.

The effect of neglecting these terms is to reduce the theoretical temperatures and this may offset to some extent the initial assumption of adiabatic flow which tends to give a high temperature estimate.

Equation (31) now becomes

$$\frac{\partial t}{\partial \theta} = \frac{\omega^2 r^2 \nu}{h J \rho \sigma} \left\{ \frac{1}{\frac{\omega h}{2} - \frac{h^3}{12 \nu r^2} \frac{\partial p}{\partial \theta}} \right\} \dots (62)$$

and differentiating the value of 'p' from equation (49) with respect to θ gives

$$\frac{\partial p}{\partial \theta} = \frac{2}{\alpha} \sum_1^{\infty} \bar{p}_n \frac{n\pi}{\alpha} \cos\left(\frac{n\pi\theta}{\alpha}\right) \dots (63)$$

This is similar to the series for 'p' and may be easily evaluated for each point on the bearing, whence the equation (63) may be integrated numerically to give the temperature distribution.

III. 4. Numerical Comparisons of the Three Solutions

In order to obtain a clear comparison of the results of the foregoing three solutions, each in turn is applied to a bearing running under a set of arbitrarily chosen constant conditions. The bearing has the same dimensions as the experimental bearing of Chapter IV, and the oil is Shell Turbo 27 as used in the experimental work. These were taken purely for convenience and for ease of comparing theoretical and practical results in later chapters. The running conditions are arbitrary, but chosen within the range of corresponding experimental values.

Running conditions and bearing dimensions are as follows:

- A. Inlet temperature = 100°F
 Rotational Speed = 10,000 rpm
- B. Parallel-surface sector thrust bearing having
- (a) four pads, and
 - (b) two pads.
- Inner diameter: (a) = 1.44"
 (b) = 1.40"

The slight difference in the inner diameters is necessary to obtain integral networks in the conformal transformations used later in the relaxation method evaluation.

- Outer diameter: (a) = 3.0"
 (b) = 3.0"

Radial oil grooves: 1/8" wide

Included angle of a sector, α :

$$(a) = 1.465 \text{ rads.}$$

$$(b) = 3.04 \text{ rads.}$$

Film thickness $h = 0.001$ " in both cases.

C. Shell 'Turbo 27' Lubrication Oil.

From Fig. 5.

The Viscosity-Temperature relationship

is

$$\mu = \mu_0 e^{-\beta t}$$

where

$$\beta = 0.02$$

The Density-Temperature relationship

is

$$\rho = \rho_0 (1 - \lambda t)$$

where

$$\lambda = 0.00043.$$

Initial Viscosity: $\mu_0 = 0.572 \times 10^{-3} \text{ lb. sec/ft}^2$

Initial Density: $\rho_0 = 53.41 \text{ lb/ft}^3$

Specific Heat: $\sigma = 0.45$

The Specific Heat, Density, Joules' Equivalent and Viscosity are in consistent units.

1. Solution III. 1 - No Side Leakage.

The solution which postulates no side leakage cannot be applied directly to a circular bearing since the derivation is in Cartesian coordinates for an infinitely wide pad. However, a first approximation to the temperature and pressure along the central arc (i.e. at the mean radius) of the bearing may be obtained by ignoring all acceleration and other radial effects, and, "Straightening" this arc along the "X" direction, taking the length of the bearing as: (included angle \times mean radius)

(a) Four Pad Bearing

The value taken for the "mean" radius is that obtained from Solution III. 2, the relaxation method - again this value is chosen to facilitate comparison.

$$\text{Mean Radius } r_m = 1.04''$$

$$\text{Included angle } \alpha = 1.465 \text{ rad.}$$

Length of central arc of pad

$$L = r \alpha = 1.52''$$

The parameter $G_1 = \frac{2 U N_0 \beta}{h^2 \sigma J \rho_0} \frac{\rho_0}{\rho_m}$ is evaluated, (Eq. 20).

The correct value of ρ_m cannot be determined until the temperature t_m is found. An initial value of G_1 is obtained by taking $\frac{\rho_0}{\rho_m} = 1$. From this value, say G_1^i , a value of ρ_m is obtained, from which the initial value of G_1^i may be adjusted. By successive adjustments, the correct value of G_1 may be obtained. It is found that only two adjustments are necessary in this case and G_1 is equal to 16.3

$$\text{The max. temp. } t_L = \frac{1}{\beta} \ln(G_1 L + 1) = 56.1^\circ\text{F from Eq. (27)}$$

$$\text{and } t_m = \frac{t_L}{2} = 28.05^\circ\text{F}$$

where t_m is the temperature at the point of maximum pressure.

$$\text{The general temperature } t = 50 \ln(16.3 x + 1)$$

The point at which maximum pressure occurs, X_m , is obtained from

$$t_m = \frac{1}{\beta} \ln(16.3 X_m + 1)$$

$$X_m = 0.56'' \text{ from the inlet edge.}$$

The maximum pressure

$$\begin{aligned} p_m &= \frac{3}{2} \lambda \sigma \rho_m J (t_m)^2 \\ &= 63.8 \text{ psi} \end{aligned}$$

And the general equation of pressure

$$\begin{aligned} p &= \frac{3}{2} \lambda \sigma \rho_m J \{ t (t_L - t) \} \\ &= 0.082 t (56.1 - t) \text{ psi} \end{aligned}$$

(b) Two Pad Bearing

Mean radius $r_m = 1.025''$

Included angle $\alpha = 3/04 \text{ rad.}$

Length of central arc of pad $L = 3.12''$

Parameter $G_{16} = 16.1$

$$t_L = \frac{1}{\beta} \ln(16.1 L + 1) = 82.5^\circ\text{F}$$

$$t_m = \frac{t_L}{2} = 41.25^\circ\text{F}$$

And the general equation for temperature is

$$t = 50 \ln(16.1 x + 1) .^\circ\text{F}$$

$$X_m = 0.95'' \text{ from the inlet edge.}$$

Maximum pressure $p_m = 139 \text{ psi.}$

General equation of pressure,

$$p = 0.0816 t (81.6 - t) \text{ psi}$$

The general equations are evaluated and curves showing the pressure and temperature for four-pad and two-pad bearings along the central arc are shown in Fig. 10.

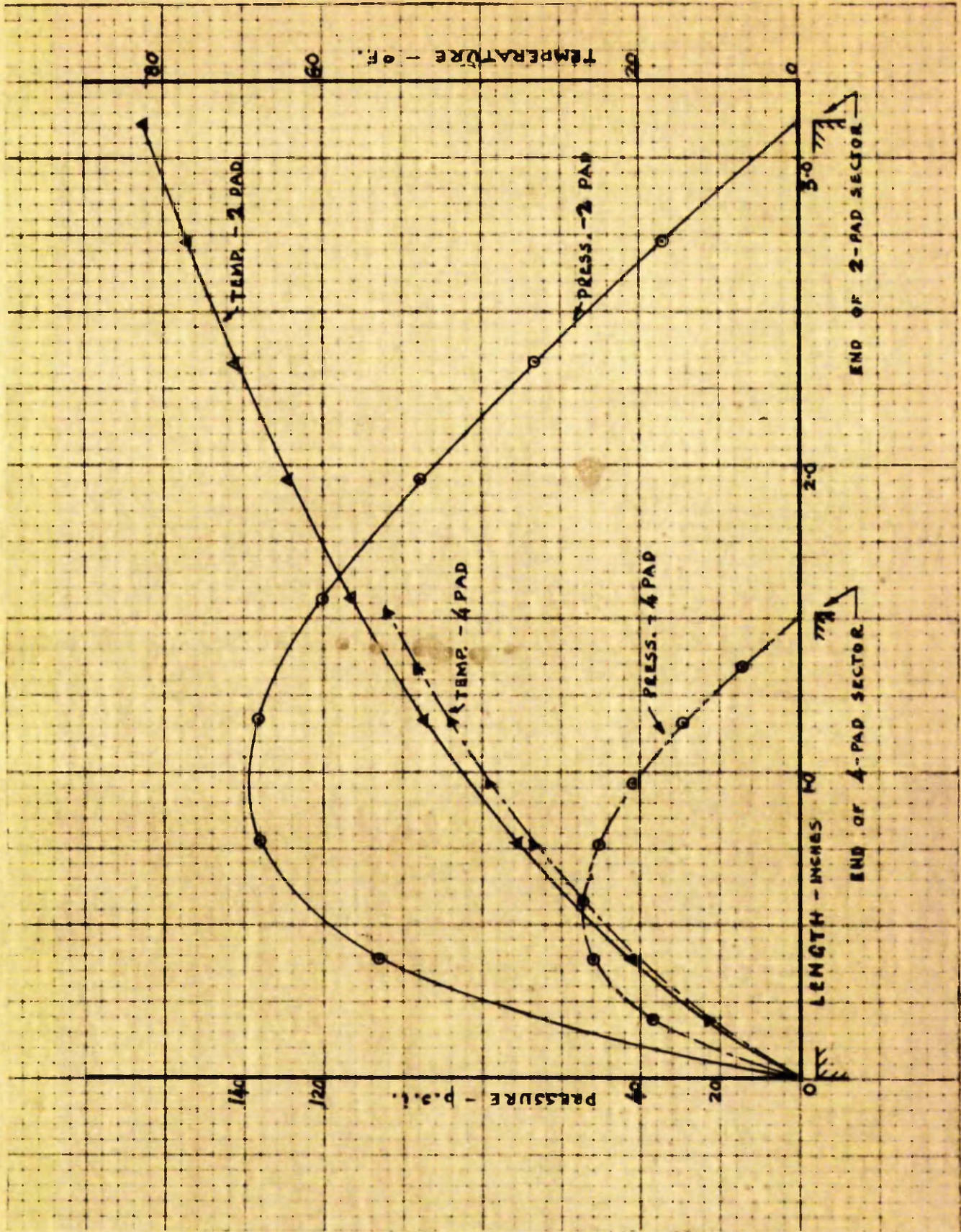


FIG.10 PRESSURE AND TEMPERATURE DISTRIBUTION FOR CASE OF NO SIDE LEAKAGE.

2. Solution III. 2 - Relaxation Method

Before the relaxation method of solution can be applied to a circular pad bearing, the variables θ and r must be changed to non-dimensional variables Θ and R , by using the transformations

$$\theta = \alpha \Theta \quad \text{and } r = r_0 e^{\frac{R}{\alpha}}$$

whereupon the sector pads, with boundaries:

$$\theta = 0 \text{ and } \alpha, \quad \text{and } r = r_0 \text{ and } r_1$$

become rectangular, with boundaries:

$$\Theta = 0 \text{ and } 1, \quad \text{and } R = 0 \text{ and } \frac{1}{\alpha} \ln \frac{r_1}{r_0}$$

For the four-pad bearing:

$$\text{Angle } \alpha = 84^\circ = 1.465 \text{ radians}$$

$$\text{Inner radius } r_0 = 0.72 \text{ in.}$$

$$\text{Outer radius } r_1 = 1.50 \text{ in.}$$

Rectangular boundaries are at

$$\Theta = 0 \quad \text{and} \quad 1.0$$

$$\text{and } R = 0 \quad \text{and} \quad \frac{1}{1.465} \ln \left(\frac{1.5}{0.72} \right) = 0.5$$

which gives a rectangular area which can be divided into an integral number of squares of side $a = 0.125$ (Fig. 11b).

For the two-pad bearing:

$$\text{Angle } \alpha = 174^\circ = 3.04 \text{ radians}$$

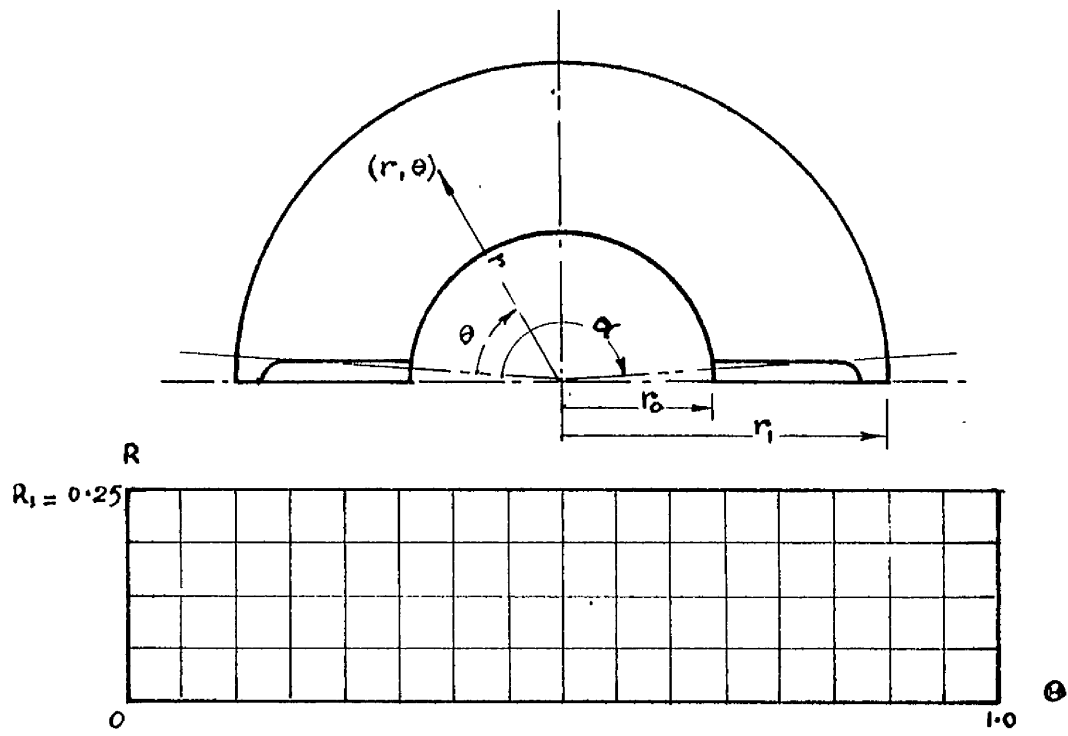
$$r_0 = 0.70 \text{ in.}$$

$$r_1 = 1.50 \text{ in.}$$

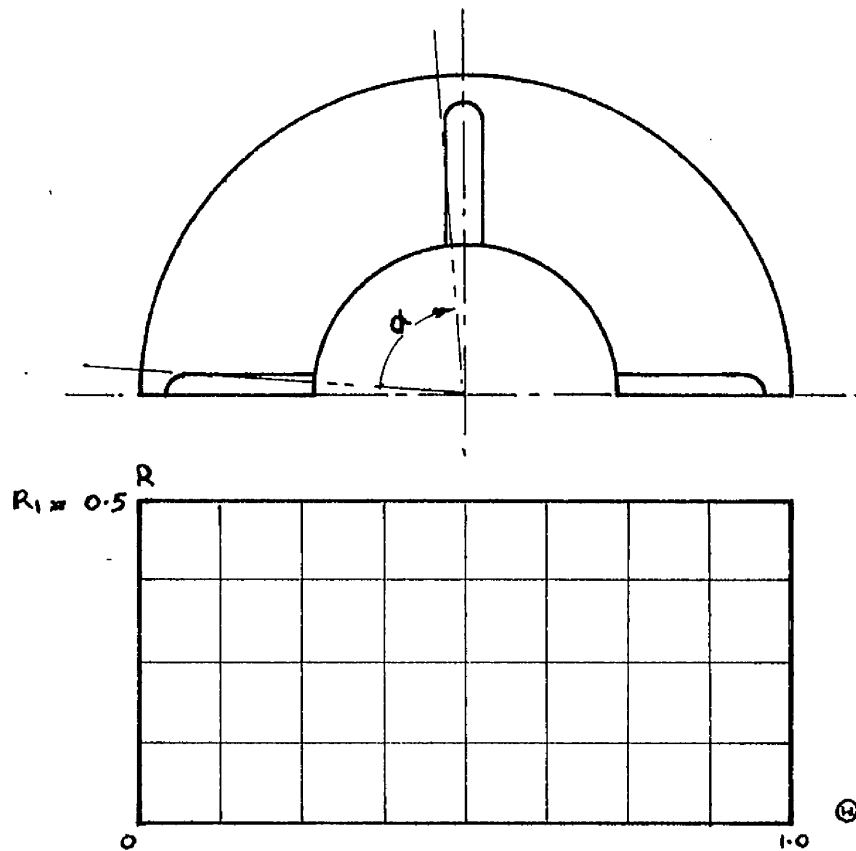
Rectangular boundaries are at

$$\Theta = 0 \quad \text{and} \quad 1.0$$

$$\text{and } R = 0 \quad \text{and} \quad \frac{1}{3.04} \ln \frac{1.5}{0.7} = 0.25$$



a) TWO PAD BEARING



b) FOUR PAD BEARING

FIG. 11 SECTOR PADS AND TRANSFORMATIONS.

which gives a rectangular area which can be divided into an integral number of squares of side $a = 0.0625$ (Fig. 11a). The evaluation is explained fully for the four-pad bearing. Only the final results, obtained by the same method, are given for the two-pad bearing.

a) Four-Pad Bearing

Temperature

The temperature distribution for the bearing pad is obtained first, from the finite difference equation (42)

$$\frac{t_1 - t_3}{2a} \left[1 - \frac{e^{-2\alpha R}}{M} \left(\frac{P_1 - P_3}{2a} \right) \right] - \left[\frac{e^{-2\alpha R}}{M} \left(\frac{P_2 - P_4}{2a} \right) \frac{t_2 - t_4}{2a} \right] = \frac{1}{D} \left\{ \frac{1}{M} \left[\left(\frac{P_1 - P_3}{2a} \right)^2 - \left(\frac{P_2 - P_4}{2a} \right)^2 \right] e^{-2\alpha R} + \frac{M e^{2\alpha R}}{3} \right\} \frac{6N_0 \omega a^2}{J \rho_0 \sigma}$$

referring to a point 'o', and the surrounding four intersections on a rectangular grid (Fig 11b).

For the bearing and running conditions specified at the beginning of Section III.4, the dimensional term is evaluated:

$$\frac{6N_0 \omega a^2 r_0^2}{J \rho_0 \sigma h^2} = 145 \text{ lb-ft-sec units}$$

An initial pressure distribution is assumed for the bearing, say $P = 0$ all over.

The temperature throughout the pad may now be obtained by a step-by-step application of equation (42) as follows:

Starting at the inlet edge, an approximation for the temperature gradient must be used for the first half grid-space, thus:

$$\frac{t_{\frac{1}{2}} - t_0}{a/2} = \left(\frac{\partial t}{\partial \theta} \right)_0$$

Since $P = 0$, Eq. (42) reduces to

$$t_{\frac{1}{2}} - t_0 = \frac{a}{2} \frac{1}{D_0} \frac{M_0}{3} e^{2\alpha R} \times 145$$

$$t_{\frac{1}{2}} = 3.02 e^{2\alpha R} \text{ deg F.}$$

which gives the temperatures at the half-space points of the first row.

Equation (42) can now be applied in full to give each succeeding row of temperatures until the bearing is covered, and the complete temperature distribution for zero pressure is obtained. (Fig. 12a)

Pressure.

From this temperature distribution ' t_1 ', the values of the "Residuals" F_c and the "Influence coefficients" a_{cn} and a_{cc} are respectively calculated for each intersection 'c' in terms of the four surrounding intersections 'n' of the grid.

From Equations (40) and (41)

$$F_c = \sum_{n=1}^4 \left[\left(\frac{D}{M} \right)_n + \left(\frac{D}{M} \right)_c \right] P_n - P_c \sum_{n=1}^4 \left[\left(\frac{D}{M} \right)_n + \left(\frac{D}{M} \right)_c \right] - 2 a^2 \frac{\partial D}{\partial \Theta} e^{2\alpha R}$$

$$\text{and } a_{cn} = \left(\frac{D}{M} \right)_n + \left(\frac{D}{M} \right)_c$$

$$a_{cc} = \sum_{n=1}^4 \left[\left(\frac{D}{M} \right)_n + \left(\frac{D}{M} \right)_c \right]$$

These values are entered on a skeleton grid, (Fig. 12b) following the convention shown in Fig. 8, Section III. 2. The effect of any change in pressure ΔP on the residuals is then:

$$-a_{cc} \Delta P \quad \text{at each point where the pressure is altered,}$$

$$+a_{cn} \Delta P \quad \text{at each of the surrounding four points 'n'.$$

The assumed values of $P = 0$ are now altered in such a way that the residuals are reduced to negligible values. (Fig. 12c).

Having obtained this pressure distribution, say $P = P_1$, a new temperature distribution $t = t_2$ corresponding to P_1 , can be calculated using Eq. (42) as above. (Fig. 12d).

0	131	20.18	35.4	46.23	56.55	63.48	72.05	75.78	83.85
0	9.05	15.25	27.0	36.45	44.7	51.25	57.75	63.14	68.45
0	6.28	11.13	20.2	27.93	34.7	40.73	45.95	51.02	55.7
0	4.36	8.0	14.9	21.08	26.5	31.66	35.85	40.35	43.77
0	3.02	5.66	10.6	15.49	19.48	23.77	27.09	30.91	33.59

TEMPERATURES AT GRID POINTS - DEG. FAHRENHEIT

FIG. 12A. FOUR PAD BEARING - EQUIVALENT RECTANGLE.
 $t = t_1$ TEMPERATURE DISTRIBUTION FOR $P = 0$.

10.64 .00432 2.55	13.55 .00352 3.16	16.52 .00281 3.77	19.46 .00240 4.38	22.29 .00225 5.00	25.15 .00188 5.57	27.99 .00169 6.18
9.92 .00229 2.41	11.90 .00189 2.82	13.87 .00161 3.21	15.91 .00141 3.64	17.95 .00130 4.05	19.94 .00120 4.48	21.99 .00104 4.95
9.38 .00116 2.51	10.74 .00102 2.83	12.03 .00991 3.16	13.44 .00081 3.49	14.77 .00074 3.83	16.28 .00067 4.24	17.86 .00061 4.56

INITIAL VALUES OF F_c , a_{cc} & a_{cn}

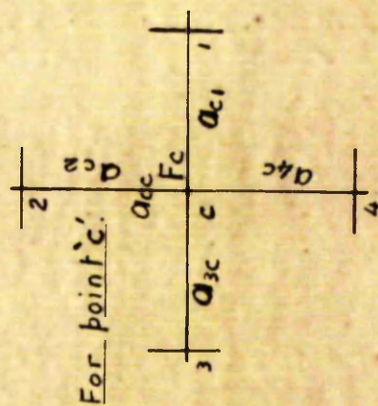


FIG. 12B FOUR PAD BEARING - EQUIVALENT RECTANGLE. RESIDUALS AND INFLUENCE COEFFICIENTS.

0	13.1	20.18	35.4	46.23	56.55	63.48	72.05	75.78	83.85
0	9.08	15.29	27.04	36.49	44.73	51.28	57.77	63.16	68.45
0	6.31	11.20	20.25	28.00	34.75	40.79	45.97	51.06	55.72
0	4.37	8.02	14.93	21.10	26.55	31.68	35.86	40.35	43.76
0	3.02	5.66	10.6	15.49	19.48	23.77	27.09	30.91	33.59

TEMPERATURES AT GRID POINTS - DEG. FAHRENHEIT

FIG. 12D. FOUR PAD BEARING - EQUIVALENT RECTANGLE.
TEMPERATURE DISTRIBUTION $t = t_2$ FOR $P = P_1$.

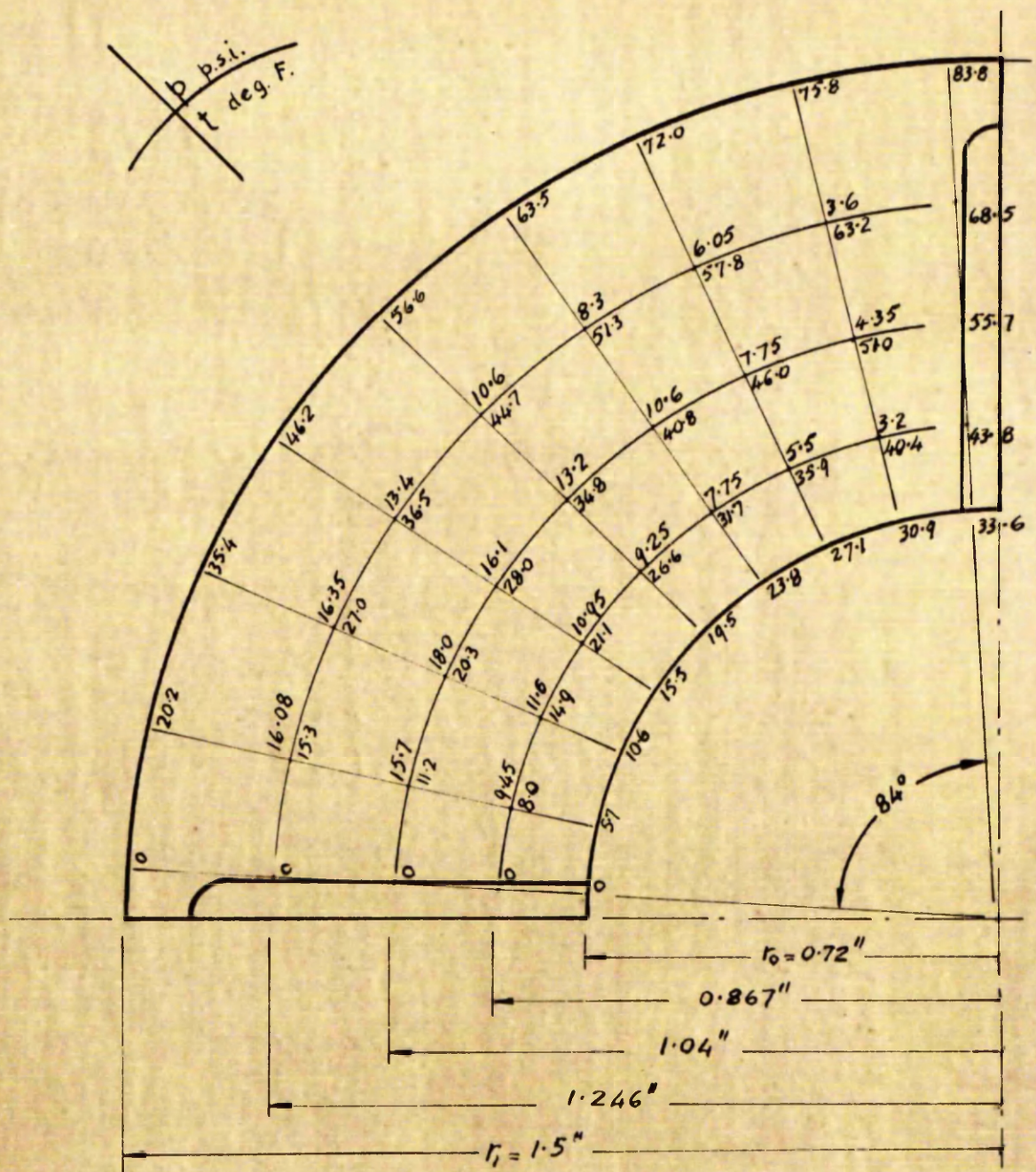


FIG. 12 E. FOUR PAD BEARING - SECTOR PAD
PRESSURE AND TEMPERATURE DISTRIBUTION.

From the temperature distribution $t = t_2$, a new pressure distribution $P = P_2$ may be found, and so on, until t and P are compatible.

However, it can be seen that temperature distributions t_1 and t_2 (Figs 12a and 12d) are very little different, since P_1 is quite small and the effect of the pressure on the temperature is negligible, so that $t = t_2$ and $P = P_1$, may be taken as final values in this case.

These pressures and temperatures on the equivalent rectangular pad may be transferred to corresponding points on the original sector pad, as shown in Fig. 12e. Pressures are obtained in psi units from the equation $p = P, \frac{6\nu_0 \omega \alpha^3 r_0^4}{h^2} \cdot 144 \text{ psi}$

Load-Carrying Capacity

The load per pad is given by Eq. (43).

$$W = \int_0^\alpha \int_{r_0}^{r_1} p r dr d\theta$$

whence $W = \frac{6\nu_0 \omega \alpha^3 r_0^4}{h^2} \int_0^1 \int_0^{R_1} P e^{2\alpha R} dR d\theta$

Integrate by dividing the rectangular pad into two equal square areas, 1 and 2, and applying Simpson's $\frac{1}{3}$ Rule in both the θ and R directions as in Section III.2 of this chapter.

$$W_1 = \frac{6\nu_0 \omega \alpha^3 r_0^4}{h^2} \frac{a^2}{9} \sum P e^{2\alpha R} K$$

$$= 36.6 (0.176)$$

$$W_2 = 36.6 (0.083)$$

$$W_1 + W_2 = 36.6 (0.176 + 0.083)$$

Therefore total load per pad $W = W_1 + W_2 = 9.43 \text{ lb.}$

Total load-carrying capacity of the bearing = 4×9.43
 $= 37.72 \text{ lb.}$

b) Two-Pad Bearing

A similar procedure to that for the four-pad bearing was followed for the two-pad bearing, and only the final temperature and pressure distributions are here shown (Figs. 13 a,b). Again, it was found unnecessary to go beyond the first temperature and pressure relaxation, since the effect of the low bearing pressures on the temperature distribution can be considered negligible.

Load-Carrying Capacity.

The two-pad sector is divided into four equal parts 1, 2, 3 and 4.

$$W_1 = \frac{6 \nu_0 \omega \alpha^3 r_0^4}{h^2} \frac{a^2}{9} \sum P e^{2\alpha R} k.$$

$$= 73.0 (0.0950)$$

$$W_2 = 73.0 (0.0555)$$

$$W_3 = 73.0 (0.0273)$$

$$W_4 = 73.0 (0.0124)$$

$$W \text{ per pad} = 73.0 (0.1902) = 13.85 \text{ lb.}$$

$$\text{Total load-carrying capacity} = 27.70 \text{ lb.}$$

136	208	36.1	47.7	57.5	65.3	72.6	78.5	84.3	89.0	94.0	97.7	102.0	105.1	109.0	111.6	115.1
93	15.5	27.4	37.2	45.4	52.5	58.7	64.3	69.3	73.9	77.7	81.9	85.5	88.9	92.1	95.1	97.9
6.35	11.2	20.4	28.3	35.0	41.1	46.4	51.3	55.8	59.9	63.7	67.2	70.5	73.6	76.5	79.3	81.9
4.36	8.0	14.85	21.0	26.4	31.4	35.8	40.0	43.7	47.4	50.4	53.9	56.5	59.7	61.9	64.9	66.8
3.0	5.6	10.65	15.3	19.5	23.5	27.0	30.5	33.5	36.7	39.3	42.3	44.5	47.3	49.2	51.8	53.5

TEMPERATURES AT GRID POINTS IN DEGREES FAHRENHEIT.

FIG. 13A. TEMPERATURE DISTRIBUTION FOR TWO-PAD BEARING SECTOR BY RELAXATION METHOD.

16.3	16.7	13.9	11.1	8.9	7.05	5.55	4.65	3.9	3.35	3.0	2.4	2.05	1.7	1.1
16.0	18.4	16.5	13.7	11.3	9.1	7.45	6.3	5.4	4.65	4.1	3.5	3.0	2.4	1.5
9.65	11.9	11.1	9.65	8.2	6.7	5.55	4.65	4.1	3.5	3.15	2.8	2.25	1.85	1.1

LUBRICANT PRESSURES AT GRID POINTS IN POUNDS PER SQ. INCH.

FIG. 13B PRESSURE DISTRIBUTION FOR TWO-PAD BEARING SECTOR
BY RELAXATION METHOD

3. Solution III.3 - Side Leakage taken into account

The general expression for the pressure at any point on the surface of a bearing sector is, from Eq. (49):

$$p = \frac{2}{\alpha} \sum_1^{\infty} \bar{p}_n \sin\left(\frac{n\pi}{\alpha} \theta\right)$$

and from Eq. (54)

$$\bar{p}_n = \frac{K \bar{g}_n}{4 - (\frac{n\pi}{\alpha})^2} \left[\left(\frac{r_0^{2 + \frac{n\pi}{\alpha}} - r_1^{2 + \frac{n\pi}{\alpha}}}{r_1^{\frac{2n\pi}{\alpha}} - r_0^{\frac{2n\pi}{\alpha}}} \right) r^{\frac{n\pi}{\alpha}} + \left(\frac{r_0^{2 - \frac{n\pi}{\alpha}} - r_1^{2 - \frac{n\pi}{\alpha}}}{r_1^{-\frac{2n\pi}{\alpha}} - r_0^{-\frac{2n\pi}{\alpha}}} \right) r^{-\frac{n\pi}{\alpha}} + r^2 \right]$$

Putting $r = \mathcal{R} r_0$ and $r_1 = \mathcal{R}_1 r_0$ and substituting the values of K and \bar{g}_n from Eqs. (47) & (56), this gives

$$p = Q \sum_1^{\infty} \frac{1}{n \left\{ \left(\frac{n\pi}{\alpha} \right)^2 - 4 \right\}} \left\{ \left(\frac{\mathcal{R}_1^2 - \mathcal{R}_1^{-\frac{n\pi}{\alpha}}}{\mathcal{R}_1^{\frac{n\pi}{\alpha}} - \mathcal{R}_1^{-\frac{n\pi}{\alpha}}} \right) \mathcal{R}^{\frac{n\pi}{\alpha}} + \left(\frac{\mathcal{R}_1^{\frac{n\pi}{\alpha}} - \mathcal{R}_1^2}{\mathcal{R}_1^{\frac{n\pi}{\alpha}} - \mathcal{R}_1^{-\frac{n\pi}{\alpha}}} \right) \mathcal{R}_1^{-\frac{n\pi}{\alpha}} - \mathcal{R}^2 \right\} \sin \frac{n\pi \theta}{\alpha}$$

$$p = Q \sum P' \quad \text{for } n = 1, 3, 5, 7 \dots \text{ etc.}$$

$$\text{where } Q = \frac{24 \omega \nu_0 b r_0^2}{h^2 \pi}$$

a) Four-Pad Bearing

To determine the value of 'b', the expansion coefficient related to bearing angle, it is necessary to know the temperature rise around the sector pad. It will be seen later in this chapter when values are compared that the temperatures obtained by Solution III.1 - (No Side Leakage) are quite accurate. Values of temperature calculated by this method at the mean radius $r_m = 1.04''$ are used to give a mean value for 'b'. Since the temperature rise around the bearing is almost linear,

$$\rho = \rho_0 (1 + b \theta) = \rho_0 (1 - \lambda t)$$

$$b = -0.00043 \frac{t}{\theta}$$

For the four-sector bearing, from Solution III.1, the temperature rise is $t_L = 56.1^\circ\text{F}$ for an included angle $\alpha = 1.465$ rads.

$$\text{Then } b = -0.0165$$

Hence, for the operating conditions already postulated, and using the initial value of viscosity $\nu_0 = 0.572 \times 10^{-3}$ lb.sec/ft².

$$Q = -271 \text{ in-lb-sec units.}$$

However, if an average value for viscosity is used, such as

$$\begin{aligned} \nu_{av} &= \frac{1}{t} \int_0^t \nu_0 e^{-\beta t} dt \\ &= 0.343 \times 10^{-3} \text{ lb.sec/ft}^2 \end{aligned}$$

then

$$Q' = -162.5 \text{ in-lb-sec.units.}$$

Equation (64) is now evaluated over the sector pad for each point on a grid in polar coordinates, similar to that used in the relaxation solution, Fig. 12e.

The calculation is carried out in a tabular form as shown in full for point No. 1, Fig. 14a. Values at other points are obtained in the same way, the work being simplified to some extent by the fact that points having the same radius differ only in the $\sin \frac{\pi n \theta}{\alpha}$ term, and also, because of the constant viscosity assumption, the pressure distribution is symmetrical about the centre line of a pad.

The pressure at a point is $p = Q' \Sigma P'$. It may be noted that the $\Sigma P'$ term depends only on the dimensions of the bearing, and a change in operating conditions affects Q' only. So that in effect, this solution for pressure is a general solution.

The complete pressure solution for a four-pad bearing sector, showing the general $\Sigma P'$ terms and the pressure p for the specified operating conditions is shown in Fig. 14b.

Four-Pad Bearing $\alpha = 1.465$ $R = 2.083$

1

Point No. 1 ($R = 1.21$, $\phi = 10.5^\circ$)

n		1	3	5	7	9
$\frac{\pi n}{\alpha}$	A	2.145	6.44	10.75	15.05	19.35
$n \left[\left(\frac{\pi n}{\alpha} \right)^2 - 4 \right]$	B	0.62	112.5	560	1540	3340
$R_1 \frac{\pi b}{\alpha}$	C	4.83	112	2.7×10^3	6.6×10^4	1.5×10^6
$R_1^{-\frac{\pi n}{\alpha}}$	D	.207	.0089	$.37 \times 10^{-3}$	$.15 \times 10^{-4}$	$.66 \times 10^{-6}$
$R_1^2 - R_1^{-\frac{\pi n}{\alpha}}$	E	4.133	4.33	4.34	4.34	4.34
$R_1 \frac{\pi b}{\alpha} - R_1^{-\frac{\pi n}{\alpha}}$	F	4.623	112	2.7×10^3	6.6×10^4	1.5×10^6
$R \frac{\pi a}{\alpha}$	G	1.505	3.41	7.75	17.6	40.0
$R_1 \frac{\pi b}{\alpha} - R_1^2$	H	0.49	107.7	2.7×10^3	6.6×10^3	1.5×10^6
$R^{-\frac{\pi n}{\alpha}}$	J	0.663	0.293	0.129	0.057	0.025
R^2	K	1.464	1.464	1.464	1.464	1.464
$\frac{E}{F} \times G$	L	1.345	0.132	.0125	.0013	.0001
$\frac{H}{F} \times J$	M	.07	.282	.129	.057	.025
$M + L - K$	N	-.049	-1.05	-1.322	-1.408	-1.439
$\sin \frac{\pi n \theta}{\alpha}$	O	.384	.924	.924	.384	-.384
$\frac{N}{B} \times O$	P'	-.0391	-.0087	-.0022	-.0003	+.0002

$$\Sigma P' = -0.041$$

Fig. 14a Specimen Tabulated Calculation of $\Sigma P'$.

Point No. 1, Four-Pad Bearing.

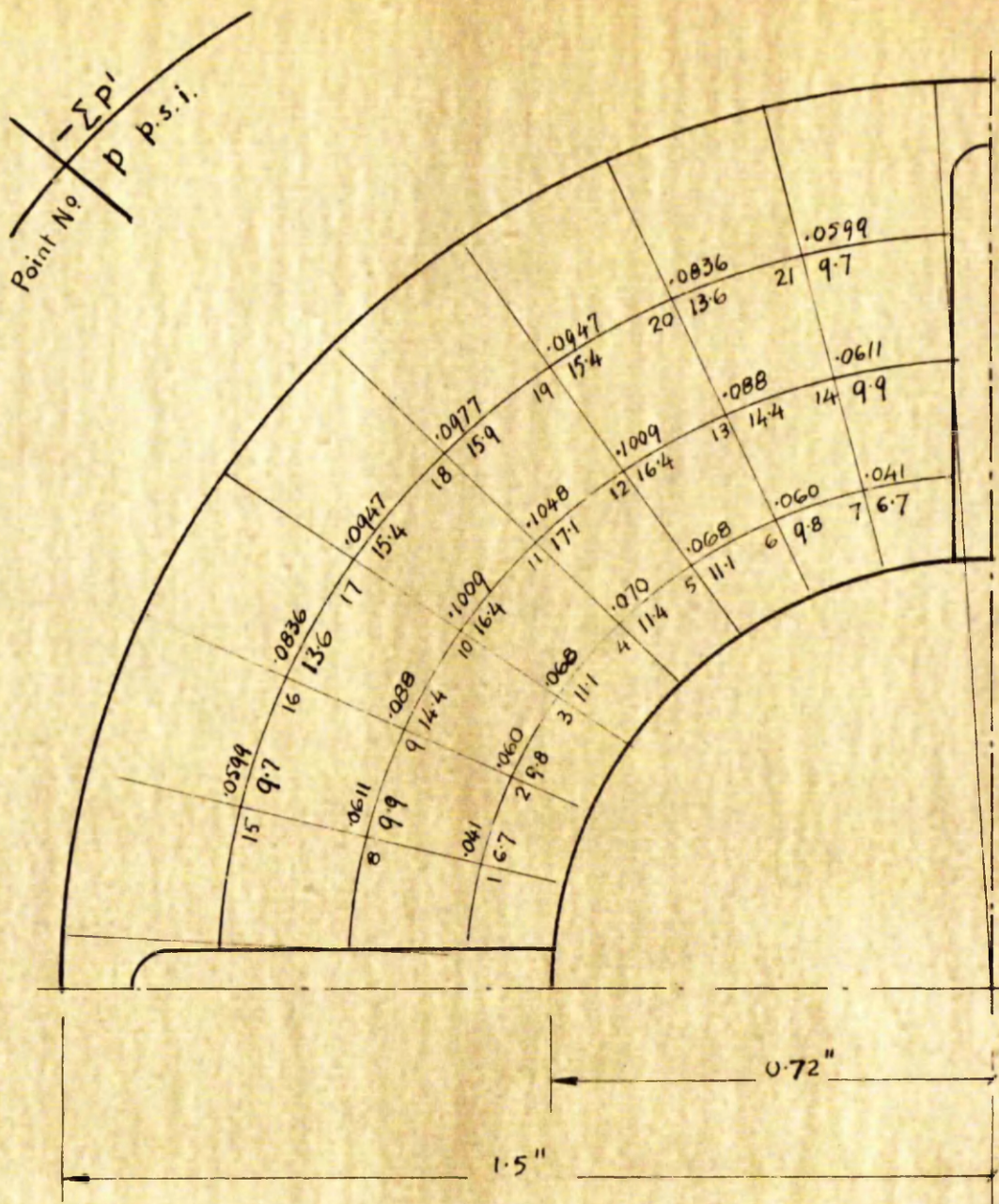


FIG 14 b THEORETICAL PRESSURE DISTRIBUTION - Solution III.3
4-GROOVE BEARING SECTOR

Four-Pad Bearing

$\alpha = 1.465$

$R_1 = 2.083$

n		1	3	5	7	9
n^2	A	1	9	25	49	81
$(\frac{\pi n}{\alpha})^2$		4.595	41.3	114.5	225.0	372
$4 - (\frac{\pi n}{\alpha})^2$	B	-0.595	-37.3	-110.5	-221.0	-368.0
$(\frac{\pi n}{\alpha} + 2)$	C	4.143	8.43	12.715	17.0	21.3
$R_1 \frac{\pi n}{\alpha}$		4.842	112.0	2630		
$R_1^{-\frac{\pi n}{\alpha}}$		0.2065	0.0089	0.38×10^{-3}		
$R_1^{\frac{2\pi n}{\alpha}}$		23.4	1.25×10^4	6.9×10^6		
$R_1^{-\frac{2\pi n}{\alpha}}$		0.0427	0.8×10^{-4}	0.145×10^{-6}		
$(R_1^2 - R_1^{-\frac{\pi n}{\alpha}})$	D	4.134	4.331	4.34	4.34	4.34
$(1 - R_1^{-\frac{2\pi n}{\alpha}})$	E	0.9573	1.0	1.0	1.0	1.0
$\frac{D^2}{CE}$	F	4.31	2.23	1.48	1.11	0.89
$(\frac{\pi n}{\alpha} - 2)$	G	0.143	4.43	8.715	13.0	17.3
$(R_1 \frac{\pi n}{\alpha} - R_1^3)$	H	0.502	107.66	2626		
$(R_1^{\frac{2\pi n}{\alpha}} - 1)$	J	22.4	1.25×10^4	6.9×10^6		
$\frac{H^2}{GJ}$	K	0.0785	0.209	0.115	0.077	0.058
$\frac{R_1^4 - 1}{4}$	L	4.46	4.46	4.46	4.46	4.46
$L - K - F$	M	0.0713	2.021	2.865	3.273	3.51
$W^1 = \frac{M}{AB}$		-0.120	-0.006	-0.001	-0.0003	-0.0001

$\Sigma W^1 = -0.1274$

Fig. 14c Specimen Tabulated Calculation for ΣW^1

Four-Pad Bearing

Load-Carrying Capacity

The load-carrying capacity of a bearing pad is obtained from Equation (60)

W per pad =

$$\frac{48 \omega \nu_0 b d r_0^4}{\pi^2 h^2} \sum_1^{\infty} \frac{1}{n^2 [4 - (\frac{\pi h}{\alpha})^2]} \left\{ \frac{R_1^4 - 1}{4} - \frac{(R_1^2 - R_1^{-\frac{\pi h}{\alpha}})^2}{(\frac{\pi h}{\alpha} + 2)(1 - R_1^{-\frac{2\pi h}{\alpha}})} + \frac{(R_1^{\frac{\pi h}{\alpha}} - R_1^2)^2}{(\frac{\pi h}{\alpha} - 2)(1 - R_1^{\frac{2\pi h}{\alpha}})} \right\}$$

for $n = 1, 3, 5, 7, \text{etc.}$

Then $W \text{ per pad} = \bar{Q} \sum W'$

For the four-pad bearing operating at the assumed conditions and

viscosity $\nu_0 = 0.572 \times 10^{-3} \text{ lb. sec/ft}^2$ the first term will be

$\bar{Q} = -131 \text{ lb-ft-sec units.}$ However, here again it is better to use the average value of viscosity

$$\nu_{\text{av}} = 0.343 \times 10^{-3} \text{ lb. sec/ft}^2$$

whence $\bar{Q}' = -78.8 \text{ lb-ft-sec units.}$

The term $\sum W'$ is also computed in a tabular fashion, shown in Fig. 14c, and is equal to -0.1274 .

Hence the load-carrying capacity of a four-pad bearing sector is

$$W = -78.8 (-0.1274) = 10.05 \text{ lb.}$$

Total load-carrying capacity of the bearing = 4×10.05

$$= 40.2 \text{ lb.}$$

b) Two-Pad Bearing

From Solution III. 1 the temperature rise at the mean radius $r_m = 1.025''$ is $t_L = 82.5^\circ\text{F}$ for an included angle $\alpha = 3.04$ rad.

$$b = -0.00043 \left(\frac{82.5}{3.04} \right) = -0.0117$$

$$\begin{aligned} \text{Average viscosity } \mu_{av} &= \frac{1}{t} \int_0^{82.5} \mu_0 e^{-\beta t} dt \\ &= 0.280 \times 10^{-3} \text{ lb. sec/ft}^2 \end{aligned}$$

$$\text{Hence } Q' = -89.2 \text{ in-lb-sec. units.}$$

Equation (64) is evaluated for the two-pad bearing in a tabular form similar to the method used for the four-pad bearing. The pressure distribution thus obtained is shown in Fig. 15b.

Load-Carrying Capacity

$$\text{Load per pad } W = \bar{Q}' \Sigma W'$$

For the two-pad bearing

$$\bar{Q}' = -84.5 \text{ lb-ft-sec. units.}$$

$$\text{and } \Sigma W' = -0.173$$

$$\text{Hence load per pad} = 14.6 \text{ lb.}$$

$$\text{Total load per bearing} = 29.2 \text{ lb.}$$

Analysis of Previous Experimental Work

The methods of Solution III.3 may be applied to the published data of Kettleborough (4) as far as available information will allow.

Taking data from Kettleborough's paper, dimensions and physical constants for the four-pad bearing are as follows:

Bearing inside diameter	d_0	=	$2 \frac{1}{4}$ "
Bearing outside diameter	d_1	=	$4 \frac{1}{8}$ "
Included angle of sector pad	α	=	83°
Area of bearing surface		=	8.68 in^2

From Fig. 6 of Kettleborough's paper

Applied bearing load		=	53 psi
Speed of rotation		=	695 rpm
Parameter $\frac{ZN}{p}$ (Z in centipoise)		=	750
Operating temperature (outlet)		=	139°F
Hence average viscosity	Z	=	57.2 centipoise
	$\mu_{av.}$	=	$0.00119 \text{ lb. sec/ft}^2$

It is necessary, in the absence of published details, to assume an oil inlet temperature of 70°F and a normal coefficient of expansion of oil, λ , of 0.00043.

$$\text{Hence temperature rise } \Delta t = 139 - 70 = 69^\circ\text{F}$$

$$\text{factor } b = -\frac{\lambda \Delta t}{\alpha} = -0.0205$$

Film thickness $h = 0.00014$ in.

From the bearing dimensions, the load term $\Sigma W' = -0.058$

$$\text{Hence, theoretical load } W = \frac{48 \mu b \alpha r_o^4 \omega \Sigma W'}{\pi h^2}$$

$$\text{Theoretical Bearing Load } W = \underline{412 \text{ lb}}$$

$$\text{Actual Bearing Load} = 53 \text{ psi} \times 8.68 \text{ in.}^2 = \underline{460 \text{ lb.}}$$

This shows very good agreement between theoretical and actual values, and serves as further confirmation of the suitability of using the methods of Solution III.3 for load capacity predictions.

Temperature by Constant Viscosity Solution

The temperature distribution obtained by this method is not satisfactory because the assumption of constant viscosity appears to have a much greater effect on temperature values than on pressure values. However, it is included here to complete the comparison.

From Equations (62) and (63) is obtained

$$\frac{\partial t}{\partial \theta} = \frac{2\omega r^2 \nu_0}{h^2 J \rho \sigma} \left\{ \frac{1}{1 - \frac{4b r_0^2}{r^2 \alpha (1+b\theta)} \sum n \left(\frac{M+L-K}{B} \right) \cos \frac{n\pi\theta}{\alpha}} \right\}$$

when M, L, K and B have been defined in the evaluation of pressure, Fig. 14a. The temperature distribution may be obtained in a similar fashion to that for pressure; upon evaluation, it was found that for the conditions specified, the quantity within the brace brackets is very close to unity.

The equation has been evaluated for $r = 1.04''$ and curves are shown on Fig. 15a and 15b.

It is seen that the temperatures thus obtained are much higher than those indicated by Solutions III.1 and III.2. Since this solution III.3 is primarily intended to give a general solution for the pressure distribution, and since Solution III.1 appears to give a short and accurate estimation of temperature, the temperature equations obtained by the constant viscosity solution may be discarded.

III. 5. Friction in a Parallel-Surface Bearing

In general, for any plane thrust bearing, the resultant shear stress at any point in a fluid film, from Newton's Law of Viscous Flow, is

$$\tau = \frac{\nu \omega r}{h} + \frac{dp}{d\theta} \cdot \frac{h}{2} \quad \dots (65)$$

The first term on the right hand side is the shear stress due to velocity, and the second, that due to pressure. The total shear force on a sector pad will be

$$F = \int_0^\alpha \int_{r_0}^{r_1} \left[\frac{\nu \omega r}{h} + \frac{dp}{d\theta} \frac{h}{2} \right] r dr d\theta \quad \dots (66)$$

Integrate the second term of the expression by parts, observing that $p = 0$ at the boundaries

Then

$$F = \int_0^\alpha \int_{r_0}^{r_1} \left[\frac{\nu \omega r}{h} - \frac{p}{2} \frac{dh}{d\theta} \right] r dr d\theta. \quad \dots (67)$$

For a normal tilting or fixed inclined pad $\frac{dh}{d\theta}$ has a finite and negative value. For a parallel surface bearing, however,

$\frac{dh}{d\theta}$ is zero, and hence

$$F = \int_0^\alpha \int_{r_0}^{r_1} \frac{\nu \omega r^2}{h} dr d\theta \quad \dots (68)$$

Thus it is seen that for the same conditions of viscosity, speed and mean film thickness a parallel surface bearing will require a slightly

lower tractive effort than a corresponding tilting pad bearing.

If the assumption is again made that temperature varies only in the ' θ ' direction, and that the variation is linear, then

$$\nu = \nu_0 e^{-\beta t} = \nu_0 e^{-k\beta\theta} \quad \dots (69)$$

$$\begin{aligned} F &= \int_0^\alpha \int_{r_0}^{r_1} \frac{\nu_0 e^{-k\beta\theta}}{h} r^2 \omega \, dr \, d\theta \\ &= \frac{\nu_0 \omega}{h} \int_{r_0}^{r_1} \frac{1}{k\beta} (1 - e^{-k\beta\alpha}) r^2 \, dr \\ &= \frac{\nu_0 \omega}{h} \frac{(1 - e^{-k\beta\alpha})}{k\beta} \frac{r_1^3 - r_0^3}{3} \end{aligned}$$

$$F = \frac{\omega \alpha}{h} \nu_0 \frac{(1 - e^{-\beta t})}{\beta t} \frac{r_1^3 - r_0^3}{3} \quad \dots (70)$$

and the average viscosity $\nu_{av} = \nu_0 (1 - e^{-\beta t}) \frac{1}{\beta t}$

$$\text{Hence } F = \frac{\omega \nu_{av}}{h} \alpha \frac{(r_1^3 - r_0^3)}{3} \quad \dots (71)$$

The ratio of tractive effort to bearing load capacity, $\frac{F}{W}$, somewhat misleadingly termed the coefficient of friction, is

$$f = \frac{\omega \nu_{av}}{h} \alpha \frac{(r_1^3 - r_0^3)}{3} \times \frac{2}{p \alpha (r_1^2 - r_0^2)}$$

where p = bearing pressure, force per unit area.

Hence

$$f = \frac{\omega \nu_{av}}{p} \frac{r_0}{h} \left(\frac{R_1^3 - 1}{R_1^2 - 1} \right) \frac{2}{3} \quad \text{where } R_1 = \frac{r_1}{r_0} \quad \dots (72)$$

(C.f. Petroff's Equation for a lightly loaded journal bearing, radius r , clearance C)

$$f = \frac{\omega \nu}{p} \frac{r}{C} (\pi)$$

Again comparing with an inclined pad bearing, for the same speed, viscosity and mean film thickness the bearing load capacity for the inclined pad bearing is much higher than that for a parallel surface thermal wedge bearing. Hence, since the tractive force is about the same for both, the coefficient of friction for the parallel surface bearing will be very much greater. Or, conversely, for the same speed, viscosity and load, the film thickness of the parallel surface bearing is much smaller than the inclined pad bearing, and since f varies as $\frac{1}{h}$, then for the same $\frac{ZN}{p}$ values, the parallel surface 'f' value will be greater than that for an inclined pad.

III. 6. Summary of Theoretical Work

The values obtained in the numerical evaluations are plotted in graphical form in Figs 15a and 15b and tabulated in Fig. 15c.

Of the three solutions, the relaxation solution III.2 is the most accurate, the final accuracy being dependent only on the size of the grid used in computation. This type of solution is awkward to use, however, involving separate calculations for each change in dimensions or running conditions. To obtain sufficient values to plot performance curves would require a prohibitive amount of work. It is necessary therefore, to use solutions which apply in a more general fashion, so that changes in performance of any single bearing can be calculated without too much trouble.

From the curves of Figs. 15a and 15b, it can be seen that the temperatures obtained by Solution III.1 - the infinitely-wide bearing solution - correspond within about 5% to those obtained by the relaxation method, for both the four-pad and the two-pad bearing. This agrees with observations of Cameron and Wood (8) who state that the temperature rise appears to be approximately the same in a finite as in an infinite bearing. On the other hand, the pressure values found by this method are much too high, indicating that side leakage does indeed have a great effect on pressure values, as was suggested by Swift (16) and others.

Again from Fig. 15a, it is seen that the temperature values obtained by Solution III.3, which involves a constant viscosity assumption, are not in agreement with the other solutions.

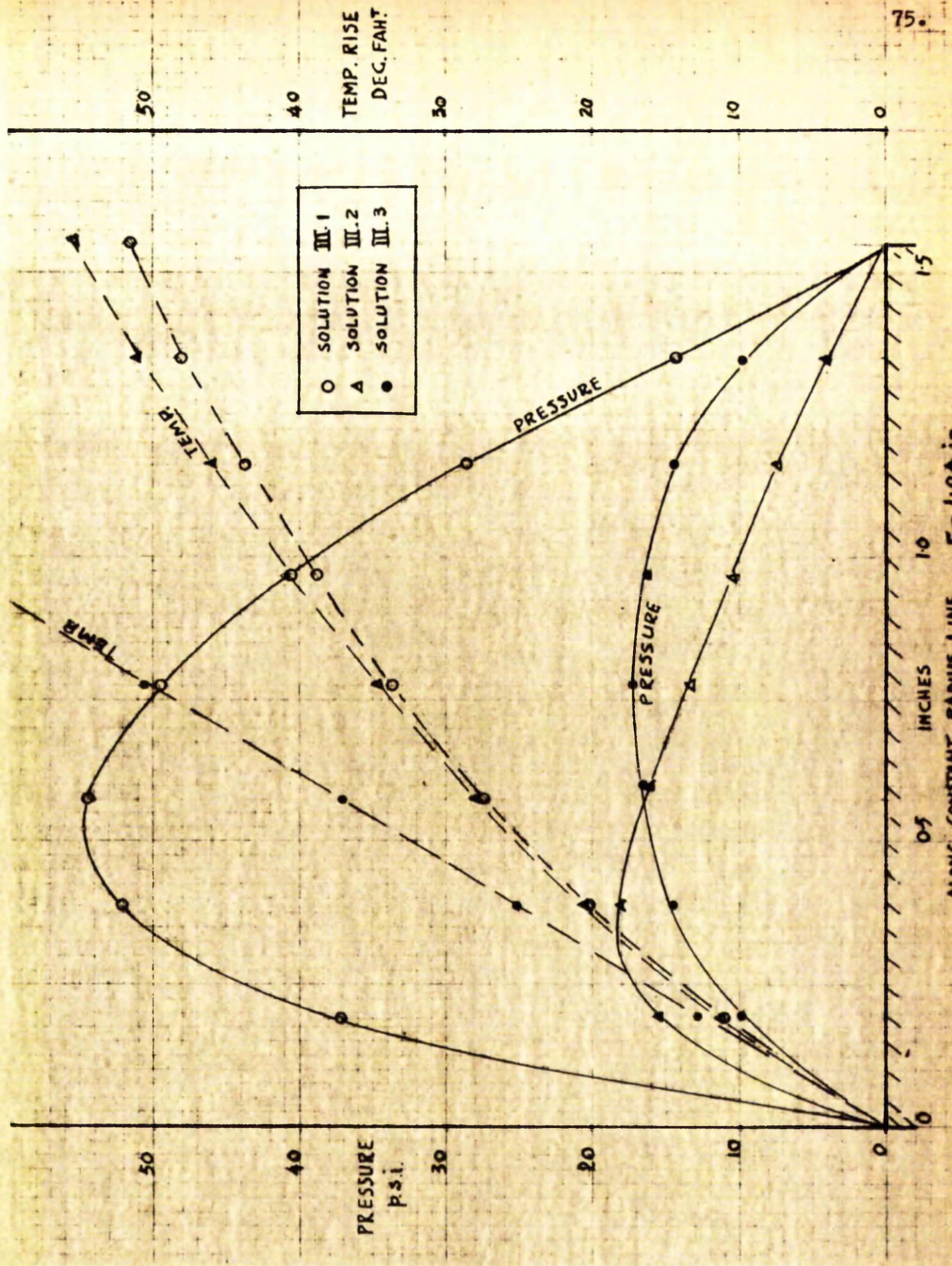


FIG 15 a THEO. CURVES OF PRESSURE AND TEMPERATURE
THREE METHODS, 4 PAD BEARING.

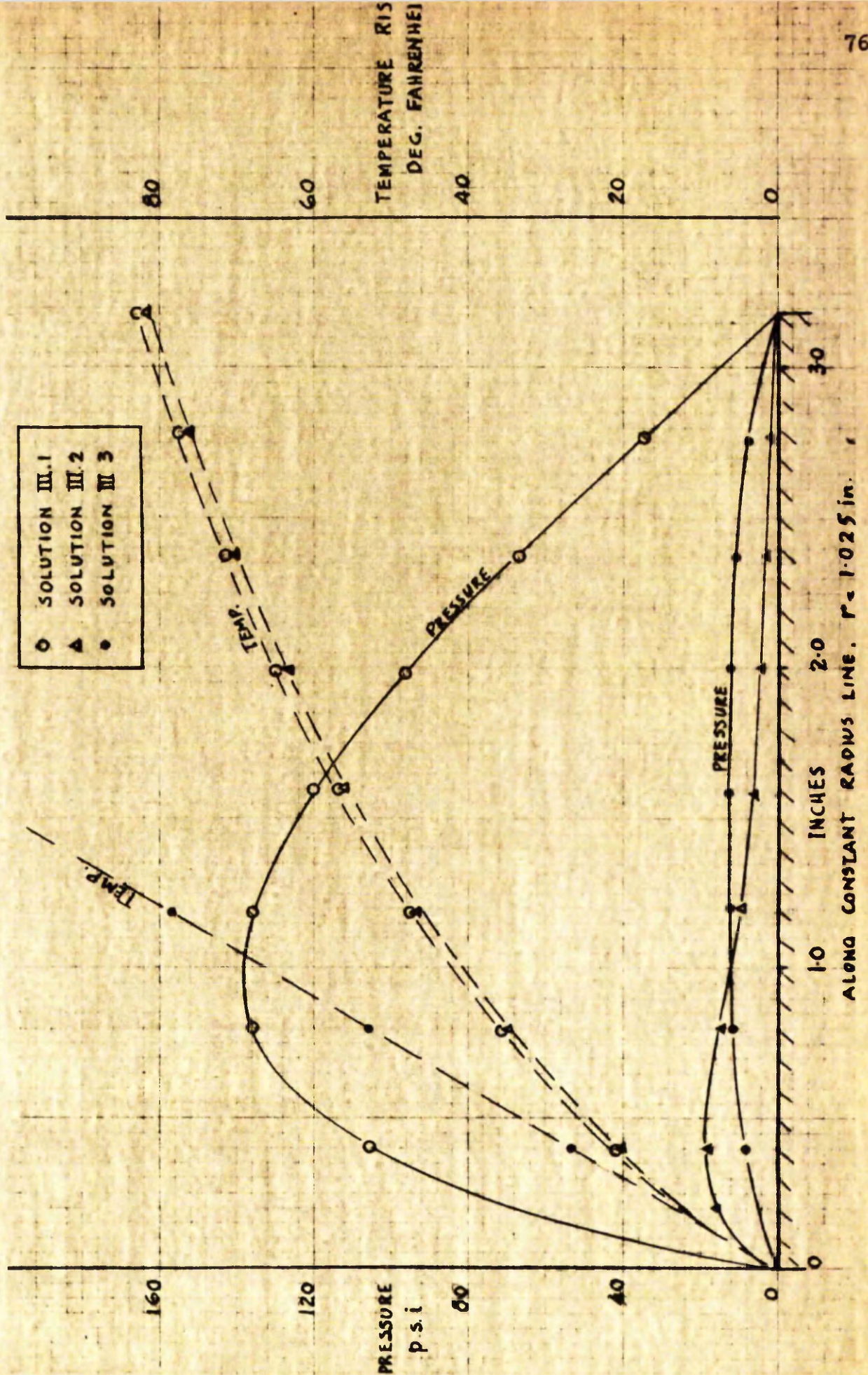


FIG 15 b

THEO. CURVES OF PRESSURE AND TEMPERATURE
THREE METHODS, 2 PAD BEARING

	Solution III.1		Solution III.2		Solution III.3	
	<u>2 pad</u>	<u>4 pad</u>	<u>2 pad</u>	<u>4 pad</u>	<u>2 pad</u>	<u>4 pad</u>
Bearing Type						
Temperature Rise t °F	82.5	56.1	81.9	55.7	--	--
Maximum Pressure p psi	139	63.8	18.4	18.0	11.7	17.1
Bearing Load W lb			27.7	37.7	29.2	40.2

Fig. 15c Summary of Calculated Values
obtained by Three Methods.

The pressures obtained by this solution which takes account of side leakage, are in reasonable agreement as to maximum values, although the curves of distribution are dissimilar. There is a very good agreement in the load-carrying capacity values, within about 5%, between this Solution III.3 and the relaxation Solution III.2 as may be seen in Fig. 15c.

It would appear that the assumption of no side leakage, but with viscosity as a variable, has little effect on temperature values, but causes wide differences in estimated pressures; and the assumption of constant viscosity, but including the influence of side leakage, has a detrimental effect on temperature calculations, but produces only a slight error in pressure and load-carrying capacity.

It is proposed, therefore, to use the following equations in the analysis of the experimental work of this thesis, Chapter V.

Temperature: from Solution III.1

$$t = \frac{1}{\beta} \ln (G_1 x + 1) \quad \dots (21)$$

Pressure: from Solution III.3

$$p = \frac{2}{\alpha} \sum_1^{\infty} \bar{p}_n \sin\left(\frac{n\theta}{\alpha}\right) \quad \dots (49)$$

Load-Carrying capacity: from Solution III.3

$$W \text{ per pad} = \int_{r_0}^{r_1} \frac{4r}{n\pi} \sum_1^{\infty} \bar{p}_n dr \quad \dots (59)$$

for $n = 1, 3, 5, 7, \text{ etc.}$

Coefficient of Friction:

$$f = \frac{\omega v_{av}}{p} \frac{r_0}{h} \frac{2}{3} \frac{(R_1^3 - 1)}{(R_1^2 - 1)} \quad \dots (72)$$

CHAPTER IV

IV. 1. Description of Apparatus

CHAPTER IVIV. 1. Description of Apparatus

Recalling the introductory chapter of this thesis, the objectives of the experimental work were;

- a) To record the operating characteristics of a parallel surface thrust bearing over a wide range of speed and load, supplementary to previously published results which are incomplete;
- b) to obtain accurate measurements of friction, as an indication of whether or not fluid lubrication was occurring, and
- c) To measure the actual temperatures around the bearing and to establish if the temperature rise thus indicated would be sufficient to account for the measured load-carrying capacity.

With these requirements in mind the apparatus was designed to include the following features:

- a) A very wide range of rotational speeds, from about 4000 to 18,000 rpm with overdrive up to 27,000 rpm; and a flexible loading system of high capacity.
- b) The whole test bearing assembly to be torque mounted, to give a direct method of friction measurement, independent of speed or load on the test bearing.
- c) Easy access to the bearing surfaces for a large number of thermocouple leads.

A general arrangement of the high speed apparatus is shown

in Figs. 16 and 17. Referring to the line diagram, Fig. 17, it may be seen that the drive is delivered from a variable speed D. C. motor through a multiple V-belt drive to an intermediate shaft and gear box. The output shaft of the gear box is connected by a flexible coupling to the test shaft, which is supported in two self-aligning ball bearings. A steel disc is shrunk on this shaft and runs between two white-metalled collars which are pressed against the disc by three hydraulic jacks working in parallel.

There are three distinct oil systems. The first circuit is for the lubrication of the gear box and the high speed ball bearings; the second is a gravity feed to the test bearing; and the third a pressure supply to the loading jacks, from a "dead weight" pressure gauge tester.

A detailed description of the component parts follows:

D.C. Motor and V-Belt Drive

The motor is a 37 horsepower D.C. motor with a speed range of 450 rpm to 1000 rpm. The motor shaft may be fitted with a 6" or a 12" P.C.D. pulley and the intermediate shaft with a 6" or a 4" pulley, to give speed ratios 1:1, 1:2, or 1:3 between the motor and the intermediate shaft. Four link type V-belts are used, the tension in the belts being adjusted by the addition or removal of links when altering the drive.

Gear Box

This unit is an ex-Rolls-Royce Merlin supercharger gear box giving a 9.5:1 step-up ratio from the intermediate to the high speed shaft. Coupled with the V-belt drive, the overall ratios are 9.5:1,

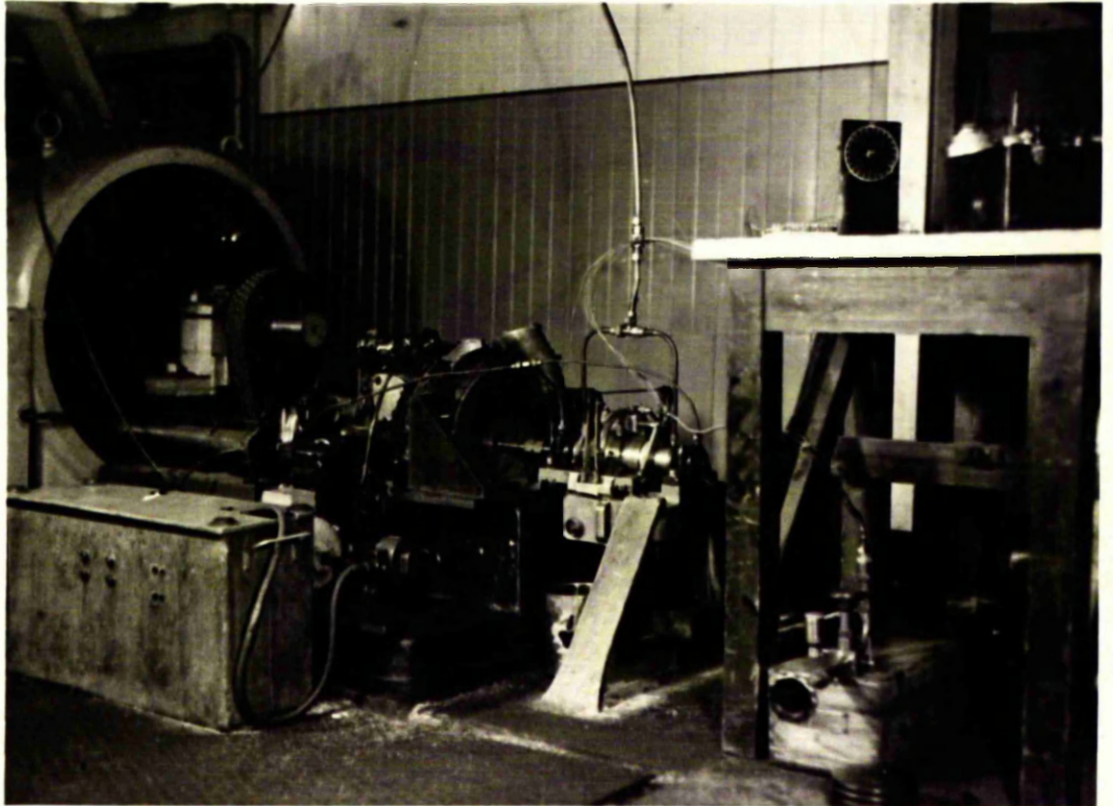


Fig. 16. General View of Experimental Apparatus

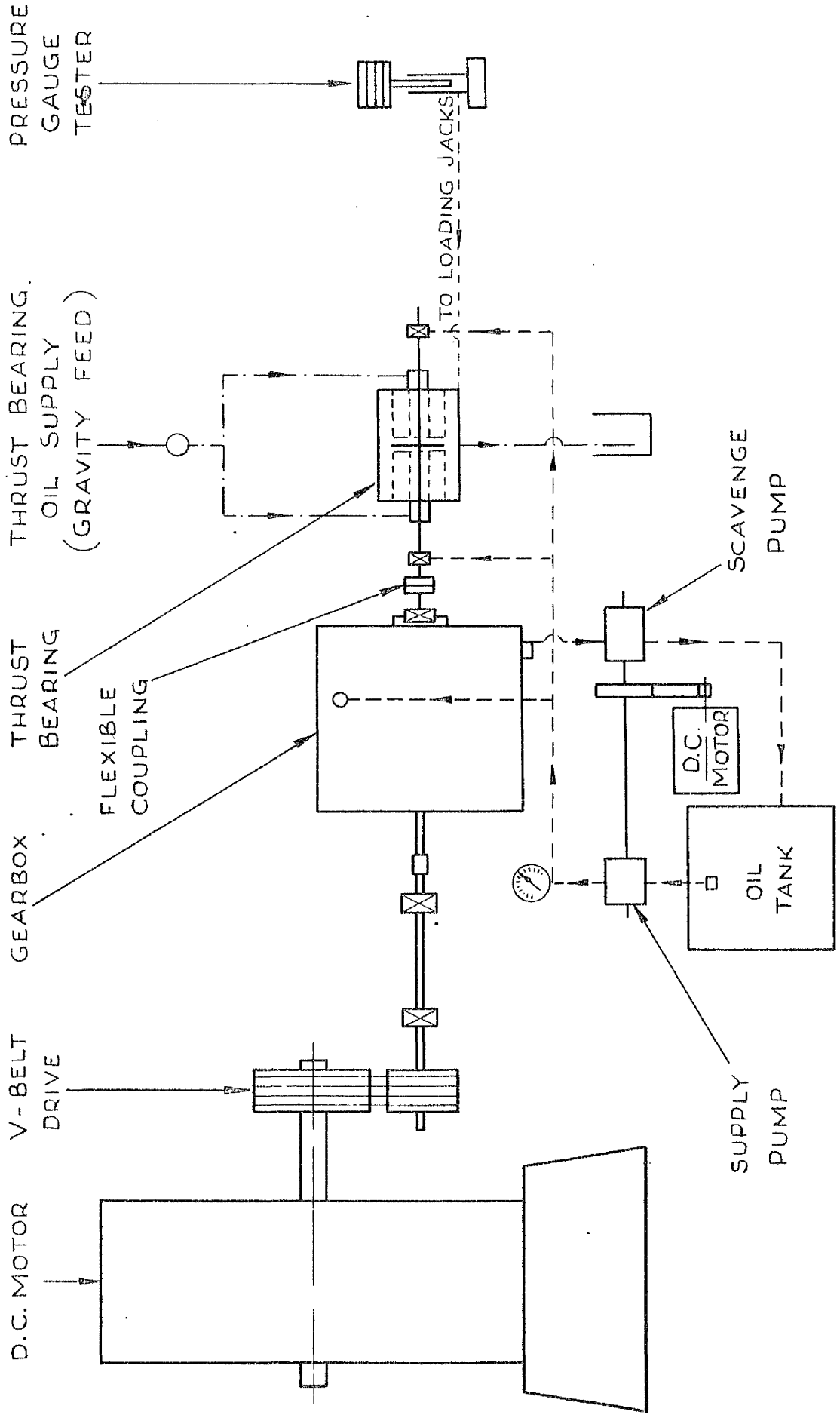


FIG 17 GENERAL ARRANGEMENT OF APPARATUS

19:1 and 28.5:1, corresponding to three-speed ranges of roughly 4300 to 9000, 9000 to 18,000 and an overdrive range of 18,000 to 27,000 rpm.

High Speed Shaft

The high speed shaft is $3/4$ " diameter silver steel, just over 12" long, on to the centre of which is shrunk a disc of medium carbon steel, 3" diameter x $3/4$ " thick. After shrinking, the two faces of the disc are finely machined in position on the shaft, flat and parallel to one another to within 0.0001". The assembly was balanced in an Avery-Schenck dynamic balancing machine. The shaft runs in two standard double-row self-aligning ball bearings. The inner races are secured to the shaft by split tapered sleeves which can be easily slackened and retightened. While this type of mounting is not usually recommended for high speed operation, it was used here for convenience in view of the frequent dismantling and reassembly required, and because continuous running at very high speeds was not envisaged.

Gear Box Lubrication

Oil is supplied to the gear box and high speed ball bearings at a pressure of 7 lb/in^2 by a gear type pump. In the gear box, the gear teeth are lubricated by fine jets, and the bearings by splash. A second gear pump acts as scavenge pump from the gear box sump, both pumps being mounted on a common shaft and driven by a small D.C. motor.

The high speed ball bearings are lubricated by means of a very fine jet directed on to the race, which atomizes the oil. At high

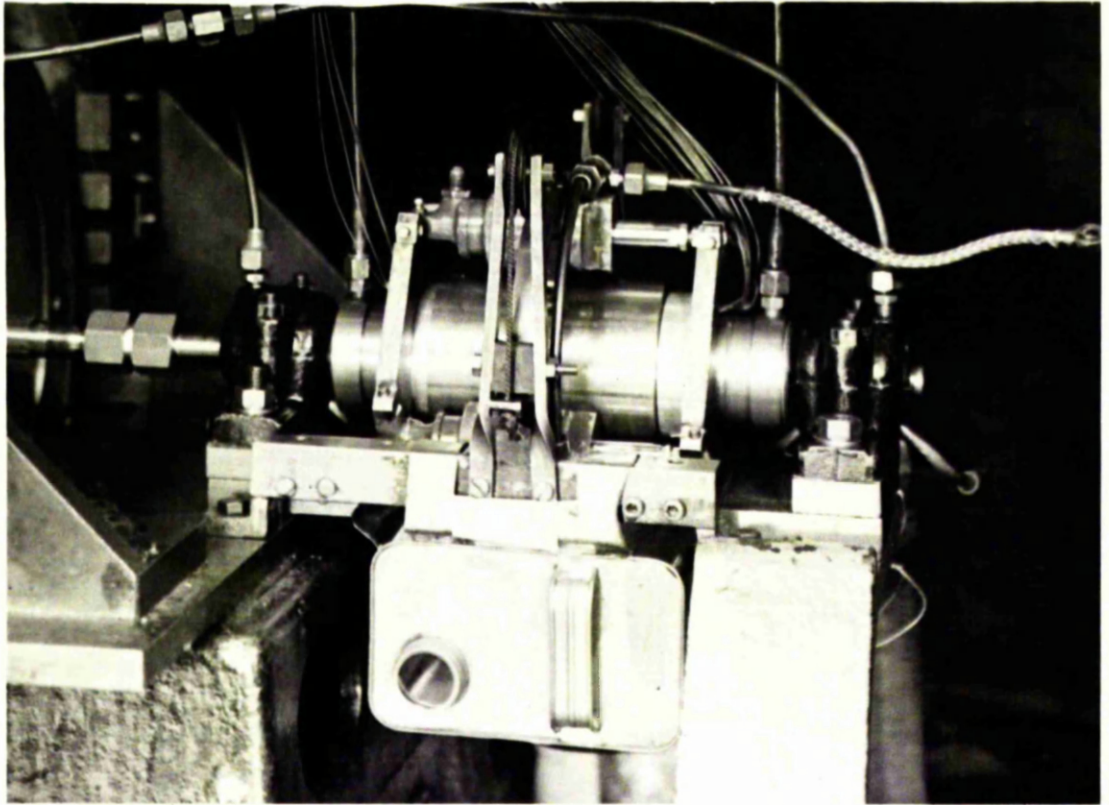


Fig. 18. Test Bearing Assembly

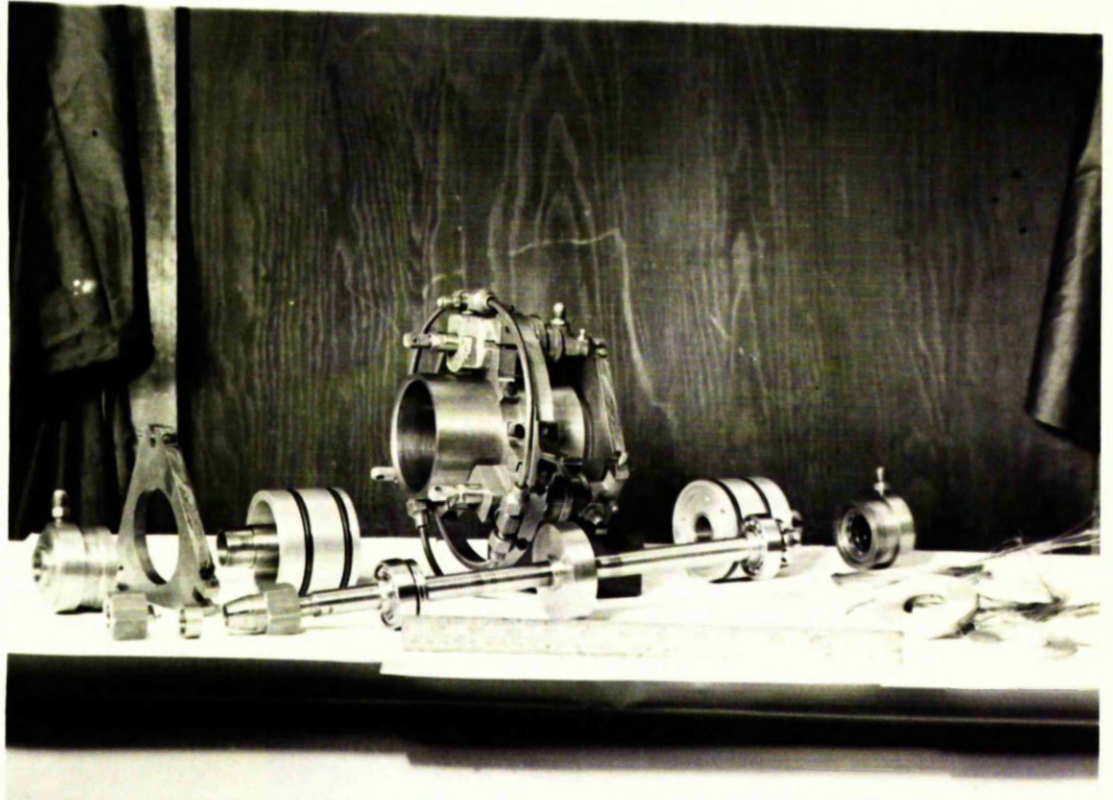


Fig. 19. Test Bearing Dismantled

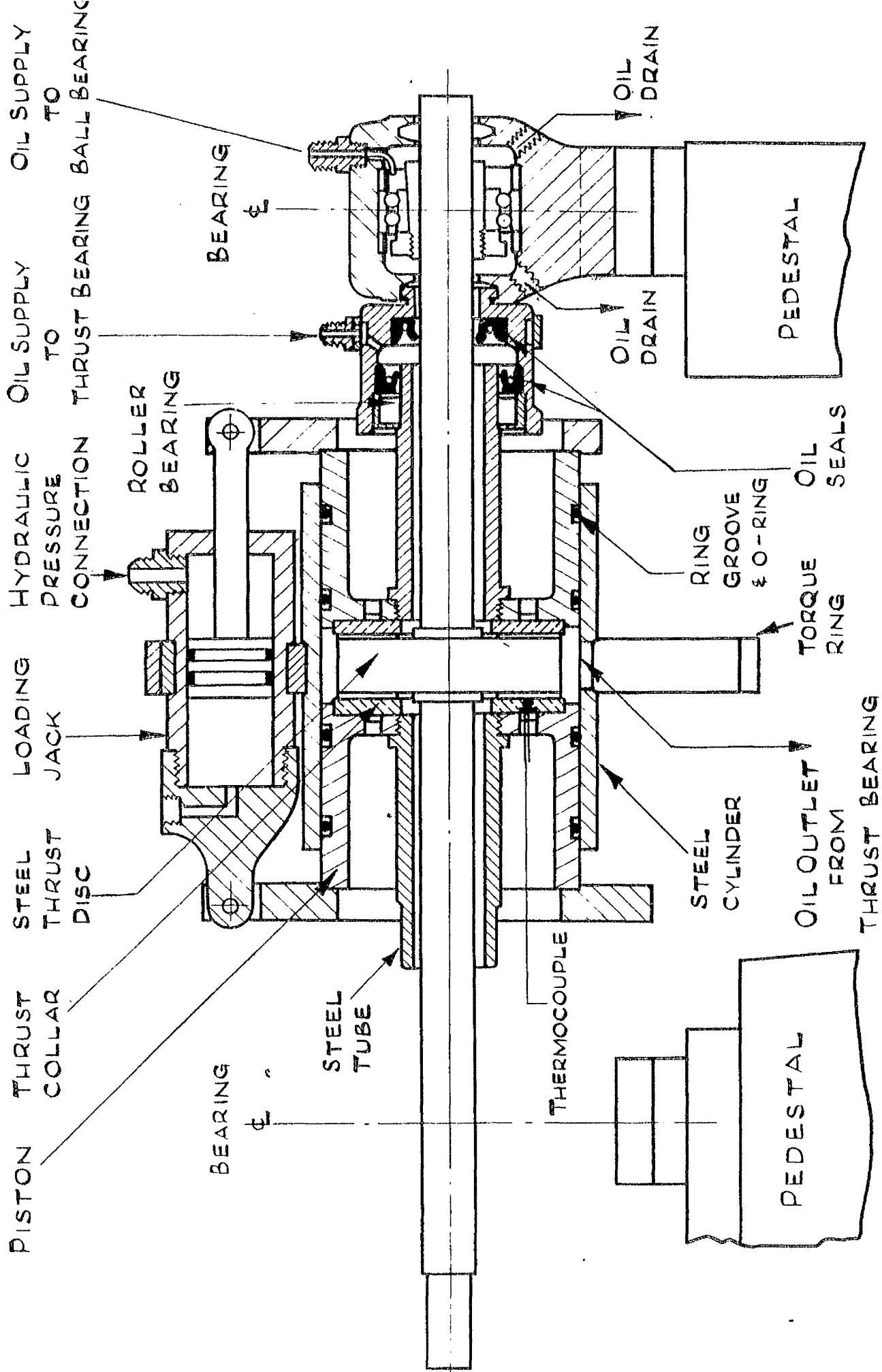


FIG 20 THRUST BEARING ASSEMBLY

speeds, it is important that too much oil is not supplied, otherwise oil churning and overheating are likely to occur. Drain tubes carry away the oil by gravity from the bottom of the bearing housings. The oil used in this system is Shell Turbo 27, a very light, high-speed oil.

Thrust Bearings.

The test bearing consists essentially of two similar white-metalled flat collars which bear on each side of a central rotating disc, Figs. 19,20. The collars exert equal and opposite forces on the disc and thus no resultant thrust force is transmitted to the high speed shaft or to the shaft bearings.

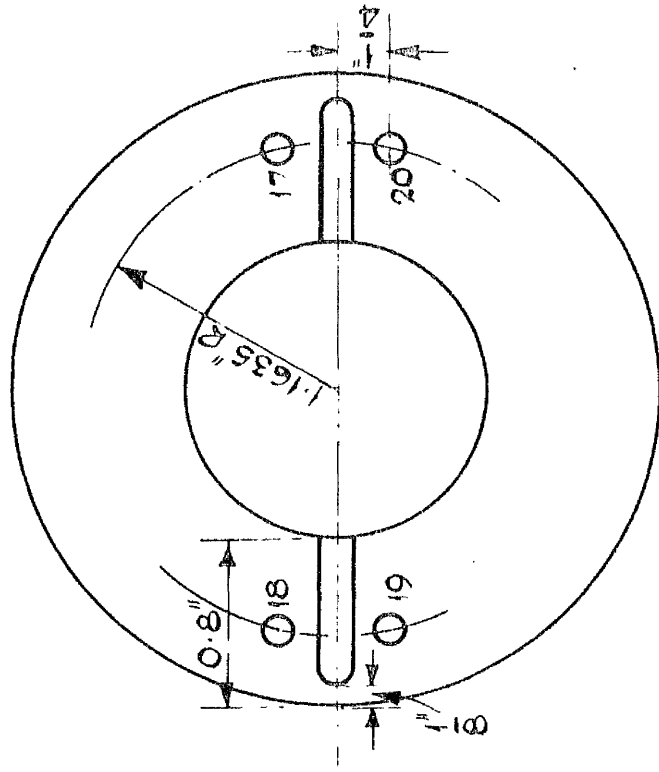
The thrust collars are 3" O.D. x $1\frac{1}{8}$ " I.D. brass plates faced with tin-based white metal. A number of grooves may be cut in the white metal and a large number of thermocouples are set in one plate of a pair. Only a few check thermocouples are set in the other, to determine whether or not similar conditions exist at both bearing surfaces. Pairs of plates, with two, three and four oil grooves, are shown in Figs. 21, 22, 23, and 24.

The collars are recessed into the faces of a pair of pistons which oppose each other inside a steel cylinder. Two synthetic rubber O-rings on each piston act as piston rings. Parallelism of the thrust faces is ensured by the close fit of the pistons in the cylinder, by the piston rings, and by accurate final machining of the white-metal faces with the plates attached to the pistons. A steel tube extends backwards from each piston, the outer end of each tube



Fig. 21. Thrust Faces - 2 Groove Bearing

COLLAR B



COLLAR A

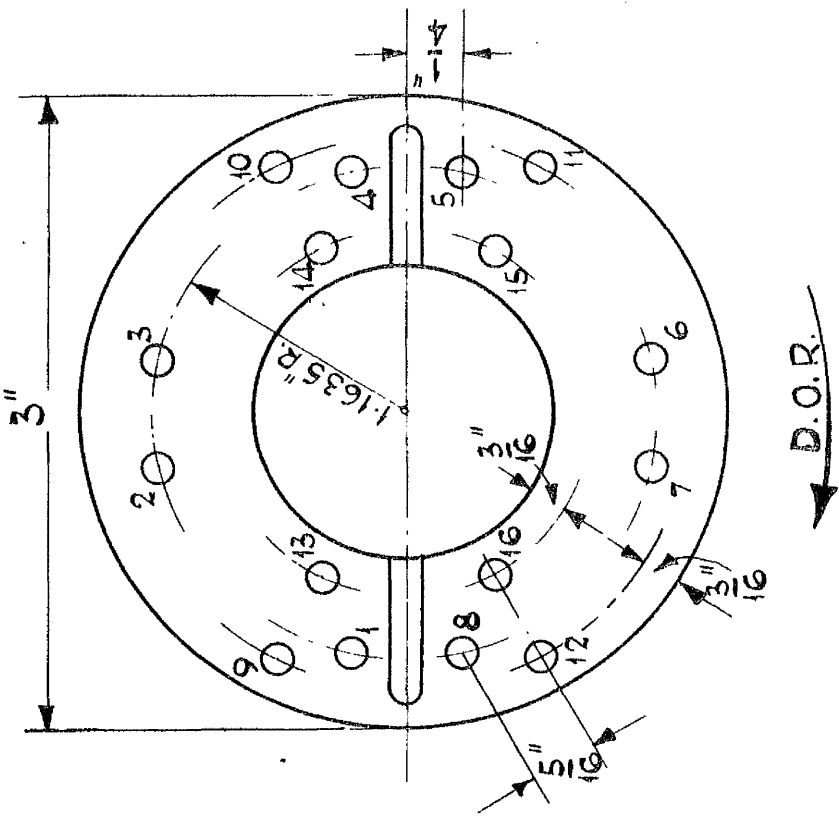
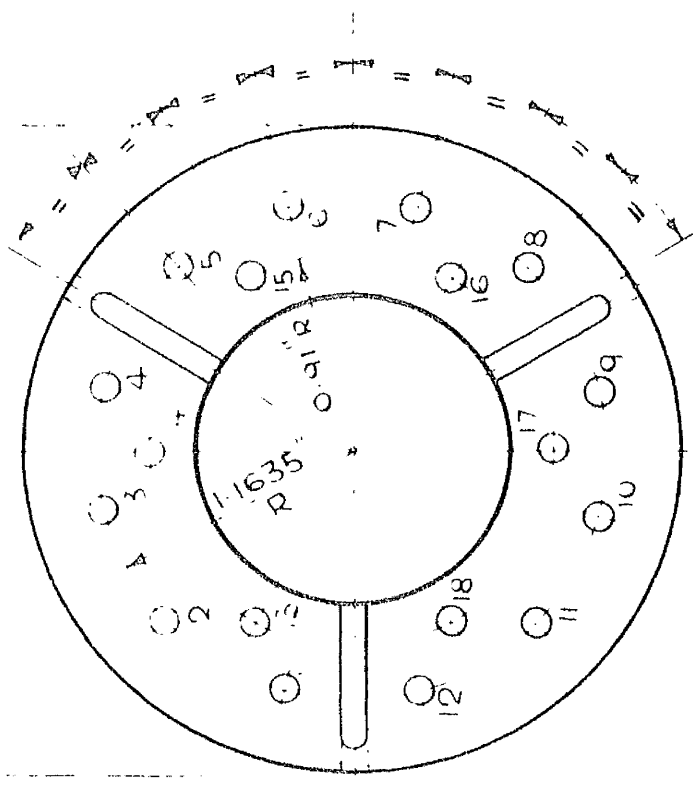


FIG 22 THRUST COLLAR BEARING FACES
WITH THERMO - COUPLE POSITIONS

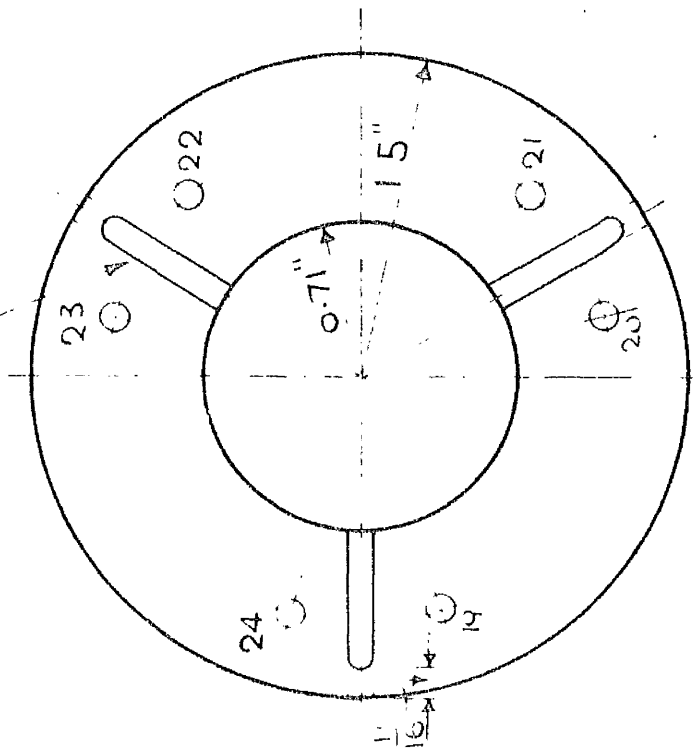
COLLAR A

3" DIA



COLLAR B

GROOVES $\frac{1}{8}$ " WIDE x $\frac{1}{16}$ " DEEP



3 GROOVE BEARING

D.O.R. OF SHAFT

FIG 23 THRUST COLLAR BEARING FACES
WITH THERMO-COUPLE POSITIONS

CASE I GROOVES STOP $\frac{1}{16}$ " FROM EDGE

CASE II SHOWN DOTTED

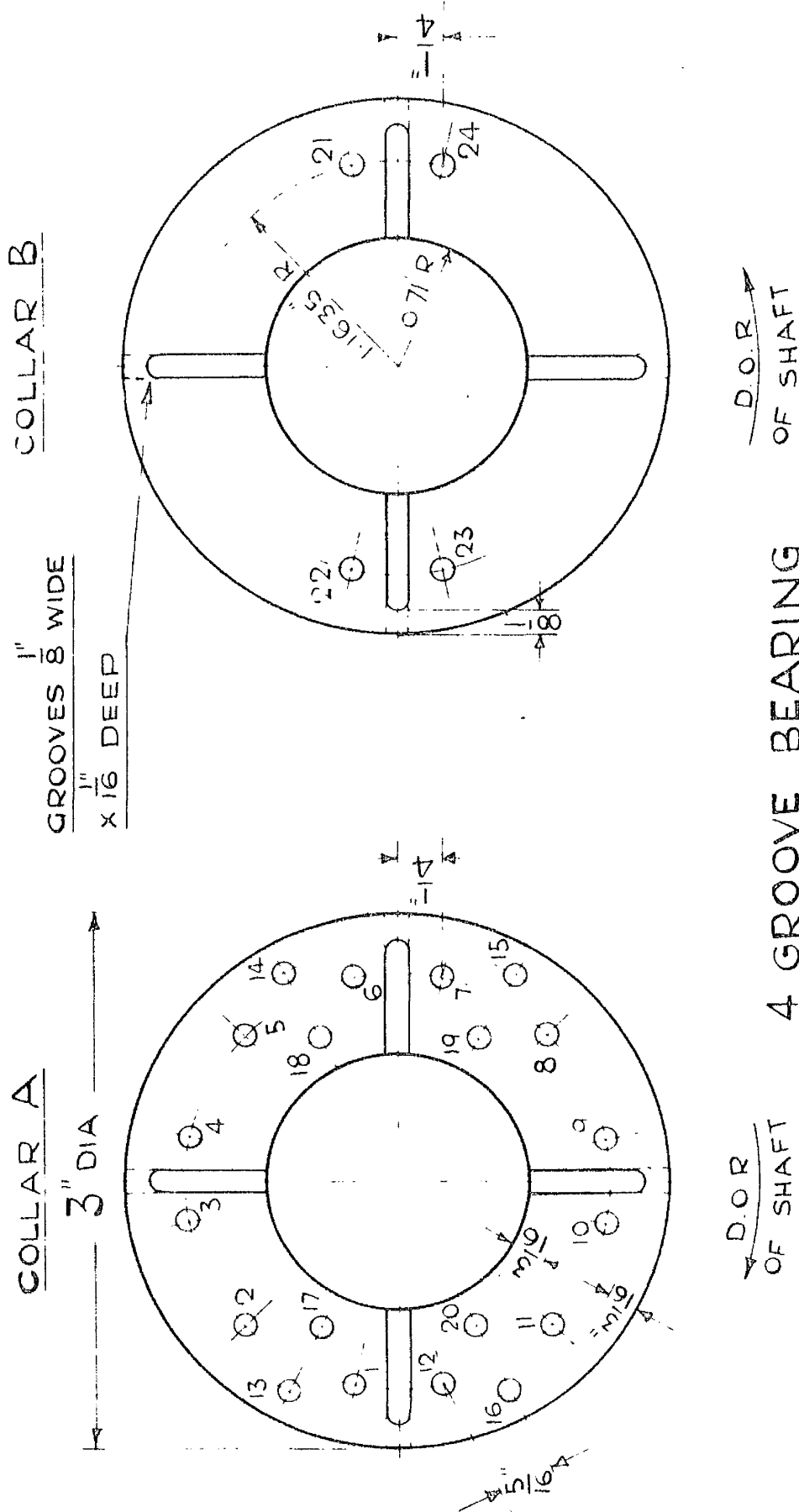


FIG 24 THRUST COLLAR BEARING FACES
WITH THERMO-COUPLE POSITIONS

CASE I GROOVES STOP 8 FROM EDGE
CASE II SHOWN DOTTED

being supported in a roller bearing which is mounted concentrically with the high speed shaft in a stationary housing (see Figs. 19 and 20). In previous designs of the type, the thrust bearings have been centred and supported by journal bearings on the high speed shaft. Such an arrangement has the obvious disadvantage that the friction torque from these journal bearings is included in the measurement of the friction torque of the test thrust bearings. This added torque is not only an unknown quantity, but also varies with speed. In the present design the only extraneous torque is a constant static friction due to the roller bearings and the oil seals on the ends of the piston tubes which do not run at speed.

Loading Jacks

The thrust load on the bearings is supplied by three small hydraulic jacks fixed parallel to the axis of the steel cylinder and spaced at 120° intervals around the outer periphery. The jacks act in parallel and are connected to triangular loading plates which bear against the outer ends of the pistons, (Figs. 19 and 20).

By mounting the loading mechanism in this way, no restraint is placed upon the test bearing as happens when the load is applied from an external source through some kind of thrust bearing, introducing a friction error varying with the load. The present design enables the test bearing friction to be measured with an accuracy which does not vary with the load.

Oil pressure to the hydraulic jacks is applied from a 'dead weight' pressure gauge tester. Part of the pressure pipe to the

jacks is flexible to reduce any restriction on the movement of the bearing assembly. A complete calibration of the loading device was carried out (Appendix II), and graphs of load/pressure are given (Fig. 35).

Temperature Measurement.

The temperature of the oil film at various points around the bearing is recorded by copper-constantan thermocouples fitted flush with the white-metal surface, as shown in Fig. 21. Tufnol plugs are screwed into the bearing plate and the bearing surface machined flat. (Fig. 25a). The thermocouple wires are inserted through two 0.015" diameter holes in the tufnol plug from the back, and the junction is soldered, filed flat and fitted into a small recess in the plug, level with the bearing surface. The surface is then dry lapped and polished on a cast iron surface plate. The accuracy of this method of measuring the temperature of a thin film is discussed in Chapter VI, p.128.

The thermocouples are connected to a potentiometer box by means of a rotary wafer switch, the wiring diagram being shown in Fig. 25b.

The main temperature measurements are made on one bearing plate only, a few thermocouples being inserted in the other plate to check that both sides of the bearing are operating under the same conditions, and to give some indication as to whether or not the interruption of the surface by a large number of thermocouples, although fitted flush, affects the operation of the bearing.

The calibration curve for the copper constantan thermocouples is given in Fig. 36.

Film Thickness Measurement

Film thickness is measure by 1/10,000" dial gauges set as

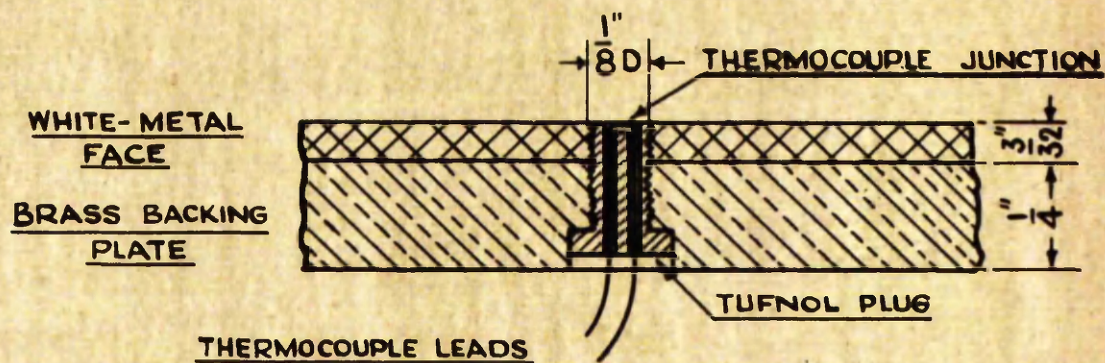


FIG. 25a DESIGN OF THERMOCOUPLE JUNCTION

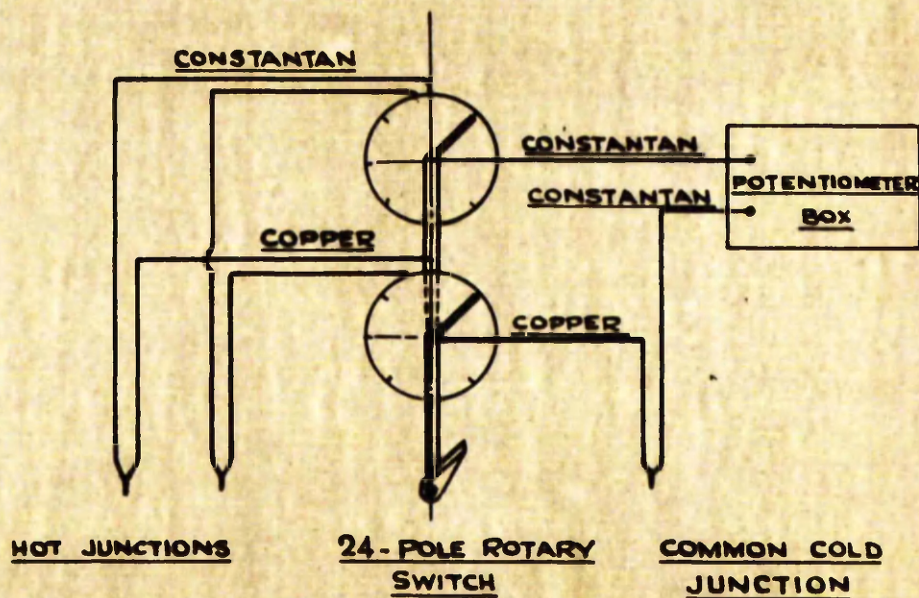


FIG. 25b THERMOCOUPLE WIRING DIAGRAM

shown in Fig. 26. Gauge 1 and Gauge 2 give directly the displacements of the housing assembly and the moving piston respectively from which the two film thicknesses are obtained since the central disc is fixed in the longitudinal direction. Readings on Gauge 3 and Gauge 4 should also be equal to the sum of Gauges 1 and 2. Thus a cross check may be made.

Great accuracy is necessary in the measurement of film thicknesses in parallel thrust bearings, since films of the order of 0.0005" thick may be expected (Kettleborough 4). It was decided that such accuracy could not be obtained in this apparatus, lacking as it does the necessary rigidity and being subject to compressive and thermal expansion effects of the same order of magnitude as the film thickness. While the present arrangement was not designed to give absolute accuracy, therefore, it is simple and straightforward and gives a reasonable indication of the film thickness.

Friction Torque Measurement

Friction torque is measured by a pure couple imposed by two diametrically opposed arms fitted on a steel ring encircling the thrust bearing assembly, as shown in Fig. 27. A single dead weight applies an equal force to each torque arm through a system of cord and pulleys and the assembly is balanced by bringing a pointer opposite a fixed mark.

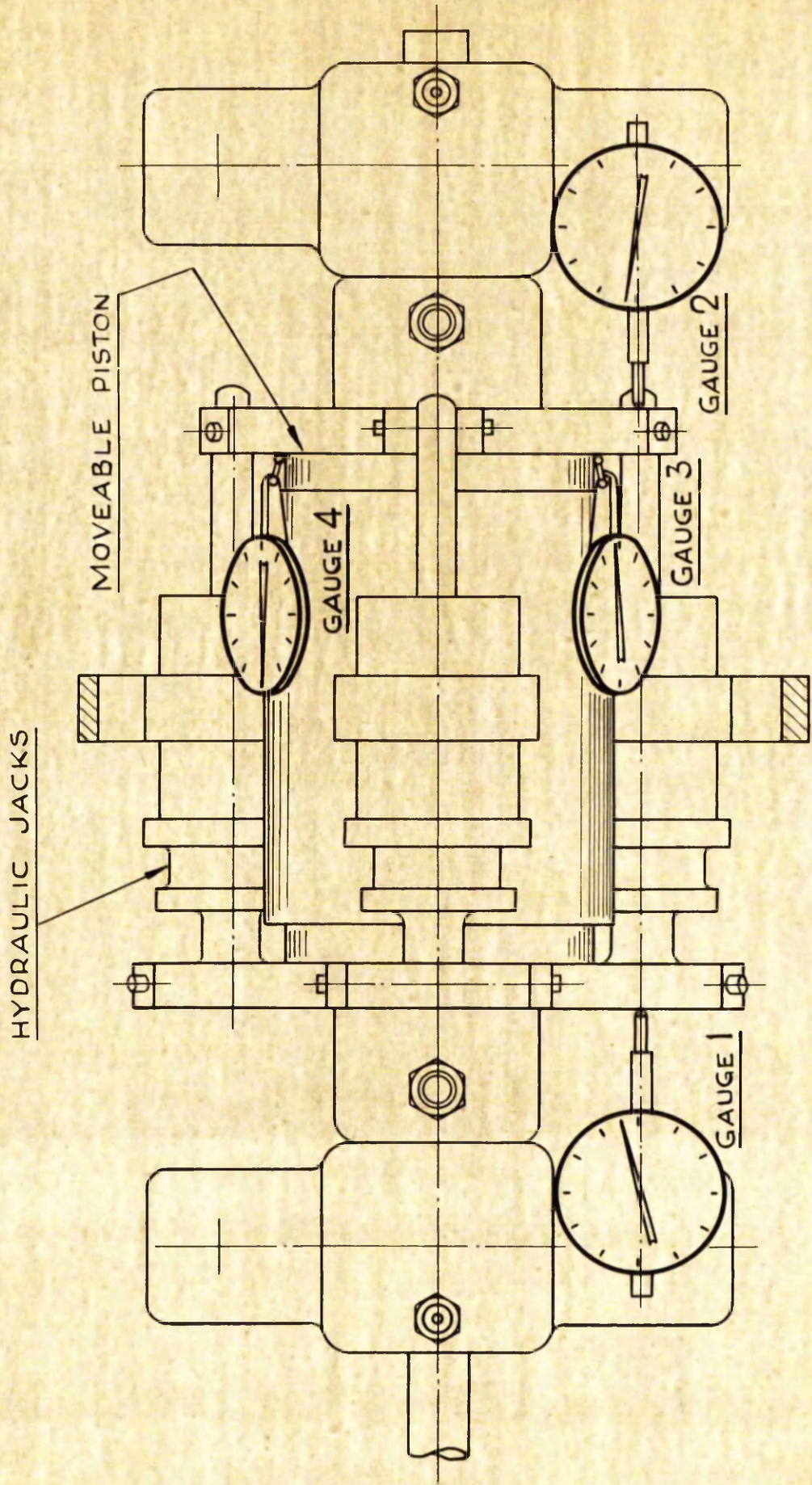


FIG. 26 POSITIONING OF DIAL GAUGES FOR FILM THICKNESS MEASUREMENT

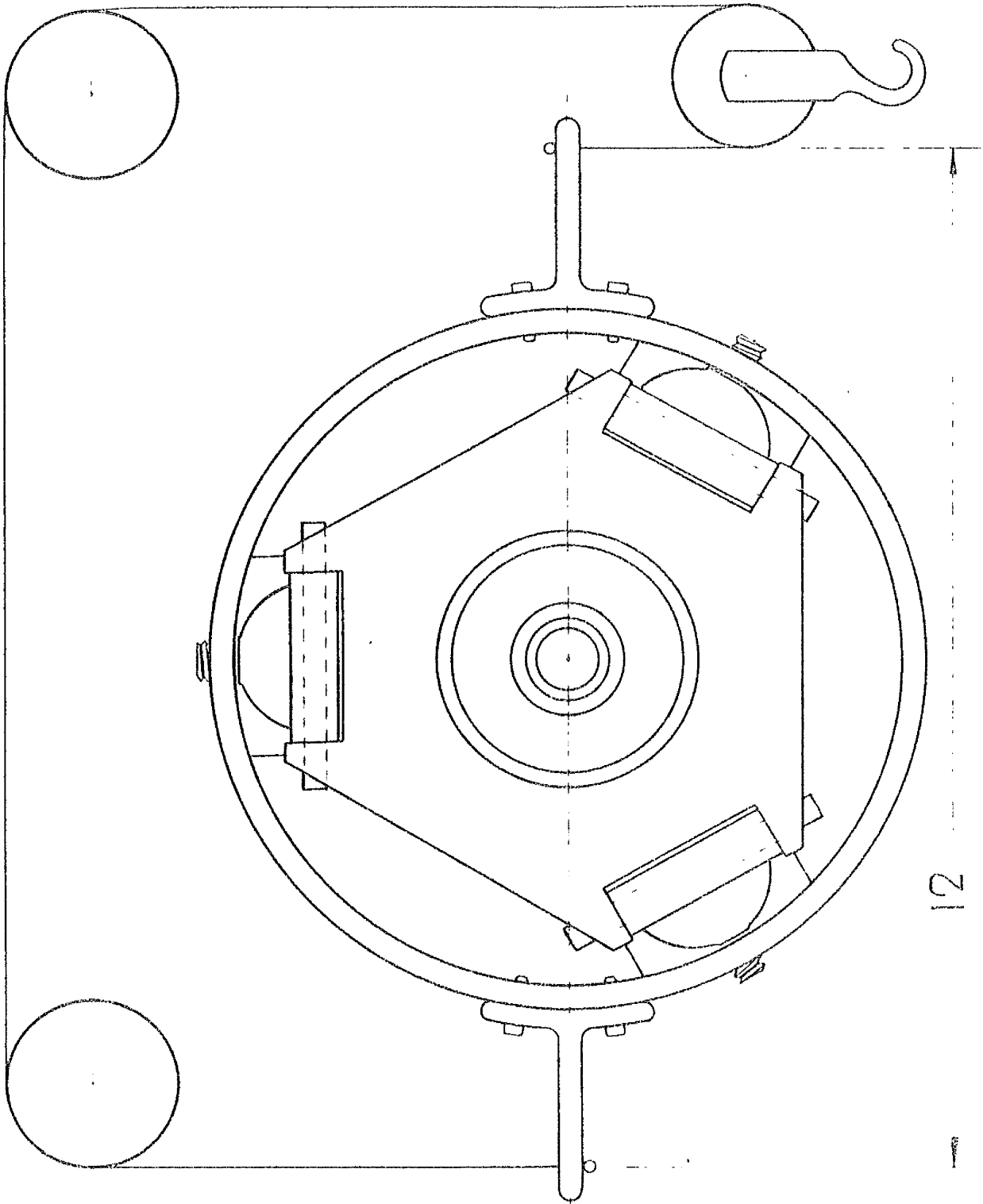


FIG 27 THRUST BEARING ASSEMBLY AND TORQUE MEASURING DEVICE

Test Bearing Lubrication

Oil is fed by gravity from a twenty gallon tank, set about ten feet above the test bearing, through $\frac{3}{4}$ " diameter copper pipe to an annular space in the end roller bearing housings. This space is sealed off by synthetic rubber seals, one on the outside of the piston tube, and the other on the high speed shaft, leaving as an outlet for the oil, an annular space between the high speed shaft and the piston tube (Fig. 20). The oil is thus supplied to the inner diameter of the thrust collars, the clearance between piston tube and shaft being large enough to prevent churning and extra friction on the assembly. From the test bearing, the oil flows to a sump and is pumped up to a settling tank, in which is placed a cooling coil, set above the supply tanks.

The oil used was Shell Turbo 27, and graphs of density/temperature and viscosity/temperature are given (Fig. 5).

CHAPTER V

- V. 1. Experimental Procedure
- V. 2. Presentation of Experimental Results
- V. 3. Discussion of Results

V. 1. Experimental Procedure

Prior to conducting any tests, initial calibrations of the loading system, thermocouples, and the friction measuring device were made and are reported in Appendix II.

Tests were carried out on bearings having two, three and four radial grooves. Of the other arrangements, plain collars with no grooves do not function satisfactorily as thrust bearings (3,4) and bearings with more than four grooves, although quite satisfactory in operation, were not used because of their smaller length of pad, which would not allow space for the requisite number of thermocouples, nor demonstrate a sufficient thermal gradient. The object of the experimental work was to correlate bearing performance with thermal wedge theory, rather than to conduct a comprehensive survey of all possible types and variations of parallel thrust bearings.

Test Procedure

Tests were normally run with the inlet oil coming from the constant head tank at constant temperature, i.e., with no oil recirculation, to ensure early temperature stabilization of the thrust bearing. The capacity of the tank was 20 gallons which limited the time of a test to about 45 minutes, depending on the rate of flow through the bearing. The oil was recirculated for tests of longer duration, but final temperatures were much higher in those cases, and for high power tests an adequate oil cooler would be required.

Before beginning a test, the appropriate load was applied to the bearing, and the four dial gauges for film thickness measurement were set to zero with the machine stationary. The load was removed and the two lubrication systems, viz., the gear box and the test bearing circuits, were brought into operation. The machine was brought up to speed with no load on the thrust bearing. This was necessary to prevent overloading the electrical motor on starting, and to avoid damaging the bearing faces. The load was then applied, and a stop clock started, from which a strict time check was kept throughout the test.

Readings of thermocouple e.m.f., film thickness, friction torque, speed and oil flow were made at regular intervals, usually at five or ten minute periods, during the course of the test. When settled conditions were attained, final readings were made and the machine stopped at no load. Immediately on stopping, the load was re-applied and a second set of 'no speed' readings of the dial gauges taken while the bearing was still hot. After allowing sufficient time for the bearing to return to room temperature, a third set of readings was taken. It was found that the gauges did not return to zero immediately after the machine was stopped (second set of 'no speed' readings), but when the apparatus had cooled to its original temperature, the gauges usually went back to within one or two ten-thousandth-inch divisions of initial zero. To allow for this effect, which seemed due to the thermal expansion of the loading pistons and other metal parts, film thickness readings were referred to the second set of 'no speed' readings as the operating zero; whilst

the fact that the gauges returned to the initial zero when cool, indicated that no bodily displacement had occurred during the test.

A period of about four minutes was necessary to read all twenty-four thermocouples. The time of starting and finishing each set of thermocouple readings was taken and, assuming an equal time requirement for each reading, the temperatures may be plotted to a base of time. By drawing a vertical ordinate, the temperatures obtaining at any instant can be found.

The rate of oil flow was obtained by deflecting the outflow into graduated containers for short periods during the course of the experiment to be measured later when the oil cooled. It was found that the flow remained quite steady, as did the running speed, throughout a test.

Several deviations from normal procedure were made to check the effect of such things as prolonged running (for several hours), change of speed or load during a test, change in oil supply quantity or temperature, and so on. None of these deviations produced any unexpected results, and it was decided that the normal type of test was sufficient to give true and consistent conditions.

Range of Testing

The range of tests was limited by several factors.

The loading system was able to place a load of over 500 lbs on the test bearing, a pressure of some 100 psi. In practice, the plane thrust bearing under test was not able to carry a load of more than 300 lb without showing signs of metal-to-metal contact and overheating.

Under normal running conditions, temperatures stabilized after about half an hour. On several occasions, however, either from known causes, such as heavy loading or restricted oil flow, or because of some unknown condition, temperatures continued to rise. Tests were normally stopped if the thermocouple e.m.f. tended to rise above 5 m.v. corresponding to a temperature of 240°F.

If metal-to-metal contact was suspected, the bearing was stripped and resurfaced by machining and lapping before further tests were carried out.

The test machine was designed for normal operation between 4,000 and 16,000 rpm with an overspeed range from 20,000 to 27,000 rpm. These speed ranges were governed by V-belt pulley sizes, and by the fact that the critical speed of the high speed shaft and disc was about 18,000 rpm. In initial calibration tests, the machine was run successfully in the overspeed range on quite a number of occasions, running extremely smoothly and quietly as might be expected. There was some difficulty in accelerating through the critical range, due to a lack of power at the drive motor and some slippage at the V-belts.

For this reason, and because the end ball bearings were not suitable for prolonged high speed running, it was decided to conduct the bulk of the tests below the critical speed, and run very high speed tests when the rest of the program had been completed.

This was done, but when the overspeed series was begun, it was found impossible to run the machine through the critical speed range without excessive vibration. The machine was stripped, overhauled, the

test shaft rebalanced, and generally reconditioned. A final attempt was made to gain the overspeed range and the drive motor was accelerated as rapidly as possible, but at about 19,000 rpm obvious failure occurred and the test was stopped. On investigation it was found that the 3/4" diameter test shaft had a permanent set of about 1/2", due to whipping, and the supporting ball and roller bearings had also failed.

When this failure occurred, the machine had been in operation for about 18 months, and the difficulty in getting through the critical speed range was undoubtedly due to imbalance caused by wear and tear during this time.

It was apparent that further testing would require extensive rebuilding and possible redesign of the test apparatus, and since a substantial amount of information had already been gained, it was decided to discontinue the experimental work at this point.

V. 2. Presentation of Results

In the course of the experimental investigations about one hundred and sixty tests were carried out, and during each test, of thirty minutes average duration, over a hundred readings of the various required quantities were obtained until steady state conditions were reached. Rather than report the bulk of these readings, it is proposed to illustrate the measurements recorded during a complete test by three typical examples, and to present average and final steady state values for the remainder in graphical and tabular form. In general, no attempt has been made to draw best curves through the experimental points, but where applicable on each graph sheet, the corresponding theoretical curve obtained from the equations of Chapter III, is shown. Thus a direct comparison of theory and experiment can be made.

Analysis of Results

Experimental readings as observed and recorded are shown for three typical tests in Tables 1, 2 and 3, Appendix I. From these recorded values, the required quantities are obtained as follows:

Load: The bearing load is obtained from the loading circuit pressure value by referring to the load calibration curve in Appendix II.

Speed: Rotational speed was recorded directly at frequent intervals throughout a test by a hand tachometer checked regularly for accuracy by a strobo-tachometer.

Temperature:

Thermocouple E.M.F. values for all stations around the

bearings were read at regular five or ten minute intervals until steady conditions were obtained, usually after thirty or forty minutes running time. The thermocouple locations are in accordance with Figs. 22, 23 and 24. The oil inlet temperature, T_o , was recorded by a thermocouple in the inner annular space of the bearing assembly near the thrust surfaces. Thermocouple e.m.f. values are converted to temperatures by means of the thermocouple calibration curve, Fig. 36, in Appendix II.

The temperature rise, t , is the difference between maximum temperature and inlet temperature, $T_{\max} - T_o$.

The average temperature, T_{av} , is taken as $T_o + \frac{2}{3} t$. It was felt that the average temperature in the bearing is higher than the simple arithmetic mean of inlet and maximum values, as may be observed in Fig. 28. While no attempt is made to justify the $\frac{2}{3}$ value, it seems to be a reasonable figure, and has been used on a previous occasion by Cameron and Wood (8).

Film Thickness:

Film thickness values are recorded on four 1/10,000 in. dial gauges. Gauges 1 and 2 are mounted on the fixed end bearing housings and measure the movement of the loading pistons thus giving film thickness directly. Gauges 3 and 4 are mounted on the outer steel cylinder, and thus measure the relative movement of the two loading pistons, i.e., they measure the sum of the two film thicknesses.

Film thickness values are obtained from the gauge reading minus the operating zero reading.

$$\text{Average film thickness } h = \frac{1}{4} \left(\text{Gauge 1} + \text{Gauge 2} + \frac{\text{Gauge 3} + \text{Gauge 4}}{2} \right)$$

Bearing Friction:

The constant static friction due to the end seals and support roller bearings was measured at the beginning of each test by applying the scheduled bearing load and recording the force required for exact balance of the static friction. This force was added to the balancing force recorded during the test, and multiplied by the radius arm of the balancing system, Fig. 27, gave the friction torque, T lb-ft.

The mean bearing radius is calculated from the uniform pressure theory, and gives the coefficient of friction

$$f = \frac{T}{W} \cdot \frac{3}{2} \left(\frac{r_1^2 - r_0^2}{r_1^3 - r_0^3} \right)$$

$$\text{or } f = \frac{T}{W} \times 10.45$$

T = Friction Torque, ft.-lbs.

W = Bearing load, lbs.

Oil Flow:

Oil flow was measured volumetrically over short periods by diverting the outflow from the test bearing into a container, and measuring, when cool, in a graduated jar. Knowing the bearing torque and speed, and the oil flow, specific heat and temperature rise, a simple energy balance gives a good and independent check on the measured quantities. It was considered satisfactory if this check was no more than about 10% in error, because of the conduction heat losses, oil leakage and other losses which were unaccounted for.

Theoretical Equations

The theoretical equations are applied to the test bearing and employed in the following ways:

Temperature

$$t = \frac{1}{\beta} \ln (G_1 X + 1) \quad \dots (21)$$

where

$$G_1 = \frac{2 \omega r_{av} \nu_0 \beta}{h^2 \sigma J \rho_0} \left(\frac{\rho_0}{\rho_m} \right)$$

$$X = r_{av} \theta \quad ; \quad X_L = r_{av} \alpha$$

r_{av} = mean radius

hence

$$e^{\beta t} - 1 = \frac{2 \omega \nu_0 \beta r_{av}^2 \theta}{h^2 \sigma J \rho_0} \left(\frac{\rho_0}{\rho_m} \right)$$

and

$$\frac{1}{\nu} - \frac{1}{\nu_0} = \frac{\omega}{h^2} \left(\frac{2 \beta r_{av}^2 \alpha}{\sigma J \rho_0} \left(\frac{\rho_0}{\rho_m} \right) \right) \quad \dots (21a)$$

where ν = outlet viscosity at $X = X_L$

For the experimental bearing and the oil used, the following are the dimensions and average values of physical properties:

$$r_o = 0.7''; \quad r_{av} = 1.03''; \quad r_1 = 1.5''; \quad R_1 = 2.14; \quad \text{Entry Temp. } 70^\circ\text{F};$$

$$\beta = 0.02; \quad \sigma = 0.48 \text{ Btu/lb}^\circ\text{F}; \quad \rho_o = 54.0 \text{ lb/ft}^3; \quad \frac{\rho_o}{\rho_m} = 1.02$$

For the Two-pad Bearing

$$\alpha = 3.04 \text{ rad.}$$

$$\frac{1}{\nu} - \frac{1}{\nu_0} = \frac{\omega}{h^2} (6.50 \times 10^{-6})$$

Three-pad Bearing

$$\alpha = 1.99 \text{ rad.}$$

$$\frac{1}{\nu} - \frac{1}{\nu_0} = \frac{\omega}{(h'')^2} (4.26 \times 10^{-6})$$

Four-pad Bearing

$$\alpha = 1.465 \text{ rad.}$$

$$\frac{1}{\nu} - \frac{1}{\nu_0} = \frac{\omega}{(h'')^2} (3.12 \times 10^{-6})$$

Load-carrying Capacity

$$W \text{ per pad} = \frac{48 \omega \nu_{av} b \alpha r_0^4}{\pi^2 h^2} (-\Sigma W') \quad \dots (59)$$

$$\text{where } b = -\frac{\lambda t}{\alpha} = -0.00043 \frac{t}{\alpha}$$

$$\text{and } \Sigma W' = \sum_1^{\infty} \frac{1}{n^2 [4 - (\frac{\pi n}{\alpha})^2]} \left[\frac{R_1^4 - 1}{4} - \frac{(R_1^2 - R_1^{-\frac{\pi n}{\alpha}})^2}{(\frac{\pi n}{\alpha} + 2)(1 - R_1^{-\frac{2\pi n}{\alpha}})} - \frac{(R_1^{\frac{\pi n}{\alpha}} - R_1^2)^2}{(\frac{\pi n}{\alpha} - 2)(R_1^{\frac{2\pi n}{\alpha}} - 1)} \right]$$

$\Sigma W'$ is evaluated in Chapter III, Section 4.

$$\text{and } \mathcal{N}_{av} = \frac{1}{t} \int_0^t \mathcal{N}_0 e^{-\beta t} dt$$

$$= \frac{\mathcal{N}_0}{\beta t} \left[\frac{e^{\beta t} - 1}{e^{\beta t}} \right]$$

$$\text{Hence } W \text{ per pad} = \frac{\omega \mathcal{N}_0}{h^2} \frac{1}{\beta} \left[\frac{e^{\beta t} - 1}{e^{\beta t}} \right] \left\{ \sum W' \right\} \frac{0.0206 \mathcal{V}_0^4}{\pi^2} \dots (59a)$$

For the 2-Pad Bearing

$$\sum W' = 0.173 \quad (\text{Ch III Sec. IV})$$

$$W \text{ per pad} = \frac{\omega \mathcal{N}_0}{(h'')^2} \frac{1}{\beta} \left[\frac{e^{\beta t} - 1}{e^{\beta t}} \right] 0.603 \times 10^{-6} \text{ lb}$$

$$= \frac{\omega}{(h'')^2} \frac{\mathcal{N}_0 - \mathcal{N}}{\beta} \times 0.603 \times 10^{-6} \text{ lb.}$$

3-Pad Bearing

$$\sum W' = 0.162.$$

$$W \text{ per pad} = \frac{\omega}{(h'')^2} \left(\frac{\mathcal{N}_0 - \mathcal{N}}{\beta} \right) 0.565 \times 10^{-6} \text{ lb.}$$

4-Pad Bearing

$$\sum W' = 0.1274$$

$$W \text{ per pad} = \frac{\omega}{(h'')^2} \left(\frac{\mathcal{N}_0 - \mathcal{N}}{\beta} \right) 0.445 \times 10^{-6} \text{ lb.}$$

Although not strictly correct, since the equations were derived by two entirely different methods, equations (21a) and (59a) may be combined to eliminate $\frac{\omega}{(h'')^2}$ giving the following:

$$\text{For the 2-Pad Bearing } W \text{ per pad} = 4.64 (e^{\beta t} + e^{-\beta t} - 2)$$

$$\text{3-Pad Bearing } W \text{ per pad} = 6.63 (e^{\beta t} + e^{-\beta t} - 2)$$

$$\text{4-Pad Bearing } W \text{ per pad} = 7.13 (e^{\beta t} + e^{-\beta t} - 2)$$

Thus it is seen that the load-carrying capacity of a parallel surface pad, for given bearing dimensions and lubricant properties, is

dependent only on the temperature rise through the pad, according to this rather loose reasoning at least.

As may be seen from Figs. 33a, b and c, this statement appears to have some slight corroboration in practice.

Coefficient of Friction

The coefficient of friction is

$$f = \frac{\omega N_{av}}{P} \frac{r_o}{h} \frac{2}{3} \left(\frac{R_1^2 + R_1 + 1}{R_1 + 1} \right) \dots (72)$$

For the experimental bearing $R_1 = 2.14$

$$\text{Hence } f = \frac{\omega N_{av}}{p} \frac{r_o}{h} 1.64$$

$$\text{or } f = \frac{\Sigma N}{p} \frac{r_o}{h} 2.49 \times 10^{-8}$$

Z in centipoise

N in rpm

p in psi

r_o, h in inches.

Energy Balance

Friction Torque = T lb-ft per bearing surface.

Work = 2 T ω ft-lb/sec for two bearings.

Flow = Q lb/min.

Heat to oil = $\frac{Q \times 0.48 \times t}{60}$ Btu/sec

Therefore 2 T ω = Q t $\frac{0.48}{60}$ x 778

$$\omega.T = 3.11 Q t$$

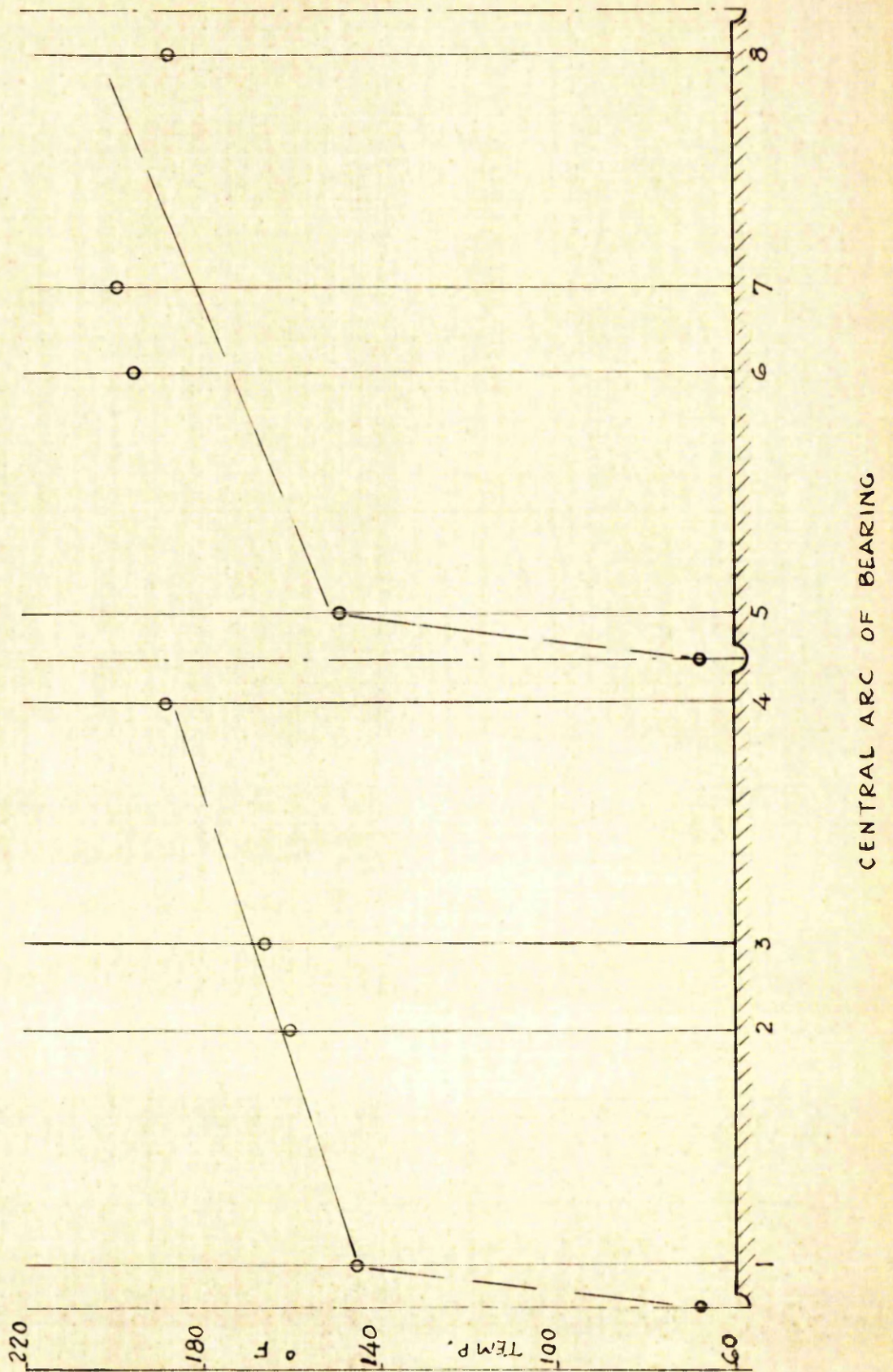


FIG 28 a TEMPERATURES AROUND CENTRAL ARC
TEST NO 2-36

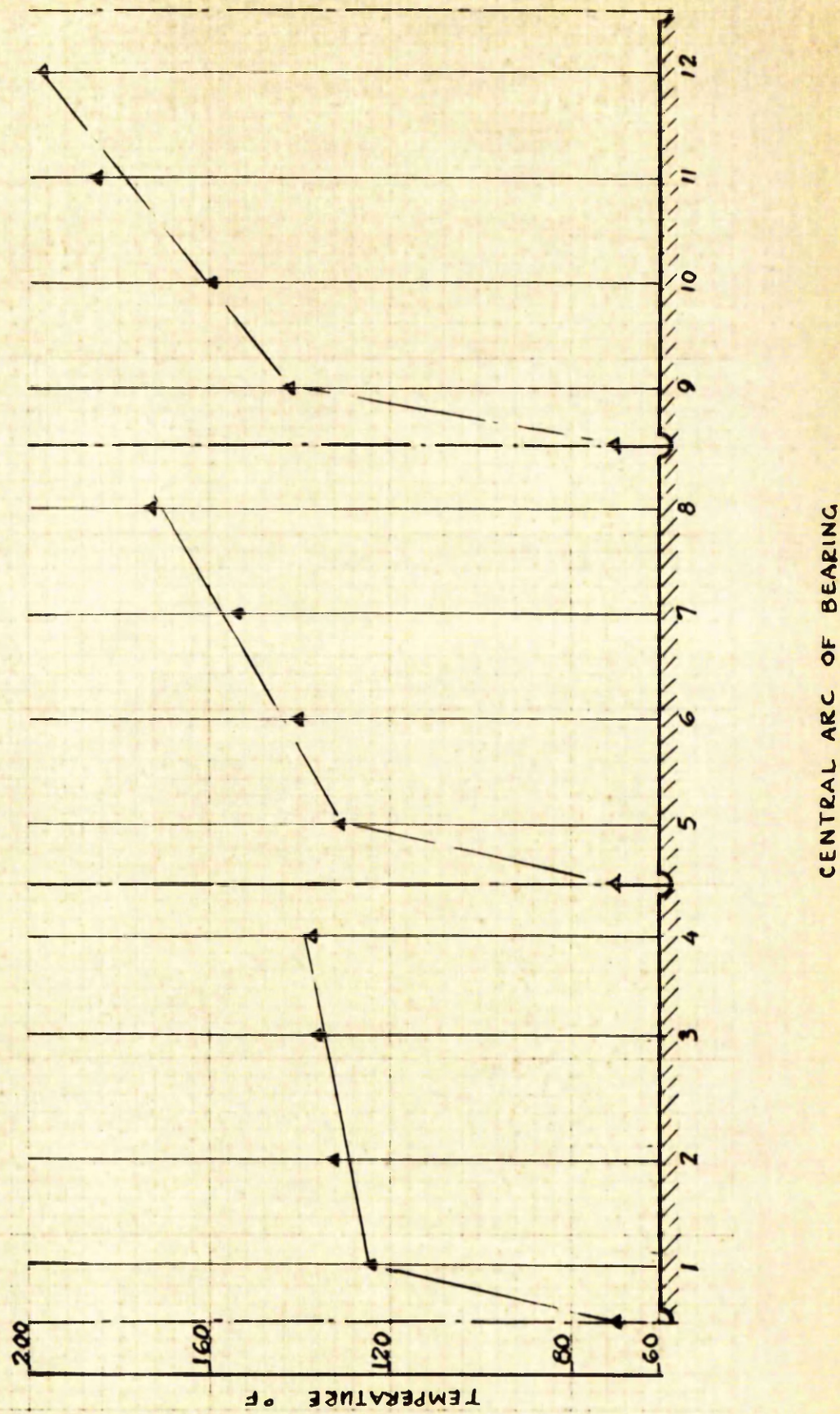


FIG. 28 b TEMPERATURES AROUND CENTRAL ARC, $r = 1.16$ in
TEST N° 3-5

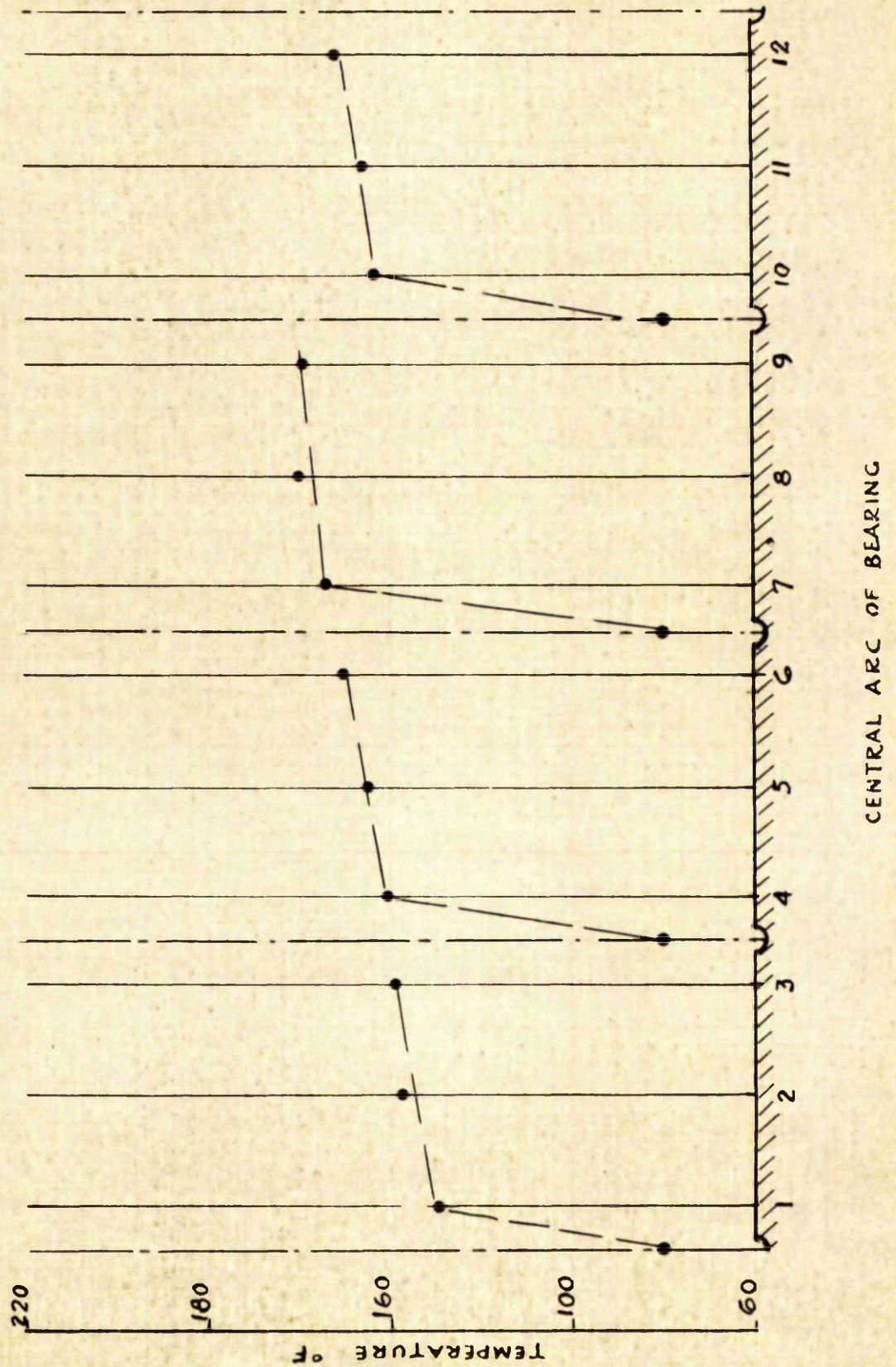


FIG 28c. TEMPERATURES AROUND CENTRAL ARC, $r = 1.16$ in
 TEST N^o 4-10

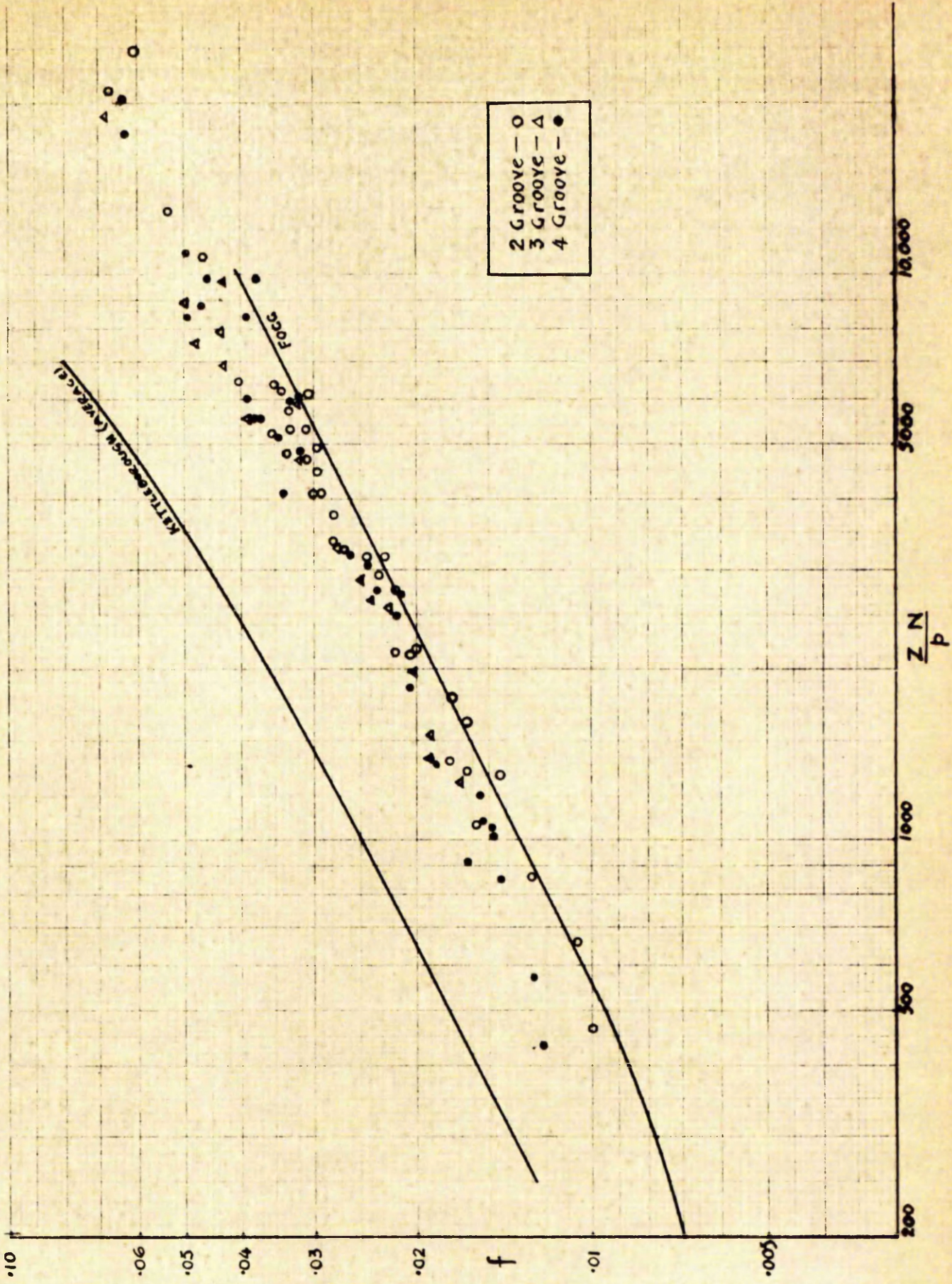


FIG. 29 COEFFICIENT OF FRICTION 'f' v. PARAMETER $\frac{ZN}{p}$
COMPARISON WITH PREVIOUS EXPERIMENTERS

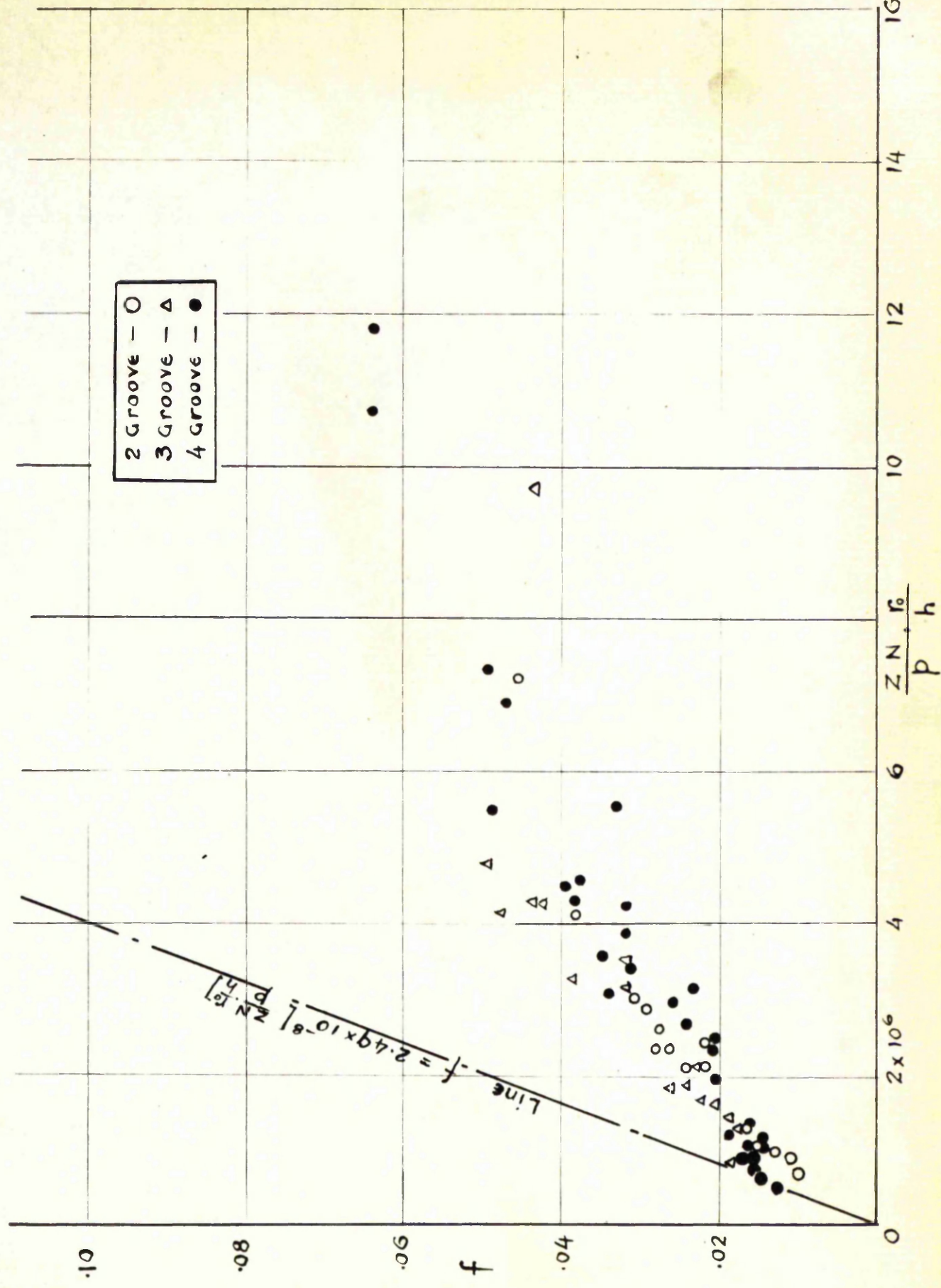


FIG 30 COEFFICIENT OF FRICTION 'f' v PARAMETER $\frac{ZN}{p} \cdot \frac{h}{2 \times 10^6}$

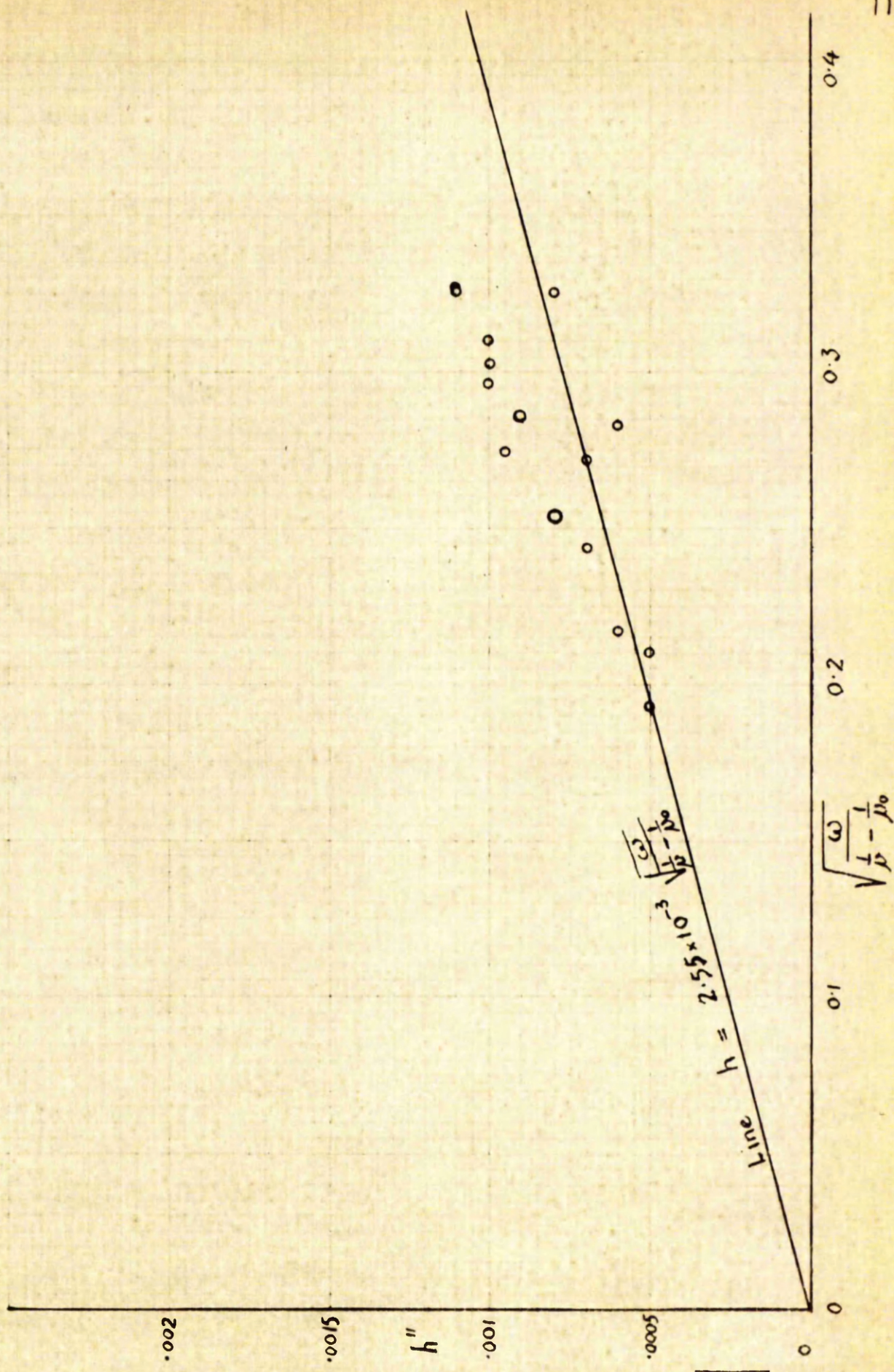


FIG. 31a. FILM THICKNESS 'h in.' v. PARAMETER $\sqrt{\frac{\omega}{\mu - \mu_0}}$
 2 GROOVE BEARING

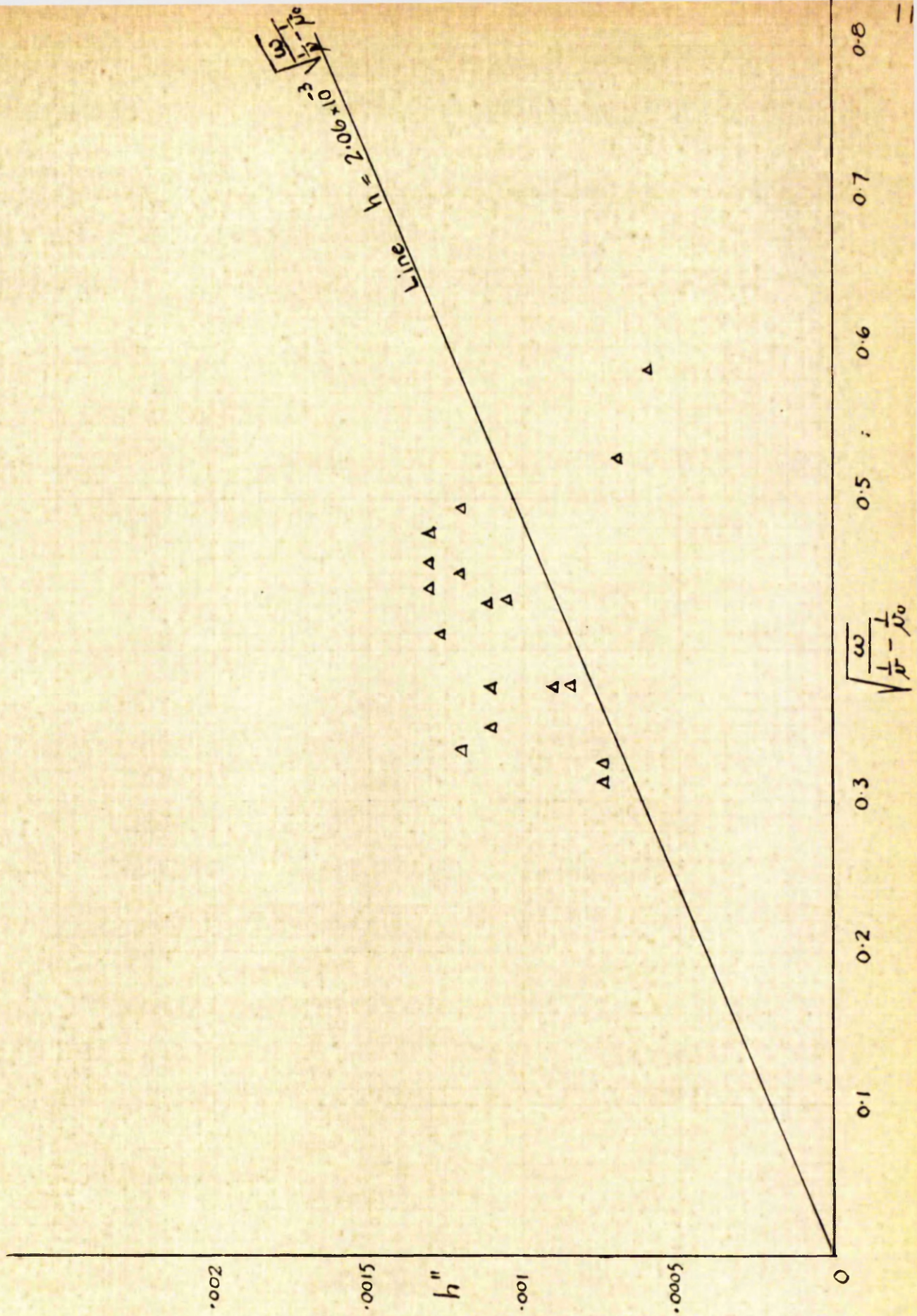


FIG. 31b. FILM THICKNESS 'h in.' v PARAMETER
3 GROOVE BEARING

$$\sqrt{\frac{1}{\nu} - \frac{1}{\nu_0}}$$

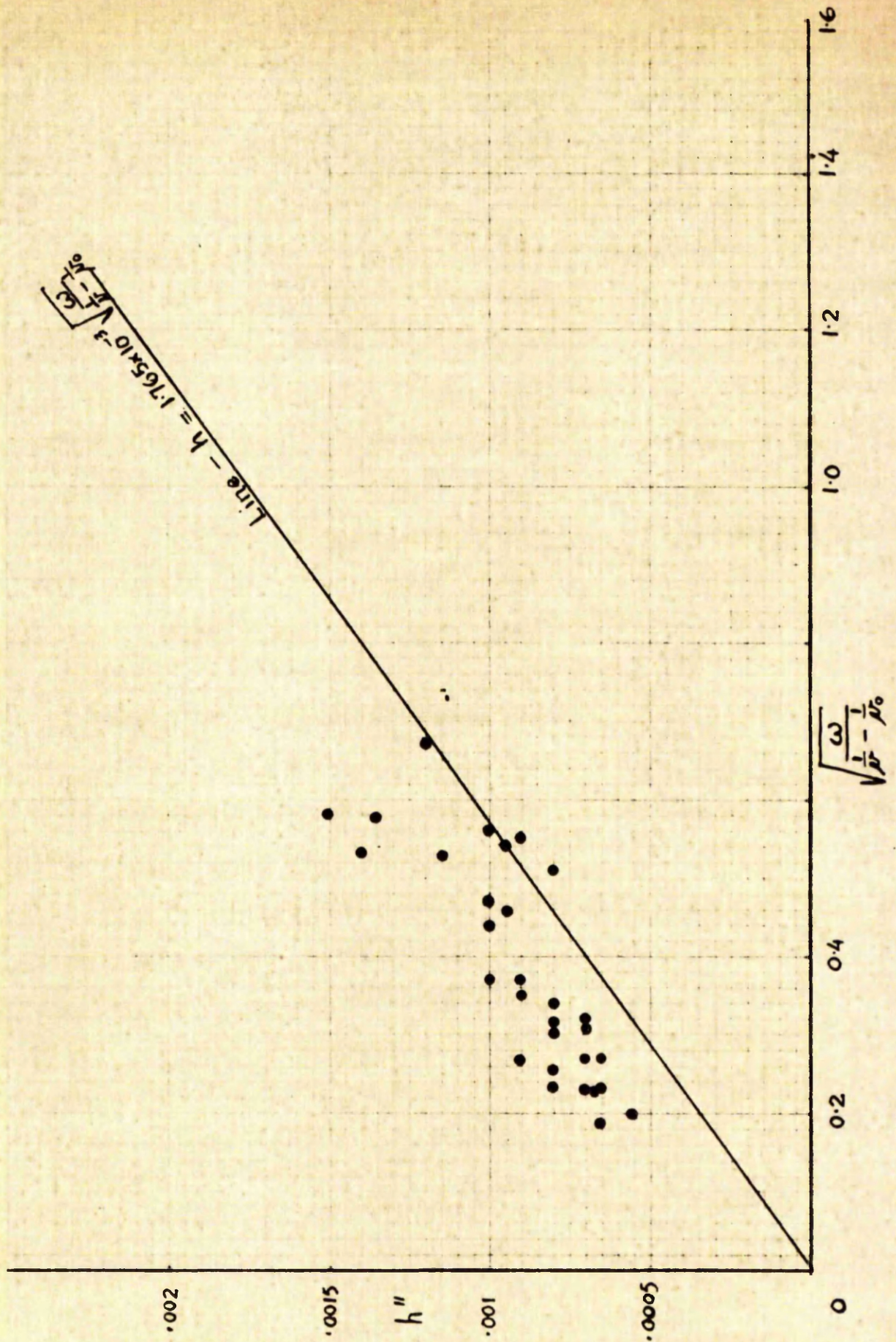


FIG. 31c. FILM THICKNESS 'h'' v. PARAMETER $\sqrt{\frac{\omega}{\nu} \left(\frac{1}{\nu} - \frac{1}{\nu_0} \right)}$
4 GROOVE BEARING

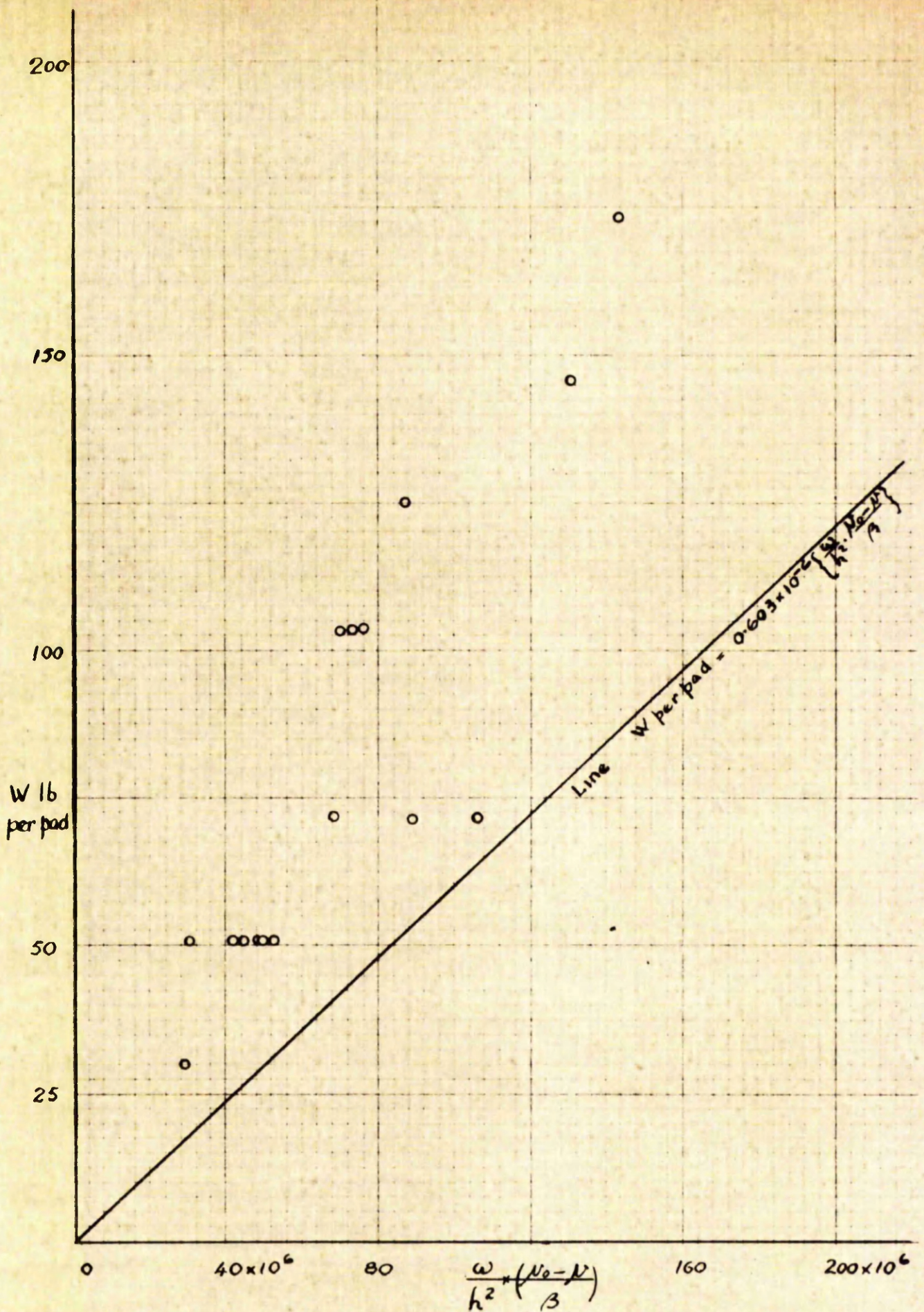


FIG 32a W per pad (lb.) v. PARAMETER
2 GROOVE BEARING

$$\left\{ \frac{\omega}{h^2} \times \frac{N_0 - N}{\beta} \right\}$$

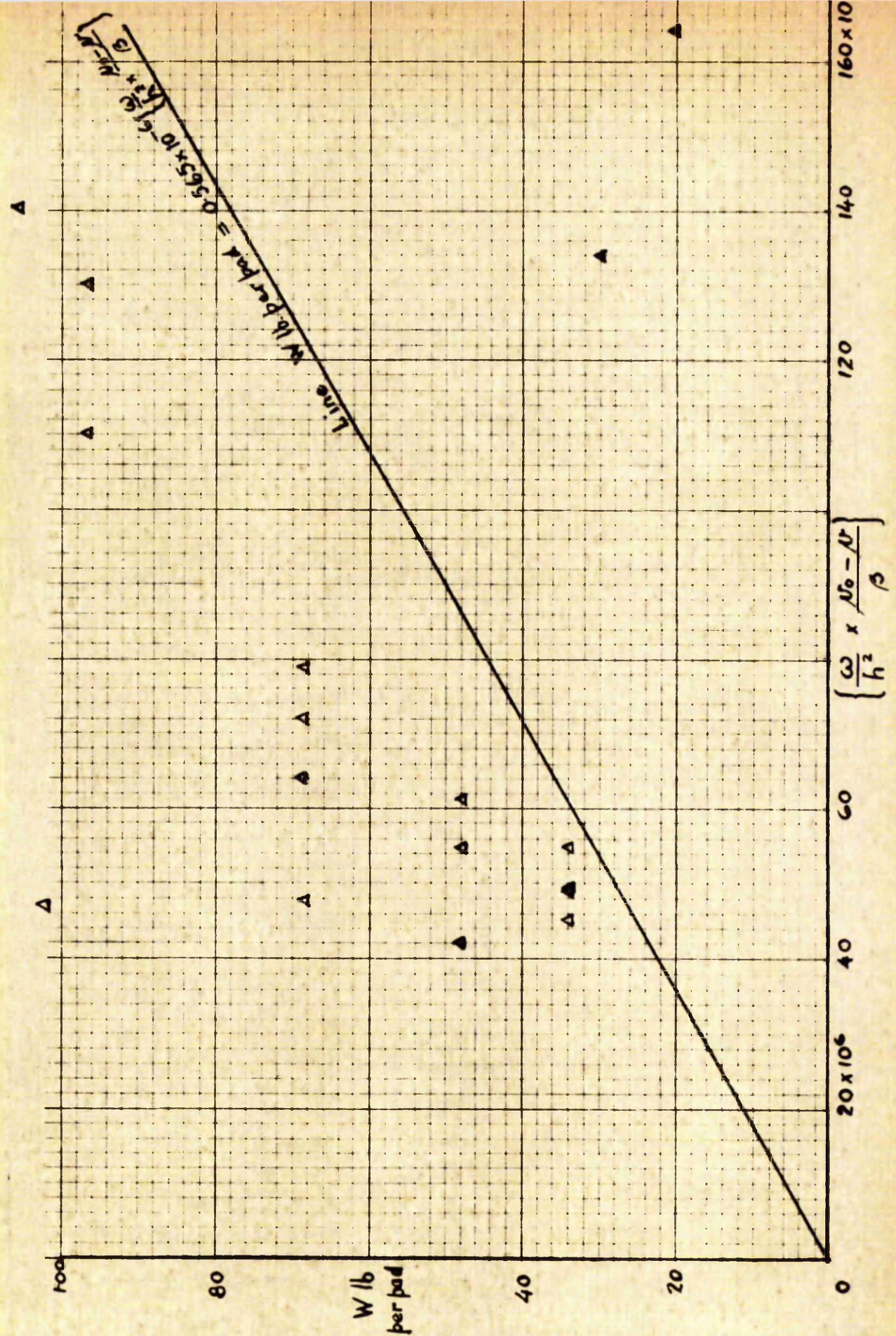


FIG. 32 b. LOAD W lb per pad v. PARAMETER $\left\{ \frac{\omega}{h^2} \times \frac{16-l}{\beta} \right\}$
3 GROOVE BEARING

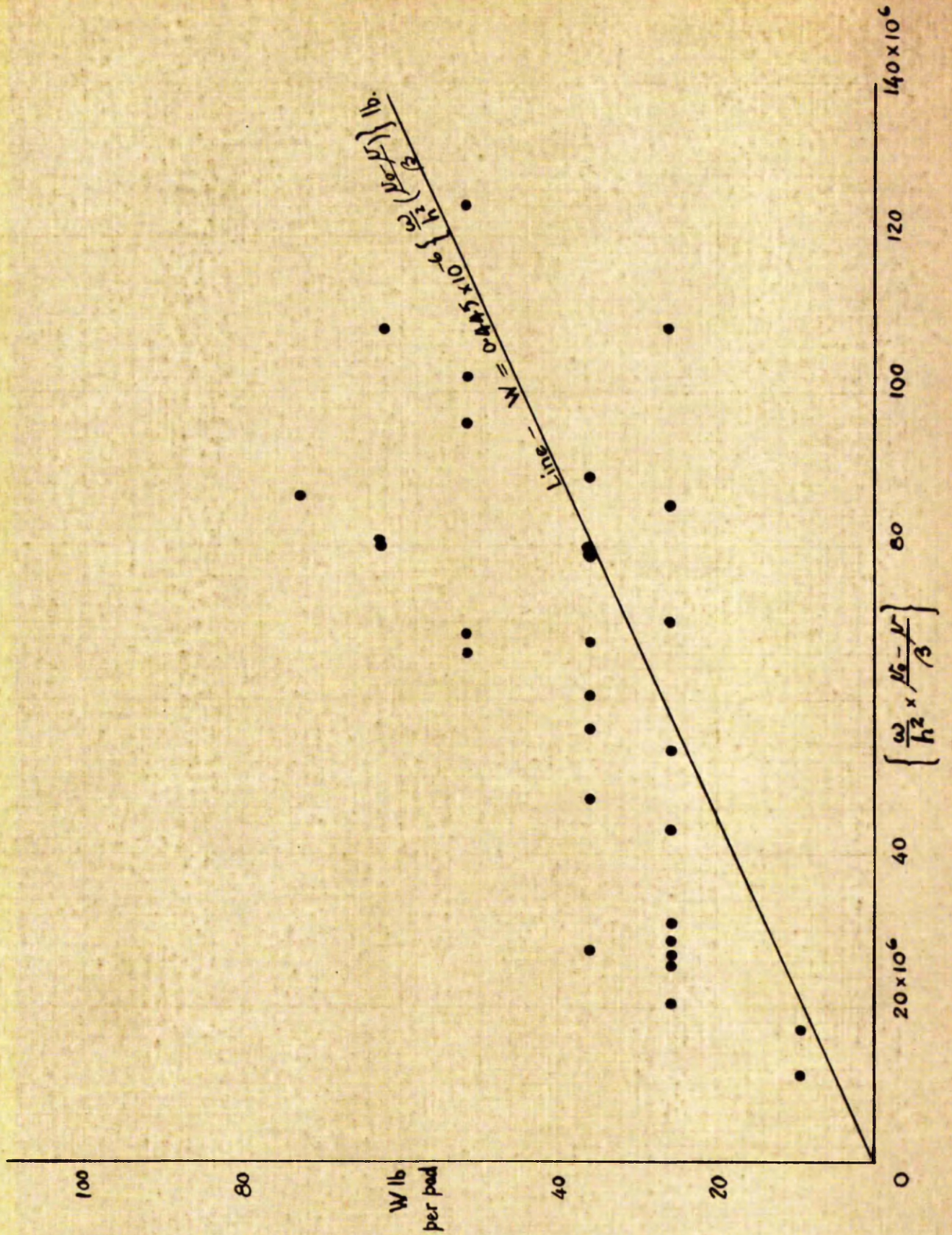


FIG 32c. LOAD W lb. per pad v. PARAMETER $\left\{ \frac{\omega}{h^2} \times \frac{M_0 - \nu}{\beta} \right\}$
 4 GROOVE BEARING

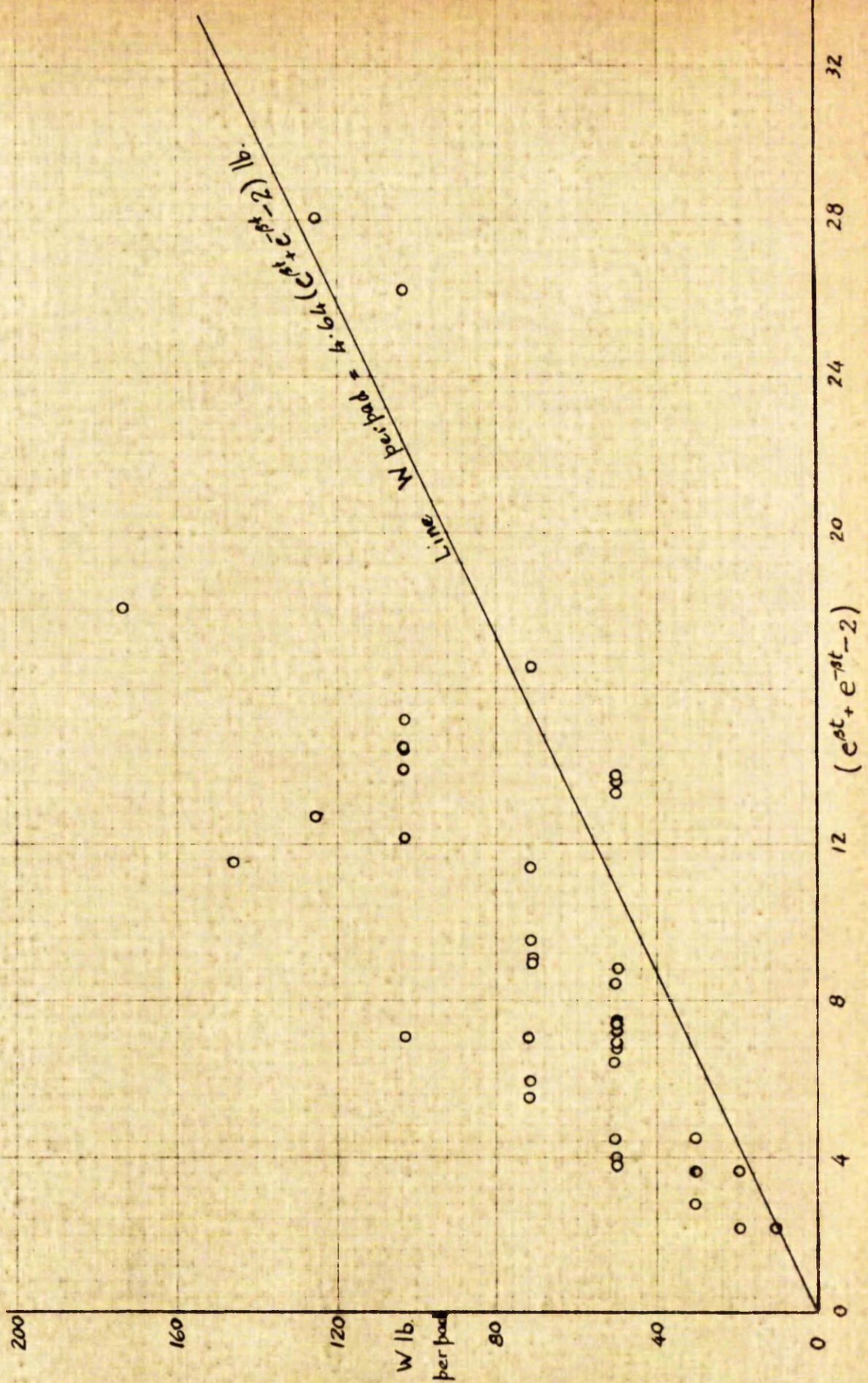


FIG 33a. W lb. per pad v. FUNCTION $(e^{\beta t} + e^{-\beta t} - 2)$
2 GROOVE BEARING

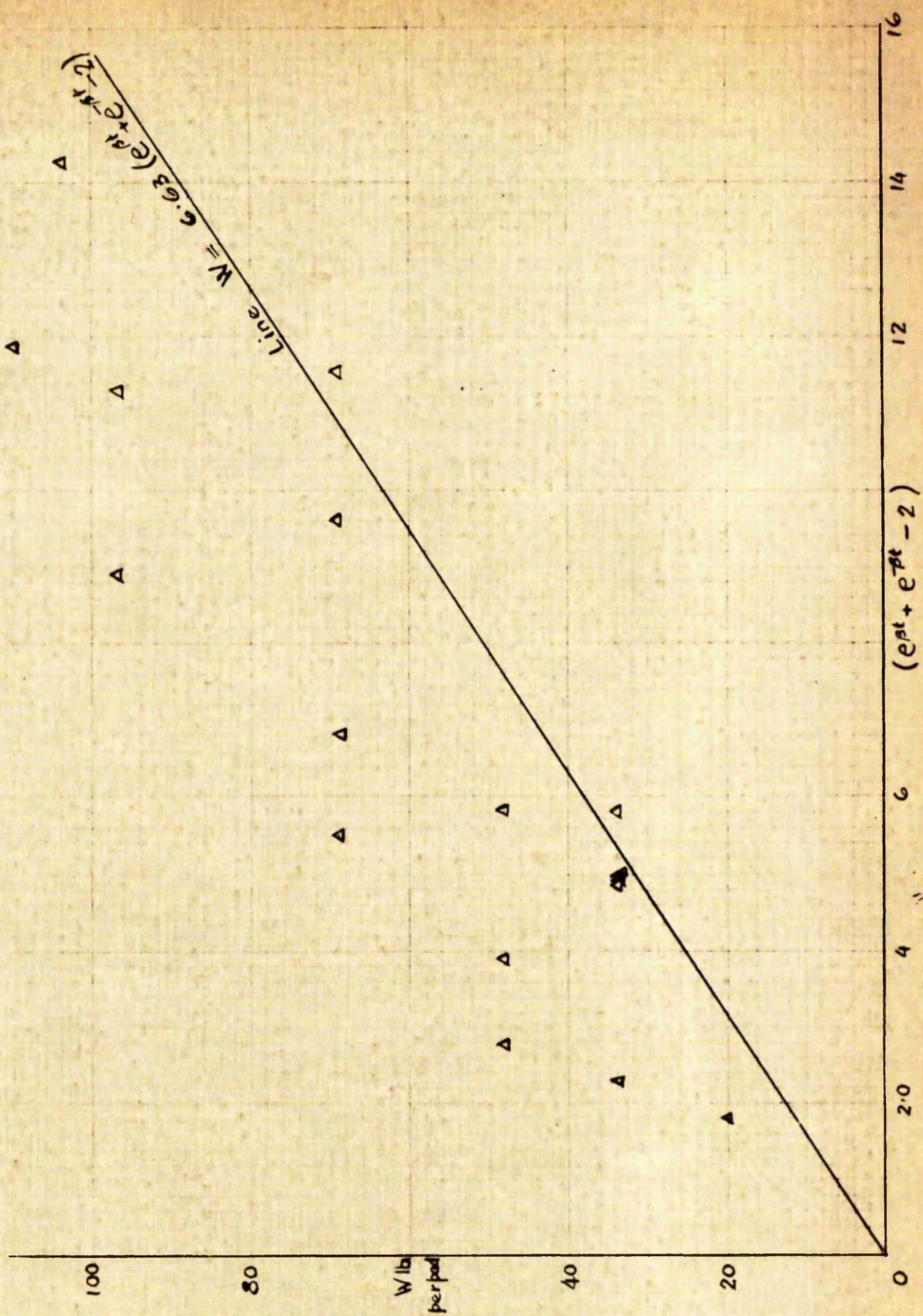


FIG. 33 b. LOAD W lb. per pad v. FUNCTION $(e^{\beta t} + e^{-\beta t} - 2)$
3 GROOVE BEARING

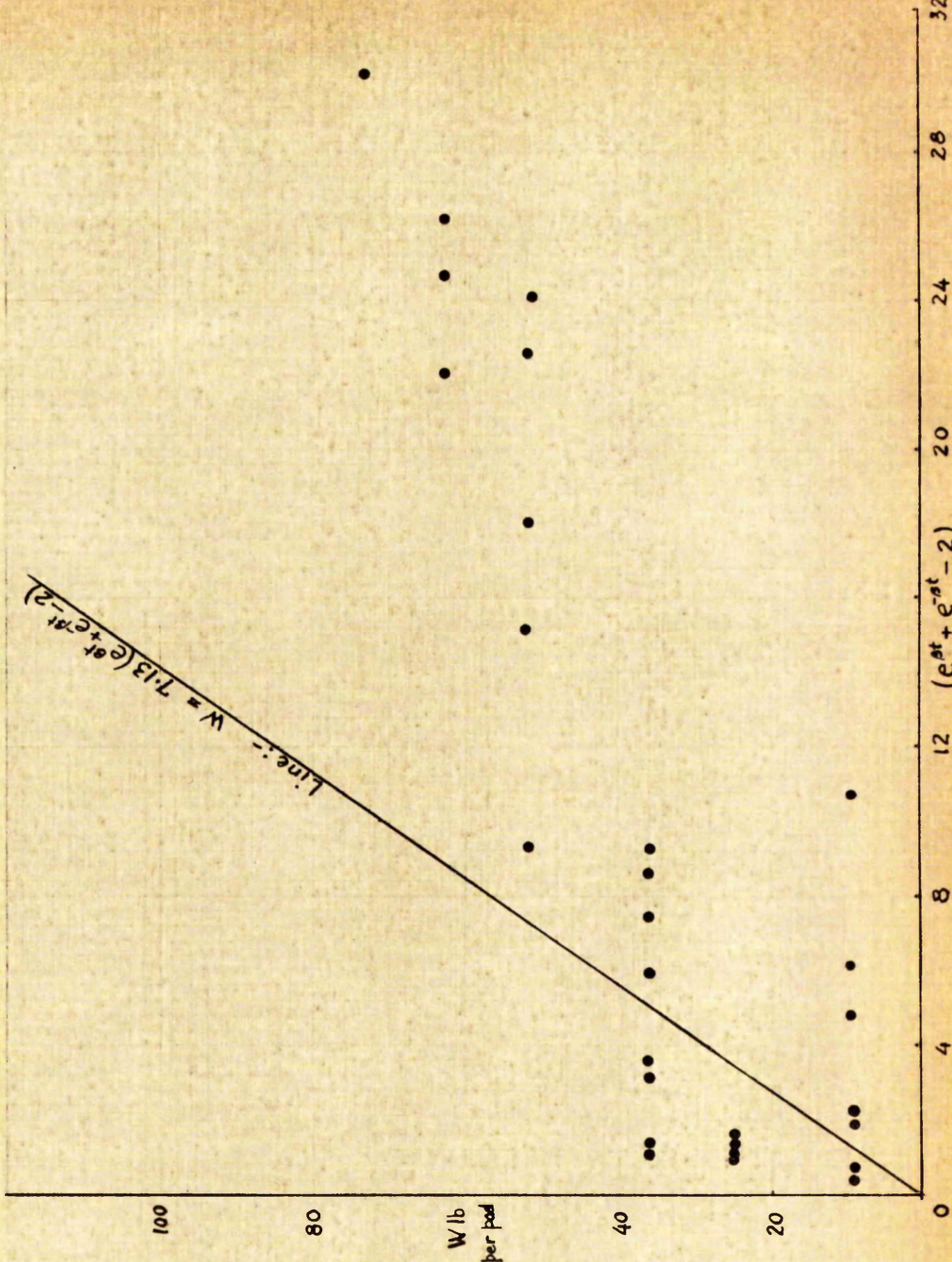


FIG. 33 c. LOAD W lb per pad v. FUNCTION $(e^{\beta t} + e^{-\beta t} - 2)$
 4 GROOVE BEARING

V. 3. Discussion of Results

The experimental results are presented graphically in Fig. 28 to 33, and the tabulated values from which the graphs are drawn are shown in Tables 1 to 10, in Appendix I.

For the three specimen tests, 2-36, 3-5 and 4-10, the temperatures which were recorded around the central arc at the mean radius 1.16 in., are plotted in Fig. 28. The temperature distributions for most other tests were similar to these.

It may be seen that a simple temperature gradient is not obtained. The oil in the grooves is assumed to be at the oil inlet temperature. There is a very rapid rise from the oil inlet temperature to the temperature shown by the first thermocouple; then there is a steady temperature rise, at a rather flat gradient, around the bearing pad.

It would appear that two factors, which were not correctly accounted for, influence the temperature readings. The actual oil temperature in the grooves is almost certainly higher than the recorded inlet temperature, which was measured by a single thermocouple in the annular supply space, and not in the grooves. Since a certain amount of oil is carried around the bearing, there will be a mixing in the grooves of fresh oil and recirculating oil, making the inlet temperature to the pad higher than the recorded value.

It was intended to test a bearing with separate inlet and outlet grooves as shown in Fig. 34.

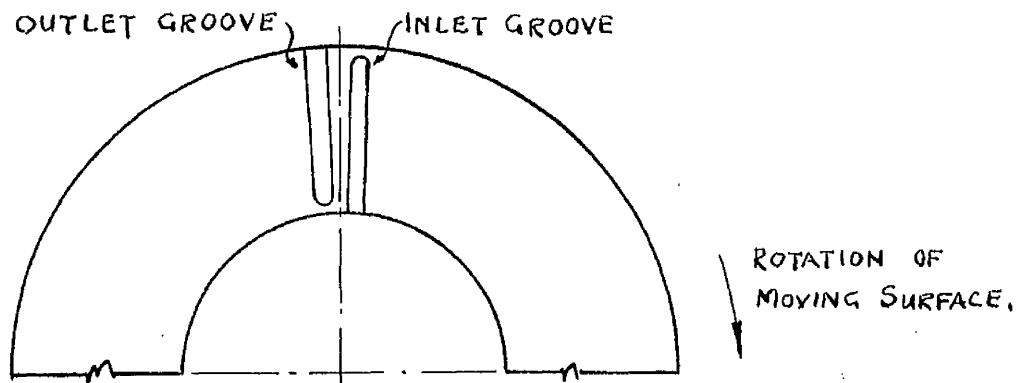


Fig. 34. Proposed Bearing with Separate Inlet and Outlet Grooves.

In this way a truer measure of the temperature rise taking place around the bearing surface itself would have been obtained. Unfortunately, the tests were halted by the breakdown of the machine before this could be done.

It is also thought that the standard method used in this work to measure oil film temperatures is not quite accurate. Thermocouples embedded in the bearing surface, although in non-conducting material, are greatly influenced by the surrounding and opposing bearing faces, and it is difficult to see how errors due to conduction and radiation can be avoided. These effects would cause a "temperature inertia," causing thermocouples to register a higher temperature at inlet and a lower value at outlet than the actual oil film temperatures.

With these arguments in mind, the temperature rise around the bearing pad, $t^{\circ}\text{F}$, was taken as $T_{\text{max.}}$ (at outlet) minus T_0 (at inlet). It is probable that both of these values as recorded are too low, so

that their difference, t , may not be too much in error. The average temperature, which gives the average viscosity Z , was taken as $T_0 + 2/3t$. It should be noted that the parameter $\frac{ZN}{p}$ is greatly affected by the value taken for Z . Previous experimenters have taken the average viscosity as obtained from one thermocouple per pad (Fogg, 3), or as the mean of inlet and outlet values (Kettleborough, 4).

As a general correlation with other workers, the coefficient of friction is plotted against $\frac{ZN}{p}$, for all tests, Fig.29. Although $\frac{ZN}{p}$ is not in consistent units and is not directly related to f , the results follow fairly well a linear pattern on a log-log scale, which has the same slope as the curves of Fogg and Kettleborough, and in fact come quite close to Fogg's results, although the magnitude of loads was much smaller than Fogg's. The difference in the three sets of results is probably in good part due to the different values employed for the average viscosity Z .

The correct non-dimensional parameter for a parallel thrust bearing is $\frac{ZN}{p} \frac{r}{h}$ as derived in Section III.5. When the coefficient of friction f is plotted against $\frac{ZN}{p} \frac{r}{h}$, the experimental results can be compared with the theoretical equation

$$f = 2.49 \times 10^{-8} \frac{ZN}{p} \frac{r}{h}$$

for this particular bearing, as shown in Fig.30. There is a marked scatter in the experimental points, but, in general, the test results lie on a flat curve. Experimental results taken from Kettleborough's paper (4) and plotted in the above manner are in close agreement with the author's results. Although correlation with the theoretical curve is very poor, the experimental points can be brought into substantial agreement if the viscosity at maximum bearing temperature is used instead of the average value.

The difference might be due to three factors:

(a) A low value of measured friction.

The friction torque as measured might have been in error, because of under-compensation for static friction effects. The static friction, due to stationary end seals and support roller bearings, was measured at no load and no speed, and added to the friction torque measured during a test. Although the static friction was independent of load and speed, it may have increased during running because of the effect of temperature on the oil seals and bearings, but this is unlikely.

(b) A high value of $\frac{ZN}{p} \frac{r}{h}$.

For a given friction value, the corresponding $\frac{ZN}{p} \frac{r}{h}$ may have been too high. The measured quantities N and r can be accepted as substantially correct.

The applied load, which gives the bearing pressure p , is also probably correct. In some early tests, however, when aluminium loading pistons were used in the steel cylinder, differential expansion caused the pistons to stick and very high loads were applied without being recorded. This fault was corrected by using cast iron pistons with a little more clearance, and rubber o-rings as piston rings.

The possibility of error in measuring Z and h is much greater. The average film temperature, which has already been discussed, could be in error by, say, 10% - between 100°F and 90°F, the viscosity changes fro

27.4 to about 36 centipoise, a difference of 30%. This difference in viscosity becomes smaller at higher temperatures, however.

In a similar way, it is doubtful if the film thickness measurements are accurate to within 0.0002", which may mean an error in the order of 20% on normal readings.

These large percentage errors which are inescapable when measuring very small or ill-defined quantities, make individual readings almost worthless. However, when a large number of tests is considered and the results plotted, the general trend of the results can be observed and compared to theoretical curves, the extent of the scatter being an inherent indication of experimental accuracy.

c) Boundary lubrication.

There is considerable doubt in the author's mind that true film lubrication occurred in all tests, especially at high loads (usually low $\frac{ZN}{p}$ values.)

Quite frequently during the course of testing, several instances of non-fluid-film lubrication and even metal-to-metal contact were noted, mainly symptomised by unstable temperatures and vibration. These obvious mal-functioning tests were discarded as has been previously noted. However, it was observed that some of these tests did not show much higher values of the coefficient of friction, the difference between tests purporting to be run under conditions of fluid-film lubrication and those which obviously were not, being fairly small. Unlike the case of the journal bearing, there does not appear to be a well-defined change between hydrodynamic and boundary lubrication for the parallel surface

thrust bearing. Following this reasoning further, it would seem that a linear plot of f against $\frac{ZN}{p}$ is not in itself a complete indication of fluid-film lubrication for a parallel surface thrust bearing.

This can be explained when one considers that in a journal bearing, when the film thickness diminishes, metal-to-metal contact takes place along a very narrow linear area, with high pressure and positive contact; whereas with the parallel surface bearing, when the film thickness is of the same order of magnitude as the surface roughness, it will be possible to have film lubrication with intermittent contact of asperities over the whole surface at low metal-to-metal pressures.

The experimental values of film thickness are in good agreement with the predicted values, Fig. 31a, b and c, although again there is a wide scatter, and the range of values along the abscissa is rather small. The scatter of the points would seem to be in accordance with the estimated accuracy of measurement, to the nearest 0.0002in. Recorded film thickness values appear to be about 20 or 30% greater than the predicted values, in the three-groove and four-groove bearings.

When the load per bearing pad is plotted against the parameter

$$\left(\frac{w}{h^2} \frac{\nu_0 - \nu}{\beta} \right)$$

in Fig. 32a, b and c, the correlation of theoretical and actual values is again apparent, although to a lesser extent, and the scatter of points is even more pronounced than on the previous graphs.

The side scatter is undoubtedly due to the h^2 term in the denominator of the parameter. It should be noted again that in this series of experiments, it was found that the maximum bearing load that could be carried safely was about 350 lb., giving a bearing pressure of some 70 psi. This load is very much lower than those reported by Fogg (2,200 lb, probable pressure 440 psi), but it is in agreement with Kettleborough (4) and with long-established marine practice for parallel surface thrust bearings.

When the load per pad is plotted against the function $(e^{\beta t} + e^{-\beta t} - 2)$ in Fig. 33a, b and c, experimental scatter is extremely pronounced and correlation of theory and practice is not good. It will be recalled, however, that $W = \text{fn}(e^{\beta t})$ is not a true mathematical relationship (Section V.2), so that exact correlation should not be expected. For the two-groove and the three-groove bearings, the trend of the experimental points appears to be fairly close to the theoretical line, and some correlation might be claimed. For the four-groove bearing, the actual load curve is at a much smaller gradient than the predicted line, giving a lower load-carrying capacity than indicated for a given temperature rise. One possible explanation for this is that the four-groove bearings ran at higher maximum temperatures (see Table 9 in Appendix I) so that the method of calculating the temperature rise, t , may have been more in error for the four-groove than for the other bearings.

From the trend of the results in Fig. 33, there is some justification for stating that the load-carrying capacity is a function of the

temperature rise around the pad for a given bearing and a given oil. On this assumption an empirical formula could probably be obtained to give better accuracy than the developed equations used in Fig. 33.

The difficulty in obtaining accurate measurements of film thickness and oil film temperature, as evidenced by the scatter of experimental points, allows no definite conclusions to be drawn. Sufficient correlation is shown, however, so that the theoretical equations

$$f = A \left(\frac{ZN^2 r}{p h} \right) + B$$

$$h = \text{const.} \left(\frac{\omega}{\frac{1}{\nu} - \frac{1}{\nu_0}} \right)$$

$$W = \text{const.} \left(\frac{\omega}{h^2} \frac{\nu_0 - \nu}{\beta} \right)$$

$$W = \text{fn}(e^{\beta t})$$

can be used with confidence to predict the performance of a parallel surface thrust bearing.

CHAPTER VI

VI. 1. Conclusions

VI. 1. Conclusions

The objectives of this research work, which were in brief, to expand the theoretical analysis to include the effect of side leakage, to demonstrate and measure the circumferential temperature gradient in a sector bearing, and to compare theoretical performance curves with actual experimental values, have been accomplished. The detailed conclusions which may be drawn from the results obtained are as follows:

(1) Theoretical Analysis

Two equations, a general expression of Reynolds equation and an energy equation, govern the hydrodynamic behaviour of a parallel surface thrust bearing. These equations have been solved by three different methods and the three solutions, III.1, III.2 and III.3, have been compared by evaluating each for the same arbitrary sets of operating conditions.

Solution III.2 which was obtained by a relaxation process, is the only solution which does not require simplifying assumptions, and thus is considered to be the most accurate. Using this solution as a basis of comparison, it is deduced that the assumption of an infinitely wide bearing, but including the effect of viscosity variation, has little effect on the temperature distribution, (also noted by Cameron and Wood, 8), but leads to large errors in pressure values.

Solution III.3 assumes constant viscosity, but includes the effect of side leakage and leads to a close approximation for pressure distribution and the correct load-carrying capacity, but temperature values are in error. This method of calculating the load-carrying capacity is given confirmation by close agreement with the published experimental values of Kettleborough (4).

Since the relaxation method of Solution III.2 requires a complete series of calculations for each change in running conditions, it is not suitable for design purposes nor does it produce theoretical performance curves. Accordingly, the general equations for temperature from Solution III.1 and for pressure and load carrying capacity from Solution III.3 are used.

Temperature: Solution III.1

$$t = \frac{1}{\beta} \ln(G, x + 1)$$

Pressure: Solution III.3

$$p = \frac{2}{\alpha} \sum_{n=1}^{\infty} \bar{p}_n \sin\left(\frac{n\pi\theta}{\alpha}\right)$$

Load Carrying
Capacity: Solution III.3

$$W. \text{ per pad} = \int_{r_0}^{r_1} \frac{4r}{n\pi} \sum_1^{\infty} \bar{p}_n dr$$

The summations are for odd values of n.

(2) Apparatus

The experimental apparatus was designed primarily as a torque-mounted thrust bearing to run at high rotational speeds, with no unbalanced end thrust, and having a large number of thermocouples in the bearing faces. These primary considerations and the fact that the apparatus was built on a rather limited budget, which necessitated using and adapting equipment which perhaps was not entirely satisfactory, but which was available, resulted in some inaccuracies of measurement.

When measuring film thicknesses by a system of dial gauges, metal expansion effects of the same order or greater than the required quantities were encountered. Although by making suitable zero adjustments, these expansion effects were taken into account, the accuracy of such measurements must be greatly reduced. To obtain the accuracy necessary to measure oil films less than 0.0005 in. thick, a very rigid housing and mounting would be required, with bearing faces flat and parallel to extremely close limits. An electrical capacitance method would measure the distance between the bearing surfaces directly, thus eliminating the effect of thermal expansion of the housing, etc. In addition, an electrical system would give a positive indication of metal-to-metal contact in the bearing.

The temperature of the oil film around the bearing pad was measured by thermocouples embedded in plugs and flush with the white-metal surface. Although this type of temperature measurement is accepted as normal and has been used by several experimentors, it is doubtful if such a method can give, with any accuracy, the temperature gradient in a very thin oil film between two extensive metal surfaces. However, since no better arrangement was available, this method was employed, with reservations. (noted on p.128, Ch. V).

The self-contained design of the test unit, in which the loading jacks were mounted around a central barrel making the friction-measuring bearings and end seals independent of load, was very satisfactory and gave accurate and easily reproducible readings for bearing friction.

The high speed aspects of the test equipment offered no serious problems. It is felt that in an arrangement similar to this, running at speeds above the critical would give improved testing conditions, with a lower noise level and a minimum amount of vibration. Operating in this speed range would entail very careful initial balancing and a close control of wear and imbalance over the period of testing.

(3) Temperature Gradient.

The temperatures recorded indicate that a thermal gradient does exist in the circumferential direction in a parallel surface thrust

bearing. However, as already explained, an accurate measurement of the temperature gradient was not obtained. An average temperature gradient was estimated from inlet and outlet oil temperatures, the temperature rise being checked by considering a simple energy balance.

The temperature gradients thus obtained are shown to be sufficient to produce the loads carried by the bearing; in this case a maximum bearing pressure of 60-70 psi required a temperature rise of about 150°F. For a bearing pressure of 440 psi, which is the estimated maximum pressure reported by Fogg (3), a temperature rise of about 290°F would be required in this bearing. The corresponding film thickness would be of the order of 0.0002 in. at a speed of 10,000 rpm.

(4) Correlation of Results.

From the equations for temperature and pressure shown above, the following operating characteristic equations have been developed:

$$\text{Coefficient of friction } f = \text{const.} \left(\frac{ZN}{P} \cdot \frac{r}{h} \right)$$

$$\text{Film thickness } h = \text{const.} \sqrt{\left(\frac{\omega}{\nu} - \frac{1}{\nu_0} \right)}$$

$$\text{Load per pad } W = \text{const.} \left(\frac{\omega}{h^2} \cdot \frac{\nu_0 - \nu}{\beta} \right)$$

$$W = \text{const.} (e^{\beta t} + e^{-\beta t} - 2)$$

The experimental points were plotted, and where applicable the corresponding theoretical curve is shown on the same sheet. Although in all cases scatter of the experimental points is pronounced, sufficient correlation is obtained to justify the use of the above equations in predicting parallel thrust bearing performance.

(5) The Thermal Wedge Bearing.

While the immediate objectives of this thesis have been achieved, it must be recognized that this accomplishment still does not constitute a complete and final study of the thermal wedge bearing. Due to certain inevitable inaccuracies in experimental technique, and to the indefinite character of the thermal wedge phenomenon, especially the ill-defined transition from film to boundary lubrication in this type of bearing, the experimental results may be open to other interpretations.

It is believed that the trend of the results is in agreement with the theory which has been developed, which would indicate that thermal wedge lubrication occurs within the range of the test conditions. The test bearing had a maximum load-carrying capacity of about 60 to 70 psi, which is in the same range as the old-fashioned parallel surface marine bearings. This load corresponds to the required temperature rise of 150°F and a film thickness of 0.0005 in. Since the test bearing was flat and parallel only within normal engineering limits, it is likely that a film thickness less than this would result in boundary lubrication and metal contact.

By extrapolating from the load graphs, Fig. 32 and 33, it would seem that a thermal wedge bearing is capable of carrying high loads, say 500 psi, but in the test bearing, this would require a temperature rise of some 300°F and a film thickness of less than 0.0002 in. These operating values would be extremely difficult to maintain in a conventional thrust bearing without oil breakdown or mechanical failure.

It would appear, therefore, that while the thermal wedge effect does exist and is appreciable in parallel surface thrust bearings, high load carrying capacity is prevented because high temperature gradients and very thin oil films cannot be achieved in normal engineering practice. There appears to be no reason why the thermal wedge method of obtaining a load-carrying fluid film should not be employed in some other type of unconventional bearing or in some field other than bearing lubrication.

LIST OF REFERENCES

- (1) H.T. Newbigin 'The Problem of the Thrust Bearing.'
Proc. I.C.E. vol. 196, p.223. 1914.
- (2) O. Lasche 'Friction Relations in High Speed Bearings.'
Traction and Transmission vol.6, p.33. 1903.
- (3) A. Fogg 'Fluid Film Lubrication of Parallel Thrust
Surfaces.' Proc. I. Mech.E. vol.155,
p.49, 1946.
- (4) C.F. Kettleborough 'Tests on Parallel-Surface Thrust Bearings.'
Engineering. p.174, Aug. 5, 1955.
- (5) G.S. Bower Discussion to paper by Fogg (3) above.
- (6) M.C. Shaw 'An Analysis of the Parallel-Surface
Thrust Bearing.' Trans. ASME, vol.69,
p.381, 1947.
- (7) H. Blok Discussion to paper by Shaw (6) above.
- (8) A. Cameron and 'Parallel Surface Thrust Bearing.'
W.L. Wood 6th Int. Congress App. Mech. Paris 1946.
- (8a) Ditto A.S.L.E. Trans. 1, 2. p.254 October 1958
- (9) D.G. Christopherson 'A New Mathematical Method for the Solution
of Film Lubrication Problems.'
Proc. I.Mech.E. vol.146, p.126. 1942
- (10) W.F. Cope 'The Hydrodynamical Theory of Film
Lubrication.' Proc.Royal Soc. vol. 197A,
p.201. 1949.
- (11) F. Osterle, A. 'Solution of the Reynolds Equation for
Charnes, E.Saibel Slider-Bearing Lubrication - VI'
Trans. ASME vol.75, p.1133. 1953.
- (12) F. Osterle, 'On the Energy Equation for Fluid-Film
A.Charnes, E.Saibel Lubrication.'
Proc. Roy.Soc. vol.214, p.133. 1952.
- (13) O.C. Zienkiewicz 'A note on a New Theory of Hydrodynamic
Lubrication of Parallel Surface Thrust
Bearings.' 9th Congrès Int. Mécan Appl.;
Univ. Bruxelles 4 p.251 1957.

- (14) A. Cameron 'The Viscosity Wedge.' A.S.L.E. Trans.
1, 2. p.248 October 1958
- (15) 'A Pocket Book of Tables'
Shell Petroleum Co. Ltd. 1951
- (16) H.W. Swift Discussion to paper by Fogg (3) above.
- (17) A.G.M. Michell 'Lubrication'
Blackie and Son, Ltd., 1950
- (18) I.N. Sneddon 'Fourier Transforms'
McGraw-Hill Book Company, 1951.
- (19) D.N. deG. Allen 'Relaxation Methods'
McGraw-Hill Book Company, 1954.
- (20) R.O. Boswall 'The Theory of Film Lubrication.'
Longmans Green and Co. 1928

ACKNOWLEDGEMENTS

The work presented in this thesis was carried out in the Department of Civil and Mechanical Engineering of the Royal College of Science and Technology, Glasgow.

The author wishes to express his gratitude to Professor A.S.T. Thomson, D.Sc., Ph.D., A.R.T.C., M.I.Mech.E., for the generous facilities which were made available and to Dr. H.L. McBroom, B.Sc., A.R.T.C., Ph.D. and Mr. W. Ferguson, B.Sc. M.I.Mech.E. for their continued interest in the work.

APPENDIX I

TABULATED EXPERIMENTAL RESULTS

Date: 27th April, 1956. 2 - Pad Bearing

Test No: 2-36

Loading Circuit Pressure: 70 psi

Speed: 8000 rpm

Thermo- couple	THERMOCOUPLE E.M.F.			
	Time Mins.			
	5	15	25	30
1	2.49	2.52	2.52	2.54
2	2.82	2.86	2.90	2.90
3	2.93	2.99	3.04	3.04
4	3.46	3.56	3.59	3.60
5	3.00	3.07	3.11	3.12
6	3.66	3.74	3.78	3.79
7	3.60	3.69	3.80	3.84
8	3.48	3.57	3.57	3.58
9	2.63	2.71	2.73	2.73
10	3.46	3.50	3.61	3.60
11	3.23	3.28	3.35	3.34
12	3.84	3.85	3.98	3.97
13	2.43	2.40	2.50	2.49
14	3.21	3.13	3.31	3.31
15	3.35	3.33	3.44	3.43
16	3.54	3.46	3.65	3.65
17	3.06	3.20	3.30	3.32
18	3.74	3.87	3.96	3.98
19	3.40	3.58	3.67	3.68
20	3.85	3.96	4.06	4.06

Time Mins.	FILM THICKNESS (1/10,000 in.)			
	Gauge Number			
	1	2	3	4
Start	0	0	0	0
1	18	2	22	21
4	21	2	27	22
9	22	7	27	23
12	23	9	30	23
19	23.5	12.5	34	25
26	24	14	34	26
33	24	14	34	26
Stop	15	7	14	13
When				
cool	-1	0	+6.5	+1

OIL INLET TEMP. deg.F 68

OIL FLOW	(1)	cc/min	382
	(2)	cc/min	370

BEARING FRICTION

Static Friction = 0.42 lb.	
Time Mins	Load lb.
1/2	0.92
10	0.77
20	0.77
30	0.77

Table 1. Test on High Speed Parallel-Surface Thrust Bearing-Direct Test Readings.

Date: 18th July, 1956

3 - Pad Bearing

Test No: 3-5

Loading Circuit Pressure: 100 psi

Speed: 9000 rpm

Thermo- couple	THERMOCOUPLE E.M.F.			
	Time Mins.			
	5	15	25	30
1	1.81	1.97	2.02	2.03
2	1.97	2.15	2.20	2.22
3	2.01	2.22	2.29	2.31
4	2.07	2.27	2.34	2.35
5	1.92	2.09	2.18	2.20
6	2.12	2.32	2.40	2.43
7	2.44	2.67	2.75	2.75
8	2.89	3.15	3.23	3.24
9	2.24	2.37	2.41	2.46
10	2.53	2.75	2.85	2.87
11	3.24	3.42	3.50	3.52
12	3.60	3.76	3.83	3.83
13	2.00	2.12	2.19	2.20
14	2.04	2.20	2.27	2.27
15	2.12	2.27	2.30	2.32
16	2.61	2.82	2.90	2.91
17	2.69	2.85	2.90	2.90
18	3.19	3.39	3.47	3.50
19	2.72	2.92	3.04	3.06
20	3.18	3.42	3.51	3.54
21	2.82	3.05	3.16	3.18
22	3.20	3.39	3.48	3.50
23	2.53	2.80	2.91	2.94
24	2.51	2.69	2.89	2.92

Time Mins	FILM THICKNESS (1/10,000 in.)			
	Gauge Number			
	1	2	3	4
Start	0	0	0	0
1	9	15	40	41
10	12.5	28	39	43
20	15.5	32	39	42
32	18.0	36	39	42
Stop	10.5	26.5	25	26
When				
cool	-4	+2.5	-2	-2

OIL INLET TEMP. deg.F		70
OIL FLOW	(1)	cc/min 735
	(2)	cc/min 720
	(3)	cc/min 730

BEARING FRICTION	
Static Friction = 0.42 lb	
Time Mins.	Load lb.
1/2	1.75
10	1.52
20	1.47
32	1.47

Table 2. Test on Parallel-Surface Thrust Bearing
Direct Test Readings.

Date: 21 May, 1956

4 - Pad Bearing

Test No. 4-10

Loading Circuit Pressure: 70 psi

Speed: 4,400 rpm

Thermo- couple	THERMOCOUPLE E.M.F.				
	Time Mins.				
	5	15	25	35	40
1	1.77	1.98	2.12	2.16	2.19
2	1.83	2.08	2.23	2.29	2.30
3	1.90	2.15	2.30	2.35	2.35
4	1.98	2.24	2.37	2.43	2.44
5	2.07	2.34	2.46	2.53	2.53
6	2.26	2.48	2.60	2.65	2.66
7	2.40	2.61	2.72	2.77	2.79
8	2.56	2.73	2.83	2.89	2.90
9	2.47	2.71	2.81	2.88	2.89
10	2.03	2.30	2.40	2.48	2.49
11	2.17	2.26	2.46	2.53	2.56
12	2.17	2.45	2.59	2.68	2.70
13	1.85	2.06	2.20	2.27	2.31
14	2.24	2.47	2.58	2.64	2.64
15	2.07	2.35	2.41	2.51	2.52
16	2.58	2.75	2.83	2.88	2.89
17	1.97	2.15	2.21	2.28	2.29
18	2.19	2.39	2.42	2.53	2.55
19	2.11	2.32	2.35	2.48	2.52
20	2.35	2.54	2.55	2.65	2.69
21	1.87	2.05	2.08	2.18	2.20
22	2.32	2.48	2.53	2.62	2.64
23	2.00	2.17	2.24	2.34	2.37
24	2.44	2.58	2.65	2.73	2.75

Time Mins.	FILM THICKNESS (1/10,000 in.)			
	Gauge Number			
	1	2	3	4
Start	0	0	0	0
1	17.5	10.0	37.0	34.0
9	24.0	7.5	31.5	31.0
19	26.0	12.5	26.5	28.0
29	27.0	15.5	22.5	25.5
39	27.5	17.0	22.5	25.5
44	28.0	17.0	21.5	25.5
Stop	19.0	13.0	9.0	11.0
When				
cool	5.0	2.5	0	1.5

OIL INLET TEMP.		deg.F	70
OIL FLOW	(1)	cc/min	345
	(2)	cc/min	320
	(3)	cc/min	335

BEARING FRICTION	
Static Friction = 0.42 lb.	
Time Mins	Load lb.
1/2	0.97
10	0.82
20	0.82
30	0.77
40	0.77

Table 3. Test on Parallel-Surface Thrust Bearing
Direct Test Readings.

Bearing Type	2-Pad	3-Pad	4-Pad	
Test No.	2-36	3-5	4-10	
Bearing Load W.lb.	144	207	144	
Angular Velocity ω rad/sec.	838	943	461	
Oil Inlet Temp. deg.F	68	70	70	
Bearing Temp. deg.F				
	Point			
	1	145	124	130
	2	160	132	135
	3	166	136	137
	4	188	137	141
	5	169	131	145
	6	195	140	150
	7	198	154	155
	8	187	173	160
	9	153	142	159
	10	188	159	143
	11	178	185	146
	12	202	197	152
	13	143	131	136
	14	177	133	150
	15	182	136	144
	16	190	160	159
	17	177	160	134
	18	202	184	146
	19	190	166	145
	20	205	185	151
	21	-	171	130
	22	-	184	150
	23	-	162	138
	24	-		
Film Thickness (1/10,000 in)				
Gauge	1	9	7.5	9
	2	7	9.5	5
	3	20	14	12.5
	4	13	16	14.5
Film Thickness (aver) 'h'		8.0	8.0	7.0
Friction Torque lb.ft		0.296	0.471	0.296
Oil Flow lb/min		0.665	1.33	0.61

Table 4. Evaluation of Test Readings.

Test No.	f	T _{max} ° F	T _o ° F	T _{av} ° F	Z _{av} centipoise	N r. p. m.	p p.s.i.	$\frac{ZN}{p}$	$e^{+st} - e^{-st} - 2$	W lb per pad
2G-0	.11	137	70	114	19.2	9000	3.7	46,500	2.08	10.0
1	.0602	136	67	113	19.6	9000	7.1	24,800	2.12	19.0
2	.0535	146	70	121	16.0	9000	11.2	12,900	2.79	30.0
3	.0306	161	74	132	12.4	9200	18.8	6,050	3.88	50.5
4	.0242	188	78	151	9.1	9200	26.6	3,150	7.11	72.0
5	.0174	207	69	161	7.7	9000	38.4	1,790	13.86	103.5
6	.067	154	69	126	14.4	10300	7.1	21,000	3.64	19.0
7	.033	186	69	147	9.6	10400	18.8	5,270	8.4	50.5
8	.0206	203	71	162	7.2	11300	38.4	2,120	12.07	103.5
9	.020	215	75	168	6.7	12250	38.4	2,140	14.46	103.5
10	.03	200	70	157	8.2	13300	26.6	4,070	11.48	71.5
12	.0232	192	70	152	8.6	9000	26.6	2,910	9.59	71.5
13	.0352	160	68	130	13.2	9100	18.8	6,380	4.46	50.5
14a	.0338	180	68	143	10.1	9000	18.8	4,830	7.46	50.5
15a	.0268	212	66	146	9.6	9000	26.6	3,240	16.55	71.5
16a	.0159	236	66	180	5.5	9000	46.4	1,070	28.03	125
15	.0465	160	68	130	13.2	9000	11.2	10,700	4.46	30.0
16	.0295	186	74	149	9.3	9000	18.8	4,470	7.51	50.5
17	.0295	180	69	143	10.3	9000	18.8	4,920	7.31	50.5
18	.0346	175	66	138	11.2	10400	18.8	6,200	6.93	50.5
19	.0227	188	69	149	9.3	9000	26.6	3,160	8.89	71.5
20	.0355	202	64	156	8.2	11800	18.8	5,100	13.76	50.5
21	.306	206	69	160	7.7	13000	18.8	5,300	13.56	50.5
22	.033	200	64	155	8.2	13200	18.8	5,710	13.27	50.5
23	.0178	237	70	181	5.5	9000	38.4	1,290	26.24	103.5
24	.0402	148	63	120	16.5	4400	11.2	6,500	3.66	30.0
25	.028	156	68	126	14.4	4400	18.8	3,360	3.97	50.5
26	.0218	164	64	130	12.9	4400	26.6	2,120	5.54	71.5
27	.0162	174	64	137	11.5	4400	38.4	1,310	7.11	103.5
28	.0124	192	68	150	9.1	4400	46.4	860	12.67	125
29	.0105	200	70	157	8.2	4400	54.3	658	11.48	146
30	.010	216	66	166	6.8	4400	64.3	465	18.05	173
31	.0265	174	68	139	11.0	5500	18.8	3,220	6.42	50.5
32	.0278	178	70	142	10.5	7000	18.8	3,720	6.77	50.5
33	.0291	184	72	147	9.6	8000	18.8	4,070	7.51	50.5
34	.0307	185	68	146	9.8	9000	18.8	4,680	8.4	50.5
35	.0217	170	68	143	10.1	5500	26.6	2,090	5.83	71.5
36	.0214	188	68	149	9.1	8000	26.6	2,740	9.10	71.5
37	.0143	210	70	163	7.1	7000	38.4	1,300	14.46	103.5
38	.0162	212	70	165	6.9	9200	38.4	1,660	15.21	103.5

Table 5. Calculated Test Results

2 Groove Bearing

Test No.	μ $\frac{\text{lb}\cdot\text{sec}}{\text{ft}^2} \times 10^{-3}$	ν_0 $\frac{\text{lb}\cdot\text{sec}}{\text{ft}^2} \times 10^{-3}$	ω rad/sec	$\sqrt{\left\{\frac{\omega}{\nu - \nu_0}\right\}}$	h in $\times 10^{-4}$	$\frac{\omega}{h^2} \left\{\frac{\nu_0 - \nu}{\beta}\right\}$ $\times 10^{+6}$	W lb per pad	$\frac{ZN}{P} \times \frac{r_0}{h}$ $\times 10^6$
2G-24	.203	1.7	460	0.326	11	28.4	30.0	4.13
25	.169	1.46	460	0.297	10	29.7	50.5	2.35
26	.146	1.6	460	0.272	7	68.2	71.5	2.12
27	.119	1.6	460	0.243	7	69.5	103.5	1.31
28	.096	1.46	460	0.217	6	87.3	125.0	1.0
29	.090	1.38	460	0.21	5	130.5	146.0	0.92
30	.077	1.5	460	0.192	5	144.0	173.0	0.65
31	.119	1.46	575	0.274	9.5	42.9	50.5	2.38
32	.113	1.38	732	0.302	10	46.3	50.5	2.61
33	.105	1.28	838	0.31	10	49.2	50.5	2.84
34	.104	1.46	942	0.326	11	53.0	50.5	3.0
35	.127	1.46	575	0.283	6	106.5	71.5	2.45
36	.105	1.46	838	0.325	8	88.8	71.5	2.4
37	.082	1.38	732	0.253	8	74.0	103.5	1.14
38	.080	1.38	960	0.286	9	76.6	103.5	1.3

Table 6. Calculated Test Results

2 Groove Bearing

Test No.	f	T _{max} °F	T _o °F	T _{av} °F	Z _{av} centipoise	N rpm	P psi	$\frac{ZN}{P}$	$e^{+st} + e^{-st} - 2$	W lb per pad
3G-1	.068	127	64	106	23.4	9000	11.3	18600	1.80	20
2	.043	134	64	111	20.6	9000	19.1	9700	2.31	34
3	.032	142	66	117	17.7	9000	27.0	5900	2.79	48
4	.0322	156	69	127	13.8	9200	27.0	4700	3.876	48
5	.0236	170	70	137	11.6	9000	39.0	2650	5.535	69
6	.0190	188	69	148	9.35	9000	55.2	1525	8.89	97
7	.0168	196	65	152	8.8	9000	63.0	1260	11.87	111
8	.0430	164	69	133	12.45	10500	19.1	6850	4.85	34
9	.0223	190	68	149	9.15	10800	39.0	2540	9.587	69
10	.0435	164	68	132	12.5	12000	19.1	7350	4.947	34
11	.050	164	68	132	12.5	13500	19.1	8850	4.947	34
12	.0482	172	70	138	11.2	12500	19.1	7350	5.83	34
13	.0395	167	67	134	12.0	12500	27.0	5550	5.835	48
14	.0266	180	72	144	10.1	12700	39.0	3290	6.815	69
15	.0203	198	69	155	8.25	13500	55.2	1990	11.276	97
16	.025	196	66	153	8.6	13000	39.0	2870	11.57	69
17	.019	215	76	169	6.3	13000	59.0	1390	14.26	104

Table 7. Calculated Test Results

3 Groove Bearing

Test No.	$\frac{\mu}{\mu_0} \times 10^{-3}$	$\frac{\mu_0}{\mu_0} \times 10^{-3}$	ω rad/sec	$\sqrt{\left(\frac{\omega}{\mu} - \frac{1}{\mu_0}\right)}$	h in $\times 10^{-4}$	$\frac{ZN}{P} \cdot \frac{r}{h}$	$\frac{\omega}{h^2} \left(\frac{\mu_0 - \mu}{\beta}\right)$
3G-1	.295	1.6	942	.585	6	21.7×10^6	164×10^6
2	.25	1.6	942	.528	7	9.7	130
3	.22	1.5	942	.492	12	3.44	42
4	.17	1.42	963	.432	10.5	3.14	54.7
5	.135	1.38	942	.376	9	2.1	72
6	.105	1.42	942	.327	7.5	1.42	110
7	.095	1.55	942	.311	7	1.26	140
8	.15	1.42	1100	.430	11	4.27	55.2
9	.10	1.46	1130	.348	11	1.62	64.0
10	.15	1.46	1255	.458	13	4.23	45.2
11	.15	1.46	1415	.486	13	4.78	48.7
12	.133	1.38	1310	.44	13	4.04	48.7
13	.14	1.49	1310	.45	12	3.24	61.5
14	.115	1.28	1330	.41	12.5	1.81	47.9
15	.092	1.42	1415	.373	8	1.64	130
16	.095	1.5	1360	.373	11	1.83	78.7
17	.084	1.12	1360	.333	12	0.81	47.2

Table 8. Calculated Test results

3 Groove Bearing

Test No.	f	T _{max} °F	T _o °F	T _{av} °F	Z _{av} centipoise	N rpm	P psi	$\frac{ZN}{P}$
4G-1	.064	102	73	93	33.5	4400	7.3	20200
2	.064	112	70	98	29.2	4400	7.3	17600
4	.032	118	68	101	26.8	4400	19.4	6080
5	.033	116	69	101	26.8	5700	19.4	7900
6	.038	121	67	103	25.4	7500	19.4	9800
7	.047	135	75	115	18.7	9100	19.4	8800
8	.034	120	69	103	25.4	4400	27.6	4080
9	.039	125	68	106	23.5	7000	27.6	6000
10	.021	150	70	123	15.5	4400	27.6	2470
11	.024	171	68	137	11.5	7200	27.6	3020
12	.015	187	66	146	9.6	4400	40.0	1050
14	.013	225	66	172	6.2	4400	48.0	570
15	.012	240	66	182	5.5	4400	56.0	432
16	.015	229	66	175	6.0	8000	40.0	1200
17	.015	210	68	163	7.2	5600	40.0	1010
18	.014	232	68	177	5.8	7000	48.0	850
19	.015	235	68	179	5.75	9000	48.0	1080
20	.021	189	68	148	9.3	8000	27.6	2710
21	.023	180	68	142	10.5	7200	27.6	2760
22	.021	168	70	136	11.5	4400	27.6	1850
23	.017	220	70	170	6.5	5600	40.0	910
24	.046	128	70	110	21.1	9000	19.4	9800
25	.031	153	68	125	14.8	9000	27.6	4860
26	.026	193	61	147	9.6	9000	27.6	3140
27	.019	228	68	175	6.0	9000	40.0	1350
36	.05	134	70	106	23.4	9000	19.4	10900
37	.035	173	78	141	11.0	9000	19.4	5100
38	.05	137	68	114	19.15	8500	19.4	8400
39	.032	174	70	139	11.0	8700	19.4	4940
40	.038	197	70	155	8.15	13100	19.4	5500

Table 9. Calculated Test Results

4 Groove Bearing

Test No.	$\frac{v}{ft^2} \times 10^{-3}$	$\frac{v_0}{ft^2} \times 10^{-3}$	ω rad/sec	$\sqrt{\left(\frac{\omega}{v-v_0}\right)}$	h in $\times 10^{-4}$	W lb per pad	$\frac{e^{+\beta t}}{e^{-\beta t}} - 2$	$\frac{\omega}{h^2} \left(\frac{v_0 - v}{\beta^6}\right)$ $\times 10^6$	$\frac{ZN}{P} \frac{r}{h}$ $\times 10^6$
4G-1	.545	1.24	462	.67	12	9.5	0.35	11.15	11.8
2	.42	1.38	462	.528	11.5	9.5	0.75	16.8	10.7
4	.36	1.46	462	.47	10	25.3	1.10	25.4	4.25
5	.38	1.42	597	.557	10	25.3	0.95	31.0	5.53
6	.335	1.49	785	.582	15	25.3	1.28	20.2	4.58
7	.25	1.16	953	.552	9	25.3	1.63	53.5	6.85
8	.345	1.42	462	.458	9.5	36.0	1.13	27.6	3.05
9	.31	1.46	733	.537	9.5	36.0	1.45	46.9	4.42
10	.19	1.38	462	.32	7	36.0	3.15	56.2	2.47
11	.135	1.46	755	.336	8	36.0	5.98	78.5	2.65
12	.105	1.50	462	.228	7	51.8	9.29	66.0	1.05
14	.08	1.50	462	.198	5.5	62.5	22.04	108.0	0.72
15	.07	1.50	462	.184	6.5	73.0	30.5	86.5	0.47
16	.075	1.50	838	.258	8	51.8	24.04	122.5	1.05
17	.085	1.46	587	.23	6.5	51.8	15.16	95.6	1.09
18	.07	1.46	733	.232	8	62.5	24.64	80.0	0.74
19	.07	1.46	942	.264	9	62.5	26.24	80.6	0.84
20	.10	1.46	838	.3	8	36.0	9.29	89.0	2.37
21	.115	1.46	755	.307	8	36.0	7.51	79.5	3.15
22	.14	1.38	462	.268	6.5	36.0	8.69	67.5	1.99
23	.08	1.38	587	.224	7.5	51.8	18.05	68.2	0.85
24	.285	1.38	942	.578	13.5	25.3	1.50	28.6	7.2
25	.18	1.46	942	.440	10	36.0	3.64	60.2	3.4
27	.075	1.46	942	.273	8	51.8	22.54	102.0	1.18
36	.25	1.38	942	.537	14	25.3	1.88	27.1	5.45
37	.13	1.05	942	.373	10	25.3	4.85	43.3	3.57
38	.24	1.46	890	.505	8	25.3	2.23	85.0	7.32
39	.125	1.38	910	.353	9	25.3	6.13	70.3	3.85
40	.095	1.38	1370	.374	9	25.3	10.78	108.5	4.27

Table 10. Calculated Test Results

4 Groove Bearing

APPENDIX II**CALIBRATION OF APPARATUS**

APPENDIX II

CALIBRATION OF APPARATUS

1. Bearing Loading Calibration

The test bearing was subjected to load by three hydraulic jacks acting in parallel (Fig. 18, 20, Ch. IV), supplied with pressure oil from a dead weight pressure gauge tester.

Initial tests were made on the jacks individually to ensure that the load/pressure characteristic of each was the same. This proved to be the case and the calibration of the loading device in its operational condition was begun.

This was done by assembling the loading jacks, cylinder and the two loading pistons complete with piston rings, but omitting the central high speed shaft and disc (Fig. 20, p.87). This partial assembly was suspended vertically by a hanger attached to the cylinder and fixed piston. A 1/4" diameter rod was hung from the moving piston and loaded with dead weights which were supported so that the loading jacks and pistons were extended to operational positions. The pressure to the jacks was increased until the load was just raised from the support. In this way, a curve of total load against pressure to the jacks was obtained covering the range of operating loads, (Fig. 35). It may be seen that movement of the pistons was minimized and the assembly was calibrated at its operational extension. Errors might possibly arise when the bearing is running because of the presence of oil and the

change in temperature of the assembly. However, after the loading pistons were modified to cast iron with neoprene O-rings operating in a steel cylinder, no thermal effects on the loading arrangement were evident. In addition to the above standard calibration, the procedure was also carried out with the piston rings dry, lubricated with heavy and light oil. No appreciable difference in the load-pressure curve could be detected.

2. Thermocouple Calibration

The thermocouples were calibrated in position on the bearing thrust plate by immersing the thrust plate (Fig. 21, p.89) in a beaker of lubricating oil and heating the oil through the expected temperature range, with the cold junction in melting ice. The curve of temperature in degrees Fahrenheit against thermocouple millivolts is given (Fig. 36) and it is seen to be in agreement with the standard copper constantan temperature - EMF curve.

3. Static Friction Calibration.

The static friction, due to the end seals and support roller bearings (Fig. 20, p.87), was measured before and after every test. With the machine stopped and unloaded, weights were added to the friction pan (Fig. 27, p.98) until a slight rotation of the assembly took place. This static friction torque was added to the friction torque reading obtained during test. The total friction torque applies to two thrust faces so that for one bearing, the friction torque reading was divided by two.

The static friction was appreciably constant and amounted to about 0.1 lb-ft per bearing, or about 20% of the test bearing friction at normal running conditions. Although this figure seems rather high, it was not thought to be a cause for concern, because the static friction was independent of load and speed on the test bearing, was well defined and could be measured accurately and often.

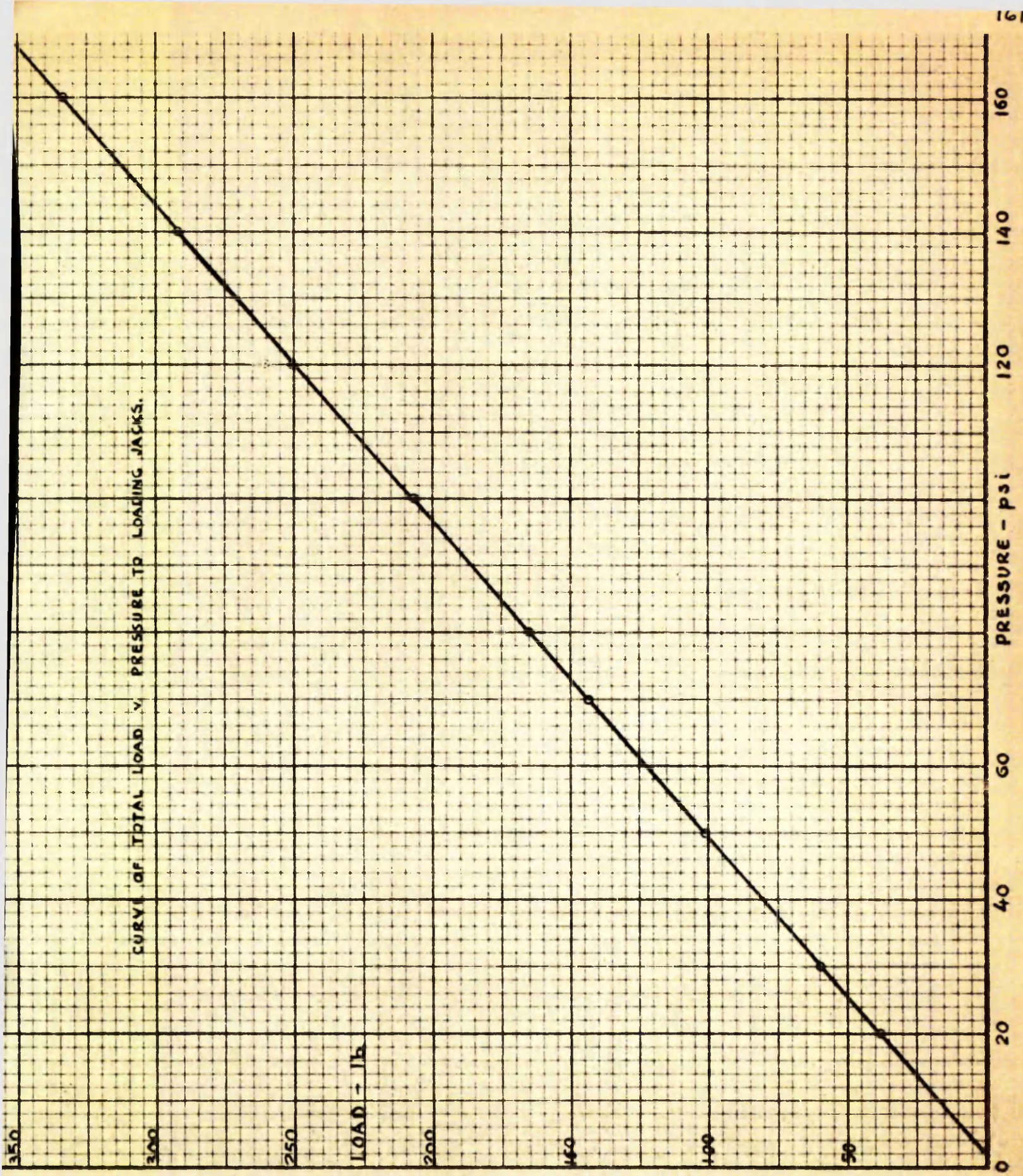


FIG 35 CALIBRATION CURVE OF LOADING SYSTEM

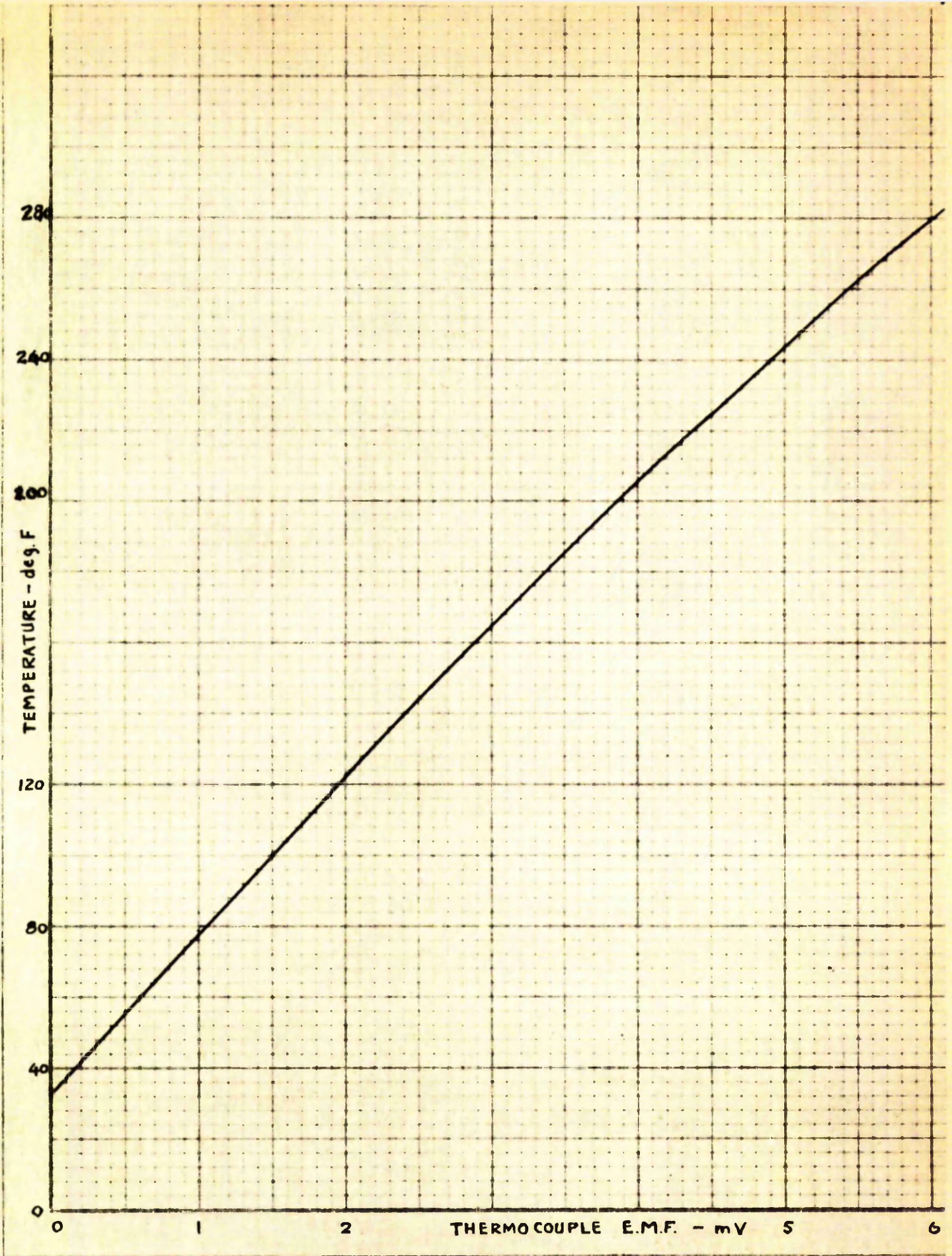


FIG 36 THERMOCOUPLE CALIBRATION CURVE

GLASGOW
UNIVERSITY
LIBRARY